Lipid metabolism and inflammation in the pathogenesis of chronic liver diseases

Sowmya Narayanan
Pittsburgh, Pennsylvania

B. S., Biochemistry and B. A., English, Chatham University, May 2010

A dissertation presented to the graduate faculty of the University of Virginia in candidacy for the degree of Doctor of Philosophy

Department of Microbiology, Immunology, and Cancer Biology

University of Virginia
June 2016

_____

_____

_____

_____

_____

ABSTRACT

Chronic liver diseases are a rising global health burden that include chronic viral hepatitis C and nonalcoholic steatohepatitis (NASH). Despite differences in their etiologies, both hepatitis C and NASH are marked by alterations in systemic lipid metabolism that are accompanied by chronic hepatic inflammation. In order to dissect how lipid metabolism and the immune response contribute to liver pathology, we investigated the role of *de novo* lipid synthesis in hepatitis C virus (HCV) infection and established novel *in vitro* systems to study the role of a newly described immune population, the innate lymphoid cells (ILCs), in NASH. We demonstrate that HCV replication, assembly, and infectious virion production are decreased upon inhibition of *de novo* lipogenesis. Suboptimal propagation of the virus is in part due to changes in the lipid composition of hepatocytes and alterations in post-translational modifications of proteins under conditions of limited *de novo* lipid synthesis. Conversely, treatment of hepatoma cells with an excess of lipids transforms them into steatotic hepatocytes characteristic of fatty liver disease. These *in vitro* equivalents of NASH hepatocytes upregulate expression of profibrogenic markers such as TGF-β, which in turn triggers expression of collagen I in hepatic stellate cells, thus initiating the fibrotic cascade seen in NASH livers. Importantly, a subtype of ILCs secretes IL-22, which facilitates tissue repair through inhibition of fibrogenesis, potentially inhibiting the transformation of hepatic lipid accumulation to chronic liver disease. Indeed, given that fibrogenesis, inflammation, and dysregulation hepatic lipid metabolism are common signatures of all chronic liver diseases, the findings from our studies collectively identify metabolic and

immunological targets that can be modulated for increased understanding of homeostatic and pathological liver biology.

In memory of Chuck Deopken, who made it all possible.

ACKNOWLEDGEMENTS

I have been exceptionally fortunate in having Young Hahn as my mentor. During my time in her lab, I have had enormous latitude in exploring various projects and several opportunities for professional development that are not commonplace to most students. In addition to helping me flourish in the lab, Young's ability to see the positive side of any situation and encouragement to balance passion for science with life outside the lab are lessons that I will remember for a long time.

Peter Krueger is not only a close friend, but also someone whom I can count on to have hours of discussion on everything from a small piece of data to the intricacies and humanness of our scientific enterprise. His creativity and ability to see the forest even before the trees is something I will always hope to emulate. Similarly, Taeg Kim has been a phenomenal mentor who never hesitated to provide advice or share his obvious love for science regardless of the hour of the day. Annie Tosello-Trampont was instrumental in helping me develop technical skills, even though I gave her more than enough reason to be frustrated with my attempts early in graduate school. I have also had the opportunity to work with two individuals who make teaching and sharing my passion for science a real joy: Albert Nieh and Fionna Surette, both of whom have not only become my very good friends, but were also incredible colleagues who did not let time sheets or career interests dictate their enthusiasm for research. I also want to thank other colleagues in the Hahn lab who made it a great place to work, especially Drew Cobb, Sue Landes, Hai-Chon Lee, Yoon-Ah Jo, and Aditya Dandekar.

My committee, Ulrike Lorenz, Tom Braciale, Kyle Hoehn, Dave Kashatus, Thurl Harris, and Ian Glomski have helped shaped my naïveté into a pragmatic approach to science. Tom has been my second mentor, who always provided encouraging and constructive feedback. Kyle and his lab members introduced me to the world lipids; their constant willingness to help and discuss lipid biology made it exciting and not daunting. Thurl is a model teacher who helped me troubleshoot the technical minutia and the conceptual possibilities of my projects.

My sincere thanks to Edik Blaise and David Peske who quantified and made large sets of data look like modern art. I am also grateful to my fellow MSTPs who shared everything from protocols and mice to their honest feedback on manuscript drafts.

The Carter Immunology Center has been pivotal in making MR6 the place where I spend more time than anywhere else. I especially want to thank the faculty and Emily Moser, who set the standard for the camaraderie that I have come to expect at the Center, which was later continued by Amy Newton and Michelle Butler.

I would not have chosen to pursue research had it not been for Dr. Pirette Appasamy at Chatham University, who introduced me to immunology and to my undergraduate mentors, Drs. Olja Finn and Pamela Beatty. Their encouragement and confidence in my abilities are the reason why I recognized scientific research as my passion and my professional home.

Thank you to my long time friend, Sara Lamars, who edited various drafts of whatever I wrote despite the excessive amounts of scientific jargon. Lastly, I am grateful to my parents and my brother for never questioning my goals and for never asking me when I will graduate.

TABLE OF CONTENTS

LIST OF FIGURES

LIST OF TABLES

ABBREVIATIONS

2-BP	2-bromopalmitate
ACC	Acetyl-CoA carboxylase
ACS	Acyl-CoA synthetases
ANOVA	Analysis of variance
Apo	Apolipoprotein
ATP	Adenosine triphosphate
BC	Biotin carboxylase
BCCP	Biotin carboxyl carrier protein
BiP	Binding immunoglobulin protein
BSA	Bovine serum albumin
CCL	C-C motif chemokine ligand
CCl4	Carbon tetrachloride
CCR	C-C chemokine receptor
CD	Cluster of differentiation
cDNA	Complementary DNA
CLDN1	Claudin-1
CoA	Coenzyme A
CT	Carboxyltransferase
CXCL	C-X-C motif chemokine ligand
CXCR	C-X-C motif chemokine receptor
DC	Dendritic cell

DMEM	Dulbecco's modified eagle medium
DMSO	Dimethyl sulfoxide
DNA	Deoxyribonucleic acid
EDTA	Ethylenediaminetetraacetic acid
eIF	Elongation initiation factor
ER	Endoplasmic reticulum
FABP	Fatty acid binding protein
FACS	Fluorescence-activated cell sorting
FAS	Fatty acid synthase
FATP	Fatty acid transport protein
FBL2	F-box and leucine-rich repeat-containing protein 2
FBS	Fetal bovine serum
FMO	Fluorescence minus one
GAG	Glycosaminoglycans
HCV	Hepatitis C virus
HCVcc	Cell culture derived HCV
HDL	High-density lipoprotein
HIV	Human immunodeficiency virus
HSC	Hepatic stellate cell
IFN	Interferon
IL	Interleukin
ILC	Innate lymphoid cell
IRE1	Inositol-requiring enzyme 1

IRES	Internal ribosomal entry site
JFH-1	Japanese fulminant hepatitis-1
LC/MS/MS	Liquid chromatography-tandem mass spectrometry
LDL	Low-density lipoprotein
LDLR	Low-density lipoprotein receptor
LPL	Lipoprotein lipase
LPS	Lipopolysaccharide
LVP	Lipoviroparticle
Mac-1	Macrophage-1 antigen
MAIT	Mucosal associated invariant T cell
MCP-1	monocyte chemotactic protein-1
MEM	Minimum essential media
MFI	Mean fluorescence intensity
MHC	Major histocompatibility complex
MOI	Multiplicity of infection
MPO	Myeloperoxidase
mRNA	Messenger RNA
MTP	Microsomal triglyceride transfer protein
NADPH	Nicotinamide adenine dinucleotide phosphate
NAFLD	Nonalcoholic fatty liver disease
NASH	Nonalcoholic steatohepatitis
NCR	Natural cytotoxicity receptor
NK	Natural killer cell

NKT	Natural killer T cell
NOD	Non-obese diabetic
NPC1L1	Niemann-Pick C1-like 1
NS	Nonstructural
NTR	Nontranslated region
OCLN	Occludin
PBMC	Peripheral blood mononuclear cells
PBS	Phosphate buffered saline
PCR	Polymerase chain reaction
PD-L	Programmed death-ligand
PDI	Protein disulfide-isomerase
PERK	Protein kinase R-like ER kinase
PFA	Paraformaldehyde
PMA	Phorbol 12-myristate 13-acetate
PPT	Palmitoyl-protein thioesterase
PT	Post-treatment
PVDF	Polyvinylidene fluoride
RIG-I	Retinoic acid-inducible gene 1
RIPA	Radioimmunoprecipitation assay
RNA	Ribonucleic acid
ROI	Region of interest
ROR	Retinoic acid receptor-related orphan receptor
ROS	Reactive oxygen species

RPMI	Roswell Park Memorial Institute medium
RT-PCR	Real-time polymerase chain reaction
SDS	Sodium dodecyl sulfate
SEM	Standard error of mean
SRB1	Scavenger receptor B1
SREBP	Sterik regulatory element-binding protein
STAT	Signal transducer and activator of transcription
T-bet	T-box expressed in T cells
TFR1	Transferrin receptor 1
TGF	Transforming growth factor
Th	T helper
TIMP	Tissue inhibitor of metalloproteinase
TLR	Toll-like receptor
TNF	Tumor necrosis factor
TRAIL	TNF-related apoptosis-inducing ligand
Treg	Regulatory T cells
TSLP	Thymic stromal lymphopoietin
US	United States
UV	Ultraviolet light
VLDL	Very low-density lipoprotein
α-SMA	Alpha smooth muscle actin

CHAPTER 1: Introduction

Included in part in "Narayanan S, Surette FA, and Hahn YS. The immune landscape in nonalcoholic steatohepatitis. *Immune Network*." (manuscript in press).

Chronic liver diseases are the 12th leading cause of death in the United States (1). These include hepatitis B and C and alcoholic and nonalcoholic fatty liver diseases, which can result in cirrhosis, or end-stage liver disease resulting from scarring due to recurrent bouts of tissue damage. The economic burden of treating cirrhosis in the United States is estimated between $14 million and $2 billion annually (2). Moreover, as cirrhosis is an irreversible process, successful treatment is limited to liver transplantation, which is available to only ~50% of patients on the waiting list due to a shortage of organs (3, 4). Despite widespread use of a prophylactic vaccine against the hepatitis B virus and recent development of antiviral agents for the treatment of hepatitis C, the number of deaths from chronic liver diseases have not decreased and instead increased by 3% between 2012 and 2013 (1). Continued investigation into the pathophysiology of chronic liver diseases is needed in order to develop novel prophylactic measures, better diagnostic markers, and alternative treatments to contain and reduce the increasing global burden of liver dysfunction.

Lipid metabolism in the liver

The liver's status as the largest internal organ is matched by the diversity and magnitude of its functions. From coagulation factor synthesis to storage of vitamins, the liver serves as the intersection point for several essential processes, central among them

being its role in nutrient homeostasis (Table 1.1). In particular, following delivery of lipids in chylomicrons synthesized in the gut, the liver repackages excess lipids for storage or distribution to extrahepatic tissues, such as adipose tissue and muscle (Figure 1.1). Specifically, triglycerides and cholesterol esters are packaged into very low-density lipoproteins (VLDL) that lose their triglyceride content in extrahepatic tissues by lipolysis via lipoprotein lipase (LPL). Unused cholesterol is then delivered back to the liver as low-density lipoprotein (LDL) and excreted as bile. Hepatic synthesis of high-density lipoprotein (HDL) also aids in recovering excess cholesterol from the periphery for delivery to the liver. In addition to supplying lipids to other tissues, the liver can store lipids in lipid droplets, intracellular vesicles bound by a single phospholipid membrane that are rich in cholesterol esters and triglycerides.

Triglycerides are esters composed of glycerol and three fatty acids. While dietary lipids constitute 15-25% of hepatic fatty acids, the majority of hepatic triglycerides are derived from free fatty acids taken up from the extracellular environment (Figures 1.1 and 1.2) (5). Transport of fatty acids across the cell membrane is primarily mediated by fatty acid transport proteins (FATPs); although they are not essential for fatty acid uptake, scavenger receptors such as CD36 have also been known to facilitate the accumulation of free fatty acids in hepatocytes (6-9). Once in the hydrophilic cytosol of the hepatocyte, fatty acids are bound by fatty acid binding proteins (FABPs) that shuttle the fatty acid to acyl-CoA synthetases (ACS) for activation via addition of a –CoA group (10, 11). Activation prevents fatty acid efflux and enables esterification and incorporation into triglycerides and phospholipids. Activated fatty acids are shuttled to various metabolic pathways by binding to acyl-CoA binding proteins (12). The fate of a given

fatty acid is determined by a number of factors including rate of uptake, chain length and saturation, and metabolic status of the liver (13).

Hepatocytes are also a major site of *de novo* lipogenesis, the process of generating fatty acids from acetyl-CoA (Figures 1.1 and 1.3.A) (14). Acetyl-CoA is derived from pyruvate following glycolysis or from citrate produced during the Krebs cycle. The rate-limiting step of *de novo* lipogenesis is the conversion of acetyl-CoA to malonyl-CoA, which is catalyzed by the enzyme acetyl-CoA carboxylase (ACC) (14). ACC is a large, biotin-dependent enzyme containing multiple functional domains: biotin carboxylase (BC), biotin carboxyl carrier protein (BCCP), carboxyltransferase (CT), and an additional domain containing phosphorylation sites that regulate enzyme activity (15). Biotin bound to BCCP is initially carboxylated at the BC domain; the activated biotin is then translocated to the CT domain where the carboxyl moiety is transferred to the methyl group of acetyl-CoA to form malonyl-CoA (Figure 1.3.B) (14). Malonyl-CoA is first combined with acetyl-CoA to form an acetoacetyl intermediate, a process catalyzed by the enzyme fatty acid synthase (FAS) (16). NADPH generated by the pentose phosphate pathway reduces the ketone group on the secondary carbon of the malonyl-CoA incorporated into the acyl chain. FAS also catalyzes subsequent rounds of addition of malonyl-CoA to the acyl chain to produce palmitic acid, a 16-carbon saturated fatty acid (16). Modification of palmitate by fatty acyl-CoA elongases and stearoyl-CoA desaturases generates a diverse pool of fatty acids.

Humans express two isoforms of ACC—ACC1 and ACC2. Although both isoforms produce malonyl-CoA, their tissue-specific expression confers distinct functions to their end product. ACC1 is found in the cytosol of lipogenic tissues such as the liver

and adipose tissue, where malonyl-CoA is used to initiate fatty acid synthesis (17, 18). ACC2 is expressed in the mitochondria of the liver, heart, and skeletal muscle, where malonyl-CoA acts to inhibit fatty acid oxidation (17-19). Coexpression of ACC1 and ACC2 thus positions the liver as a central regulator of fatty acid metabolism.

The complexities of hepatic lipid metabolism are illustrative of the enormous flux of nutrients into and out of the liver. The liver's central role in the processing of potentially immunogenic molecules from food, in addition to toxins and microbial by-products draining from the gut, requires local immune responses to be held in a suppressed state to avoid frequent bouts of inflammation (discussed below). It is this confluence of the liver's role in lipid metabolism and its unique tolerogenic immune environment that is the focus of my dissertation. Specifically, I describe the investigation of two liver diseases, hepatitis C and nonalcoholic steatohepatitis, which are chronic inflammatory diseases intimately linked with hepatic lipid metabolism.

Hepatitis C

Hepatitis C is a chronic inflammatory disease that poses a significant health burden as it affects over 150 million people worldwide, resulting in over 350,000 deaths per year (20). First recognized in the mid-1970s as the cause of unexplained liver dysfunction in patients that received blood transfusions, hepatitis C is presently the leading cause of liver transplants in the United States (21, 22). The etiological agent of hepatitis C is the hepatitis C virus (HCV). Upon infection, over 80% of patients develop chronic low-grade inflammation that frequently results in end-stage liver diseases such as cirrhosis and hepatocellular carcinoma. However, hepatitis C follows a silent course of

disease in the majority of infected individuals and typically presents with symptoms 2-4 decades after exposure (23).

Until recently, the standard treatment for hepatitis C was pegylated interferon (IFN)α and the nucleoside analog, ribavirin. This combination was effective in only 8-50% of patients and had a number of side effects, including flu-like symptoms, diarrhea, and anemia (24). It was only in 2011 that teleprevir and boceprevir, the first generation of viral protease inhibitors, were introduced for widespread patient use. Although these agents significantly improved the rates of sustained virological responses (undetectable viral RNA in blood) to >65%, they were administered in combination with IFNα and ribavirin, required multiple daily doses, and resulted in adverse side effects including severe anemia and rash (25-27). The second and third generation direct acting antivirals currently in use are not only well tolerated, but have also increased the rates of sustained virological responses to >90% (28-30). While remarkably effective, these drugs are highly cost-prohibitive as the approximate cost per sustained virological response is US $150,000 (31). In addition, although increasing screening of blood products and safer medical practices have dramatically reduced the incidence of acute hepatitis C in the last two decades, HCV-related deaths now surpass the number of human immunodeficiency virus (HIV)-related deaths in the United States (32). The development of cost-effective prophylactic vaccines has thus reemerged as the next frontier in the field.

Such rapid and remarkable progress in the treatment of hepatitis C was not always the pace with which HCV was understood. Despite the discovery of non-A, non-B hepatitis in the 1970s, the transmissible agent responsible for hepatitis C was not identified until 1989 (33). The intervening years were met with several technical

difficulties, including the lack of an animal model, as sera from patients were unable to establish productive disease in most primates with the exception of chimpanzees (34, 35). Inoculation of chimpanzees with serum from a patient with particularly severe disease allowed further characterization of the infectious agent as a 30-60 nm sized particle, which was inactivated by chloroform, and produced membranous tubules in infected animals, tentatively identifying it as an enveloped RNA virus (36-38). Subsequent experiments introduced a cDNA library from infected chimpanzees into bacteria, and the resulting proteins were screened for reactivity against patient sera (33). The elusive cause of post-transfusion hepatitis was thus finally identified as the hepatitis C virus. At present, there are over 50 subtypes of HCV spanning 7 genotypes that vary in geographical distribution, disease characteristics, and sensitivity to treatment (39). Moreover, host selective pressure and an error-prone polymerase can generate quasispecies within an infected individual that can vary 1-9% in sequence, making HCV a formidable, yet fascinating pathogen (40).

HCV genome and life cycle

HCV is classified in the genus *Hepacivirus* within the *Flaviviridae* family of viruses. All members of the *Flaviviridae* family are enveloped, single-stranded positive-strand RNA viruses. HCV's 9.6 kb genome consists of nontranslated regions (NTR) in the 5' and 3' ends that flank a single open reading frame encoding a 3000 amino acid long polyprotein. The polyprotein is cleaved into three structural proteins—core, E1, and E2—and seven non-structural proteins—p7, NS2, NS3, NS4A, NS4B, NS5A, and NS5B (Figure 1.4).

The life cycle of HCV begins with viral entry into hepatocytes through binding of host receptors on the basolateral surface (Figure 1.5) (41). Initial attachment of HCV to hepatocytes is thought to proceed via interactions with the low-density lipoprotein receptor (LDLR) and glycosaminoglycans (GAGs) on heparan sulfate proteoglycans (42-44). As described below, binding of HCV to the LDLR and GAGs is mediated by interactions with virion-associated apolipoprotein E (ApoE). However, while LDLR and GAGs are thought to enhance HCV entry, they are not as essential as CD81, scavenger receptor B1 (SRB1), and the tight junction proteins, claudin-1 (CLDN1) and occludin (OCLN). Although the mechanics of HCV entry are still under investigation, current data suggests that E2 initially binds SRB1, which exposes the binding site for CD81 (45-47). Binding of E2 to CD81 promotes lateral movement of the virion to sites between hepatocytes, where CLDN1 and OCLN facilitate internalization of HCV (48). More specifically, CLDN1 interacts with CD81 to mediate post-attachment steps of viral entry, but does not associate with HCV proteins (49, 50). The role of OCLN is less well-defined and it is not known whether it directly interacts with viral proteins (51, 52). Nonetheless, hepatic expression of CD81 and OCLN is sufficient to render mice permissive to HCV infection (53-55). In addition, HCV's tropism to the liver is partly dictated by SRB1 as it is expressed at high levels in hepatocytes in contrast to other host receptors that participate in HCV entry (41). Lastly, the transferrin receptor 1 (TFR1) and the cholesterol receptor Niemann-Pick C1-like 1 (NPC1L1) were also found to have a role in viral entry as knockdown of either receptor inhibited HCV entry *in vitro* (56, 57).

Entry of HCV into the hepatocyte is completed by clathrin-mediated endocytosis, after which the viral genome is release into the cytosol by low-pH-mediated fusion, a

process regulated by the envelope protein E1 and perhaps E2 (58-62). Subsequent translation of the (+)-strand RNA proceeds through the HCV internal ribosomal entry site (IRES) as HCV RNA lacks the 5'-7-methylguanosine cap found in eukaryotic mRNAs (63). As a result, the HCV IRES overrides the need for group 4 elongation initiation factors (eIF), which bind the 5' cap of host mRNAs; instead, translation of HCV RNA only requires eIF3, eIF2, and eIF5 (64). Translation of the viral genome then proceeds through a single open reading frame, producing a 3,000 amino acid long polyprotein encoding 10 viral proteins (65, 66). Host signal peptidase and signal peptide peptidase cleave the structural proteins and the junction between p7 and NS2 (67-69). The remainder of the polyprotein is processed by viral proteases; NS2 is an autoprotease that cleaves itself from NS3, while the serine protease NS3, with the cofactor NS4A, liberates the remaining non-structural viral proteins (70-73).

The newly synthesized HCV non-structural proteins then assemble onto host endoplasmic reticulum (ER) membranes to form replication complexes, similar to the double membraned vesicles used by other (+)-sense RNA viruses. Such characteristic changes in the ER membrane are identified as membranous webs and are orchestrated by NS4B and NS5A (74). Sheltered from degradation within these webs, HCV RNA replication is initiated in the absence of a primer and generates a (-)-strand intermediate, which in turn serves as a template for synthesis of (+)-strand RNA (75, 76). The ratio of (+)-strand to (-)-strand varies across experimental systems and viral genotypes, but averages at 10:1 and decreases to 6:1 within replication complexes (77-79). Replication of HCV RNA exclusively requires NS3-NS5B. In addition to its role as a protease, NS3 also has nucleotide triphosphatase and helicase functions, which are thought to displace

complementary RNA or resolve secondary RNA structures prior to replication (80, 81). NS5A is the most multifunctional protein in the HCV proteome and facilitates replication through multiple ways, including protein-protein interactions and protein-RNA interactions (82-85). NS5B is the viral polymerase that is responsible for the synthesis of both (-) and (+)-strand HCV RNA (86, 87).

Current knowledge of the shuttling of viral RNA to translation, replication, and packing into virions is tenuous, as the fate of a given (+)-strand RNA is not well understood. For instance, it is not known whether (+)-strand RNA must be translated before it can serve as a template for (-) strand synthesis. Conversely, once synthesized from a (-)-strand template, trafficking of the nascent (+)-strand for additional rounds of replication, translation, or packaging into virions is not completely defined. As synthesis of the (-)-strand proceeds in a 3'-5' direction, translation cannot occur simultaneously with synthesis of (-)-strand RNA (75, 88). Modeling studies further predict that the initial synthesis of (-)-strand RNA is at or near the site of translation, as it requires the polymerase NS5B to be supplied in *cis* (76). The (-)-strand RNA is subsequently enclosed within double membraned vesicles, which are the site of (+)-strand synthesis. The majority of the newly synthesized (+)-strand RNA are then exported back to the cytosol, where they can reinitiate translation or be assembled into viral particles (76).

Assembly of replicated viral RNA into nascent virions is a concerted effort that requires all viral proteins except the polymerase. Although the roles of p7, NS2, NS3/4A, and NS4B in HCV assembly are not fully defined, the functions of the nucleocapsid core protein, the envelope glycoproteins, and NS5A are better understood. For example, assembly is dependent on the association of core with the surface of cytosolic lipid

droplets (89, 90). Lipid droplets are highly mobile intracellular structures composed of triglycerides and cholesterol esters enclosed within a single phospholipid membrane. As lipid droplets are thought to bud from the ER membrane, they are typically located in close proximity to the ER, the site of HCV replication. NS5A also localizes to the surface of lipid droplets and is thought to shuttle newly synthesized RNA from the ER to the site of assembly (90). However, given the low efficiency of assembly in live cells, the precise location of HCV assembly, e.g., the surface of lipid droplets or lipid droplet-associated ER membranes, is unclear (91). Nonetheless, once the viral RNA is encapsulated by the icosahedral nucleocapsid, it is enveloped by host ER membranes decorated with E1 and E2 heterodimers, which are held facing the ER lumen after being cleaved from the polyprotein (92-94).

Although the minimum requirements for an HCV particle are assembled at this point, the virus continues to mature through the ER. Specifically, newly formed virus particles are complexed with apolipoproteins in a process that remains enigmatic (95, 96). One possibility is that as the virus buds into the ER lumen, it associates with precursors to lipoproteins in the ER lumen containing triglycerides, cholesterol esters, and the apolipoproteins E and C (ApoE and ApoC). Fusion of the lipidated virus with ApoB that is lipidated simultaneously, but independently of the virus, produces a viral particle known as the lipoviroparticle (LVP). The virus is subsequently exported through the Golgi and released via a noncytolytic pathway (91).

HCV and lipids

HCV's association with lipoproteins produces a heterogenous mixture of secreted viral particles that range in density from 1.20 g/mL to 1.03 g/mL (97-100). Particle infectivity is inversely proportional to density (100, 101). As a result, LVPs, which harbor on average 40% of viral RNA in blood, constitute the most infectious form of HCV. The increase in infectivity is in part due to enhanced viral entry, as lipoproteins on the LVP can bind SRB1 and LDLR (101, 102). Furthermore, the presence of lipids likely masks the binding sites of neutralizing antibodies, enabling HCV to evade anti-viral host responses (103). However, the benefits of associating with lipids are not limited to viral entry and circumventing host immune responses, as multiple steps of the HCV life cycle rely on host lipids. As described above, HCV replication occurs within double membraned enclosures on the ER membrane. These membranous webs are highly detergent resistant and enriched in cholesterol and sphingomyelin (104, 105). Moreover, lipid droplets play a critical role in viral assembly. Maintaining adequate supplies of intracellular lipids is therefore essential for the propagation of HCV.

Indeed, in addition to directly facilitating viral entry, replication, assembly, and export, lipids also serve as modifiers of host and viral proteins. Addition of a geranylgeranyl group, which is derived from the cholesterol synthesis pathway, to the host factor F-box and leucine-rich repeat-containing protein 2 (FBL2) is necessary for optimal viral replication (106). *S*-palmitoylation is another type of lipid-based post-translational modification of proteins in which a fatty acid is added to a cysteine residue. Palmitoylation of proteins can dictate localization to membranes, folding, and ultimately function. As a result, inhibiting the palmitoylation of HCV core disrupts its ability to trafficking to ER membranes, resulting in decreased virion assembly and release (107).

Similarly, palmitoylation of HCV NS4B was previously shown to permit its polymerization and interaction with NS5A, where depalmitoylated NS4B was unable to form the replication complex resulting in a marked loss of viral replication (108). A more recent study, however, found that the majority of NS4B present in replication complexes is not palmitoylated (109). Although these contradictory findings indicate the need for further investigation, they nonetheless underscore the importance of fatty acids in potentially regulating viral protein function and in turn, influencing the outcome of disease. Thus, considering the extensive roles of lipids in HCV infection, hepatic synthesis and processing of lipids may serve as an intracellular determinant of HCV's tropism to the liver.

Acute changes in extracellular lipids also impact HCV virulence. To date, two studies demonstrate that in the post-prandial state, the amount of viral RNA is increased in very low-density fractions, which include chylomicrons and VLDLs (110, 111). While Diaz, et al. interpret their findings as preliminary evidence of intestinal involvement in HCV infection, Felmlee, et al. suggest that the virus migrates via intravascular transfer into more buoyant fractions. Although the exact mechanism is not resolved, these findings collectively suggest that in addition to the essential functions of intracellular lipids, extracellular lipids also play a distinct role during HCV infection.

HCV's dependence on intracellular and extracellular lipids manifests as a number of clinical consequences. As an example, steatosis, or the accumulation of intracellular lipids in hepatocytes, is present in ~50% of patients and was used as a diagnostic marker for non-A, non-B hepatitis before the development of serological tests for HCV (112-114). The association of HCV with steatosis rises to ~80% in patients infected with

genotype 3 virus (115-117). The extent of steatosis parallels the level of viral RNA in the liver and serum and can persistent even after sustained virological response is achieved in non-genotype 3 patients (115, 118, 119). Steatosis can drive hepatic inflammation in non-HCV models of fatty liver disease (120). Expression of viral proteins thus augments local production of inflammatory cytokines that enhance the development of fibrosis. Furthermore, patients infected with genotype 3 HCV are more resistant to treatment with the direct acting antivirals (121). Hepatic lipid metabolism thus significantly influences the pathogenesis of hepatitis C.

Nonalcoholic steatohepatitis

Nonalcoholic fatty liver disease (NAFLD) is a formidable health problem as it is the third leading cause of liver transplants in the United States and is predicted to surpass viral hepatitis and alcoholic cirrhosis as the leading cause in the next decade (122). NAFLD is characterized by extensive steatosis, or the accumulation of triglycerides in lipid droplets within hepatocytes. The etiology of NAFLD consists of complex interactions that often stem from obesity-related insulin resistance resulting in systemic dysregulation of glucose and lipid metabolism. Specifically, sedentary lifestyles combined with diets high in carbohydrates and saturated fats induce adipocyte dysfunction, resulting in increased uptake of free fatty acids by the liver. Hepatic steatosis is further exacerbated by the upregulation of *de novo* lipogenesis, which occurs despite a parallel rise in insulin resistance (123). A subset of patients is also predisposed to developing steatosis due to mutations in a number of genes, many of which regulate lipid metabolism (124, 125). While simple steatosis is considered relatively benign, it can

progress to nonalcoholic steatohepatitis (NASH), which is marked by the infiltration of immune cells into the liver. NASH can lead to the development of hepatic diseases such as fibrosis, cirrhosis, and hepatocellular carcinoma, and is also associated with an increased risk of cardiovascular disease (126). At present, treatment of NAFLD is largely limited to diet and lifestyle modifications while the gold standard for diagnosis is an invasive liver biopsy. Continued investigation of the molecular events that regulate disease progression are thus necessary to identify novel targets for the diagnosis and treatment of NAFLD.

The exact triggers that propel steatosis to NASH are not known; increased levels of free fatty acids, oxidative damage, hepatocyte death, and altered gut permeability can all contribute to the activation of local immune responses. Sustained activation of immune responses stimulates production of profibrogenic factors by hepatic stellate cells, initiating a tissue repair response that can manifest as end-stage liver diseases if left unchecked. Indeed, the contribution of the immune response to NAFLD progression is critical as deficiency or inhibition of innate or adaptive immune cells in mice results in less severe or no disease (127, 128). Recent advancements in our understanding of the roles of specific immune cells in the pathogenesis of NAFLD have identified new avenues, including innate lymphoid cells (ILCs), which are discussed in further detail below.

Hepatic immune responses

The liver is a unique immunological site as it is continually exposed to highly immunogenic content draining from the gut. This quasi-mucosal nature of the liver

microenvironment requires homeostatic suppression of both immune cells resident in the liver and those in transit through the liver's sinusoids. The myeloid arm of liver-resident immune cells is enriched in macrophages and dendritic cells (DCs) that induce anergy in T lymphocytes, promote the generation of regulatory T cells (Tregs), or maintain hyporesponsive natural killer (NK) cells via secretion of immunosuppressive factors such as IL-10 (129, 130). The lymphocytic compartment is enriched in NK cells as they comprise ~30% of lymphocytes in the human liver (131). Although hepatic NK cells can produce lytic agents and cytokines, including granzyme B, IFN-γ, and TNF-α, they also contribute to maintaining immune tolerance via fratricide of activated T cells (132). Similarly, another innate lymphocyte population in the liver, the natural killer T (NKT) cells, can limit T cell responses by inducing the upregulation of the inhibitory molecules PD-L1 and PD-L2 on hepatic antigen presenting cells (133). Moreover, interactions with T cells are not limited to hematopoietic cells, as they can be primed, albeit inefficiently, by hepatocytes, liver sinusoidal endothelial cells, and hepatic stellate cells (134-136). Despite the multitude of mechanisms that dampen hepatic immunity, the liver retains the ability to stage robust immune responses upon inflammatory insult, such as injured hepatocytes in NASH, through recruitment of monocytes, granulocytes, and additional lymphocytes. Delineating the interplay among these populations will increase our understanding of the molecular switches that convert a quiescent immune environment into a cellular battlefield during chronic inflammatory diseases like NASH. Below, I describe the role of a newly described population of cells, the innate lymphoid cells (ILCs) in the pathogenesis of NASH. The contribution of cells of the myeloid lineage

(monocytes, macrophages, dendritic cells, and neutrophils) and other lymphocytic lineages (NK cells, NKT cells and T cells) is detailed in the appendix.

Innate lymphoid cells (ILCs)

Innate lymphoid cells (ILCs) are emerging as potent regulators of inflammation and metabolic disease. ILCs are classified into three groups that arise from the common lymphoid progenitor (Figure 1.6) (137). Group 1 ILCs include NK cells and ILC1s, which are analogous to Th1 cells in that they are regulated by the master transcription factor T-bet and produce IFN-γ in response to IL-12. Group 2 ILCs are governed by the transcription factor GATA3 and respond to IL-25, IL-33, and TSLP by producing Th2 cytokines, including IL-4, IL-5, and IL-13. Lastly, group 3 ILCs parallel Th17 cells by expression of RORγt, are activated by IL-1β and IL-23, and secrete IL-17 and IL-22, and in some cases, IFN-γ. Much like CD4 T cell subsets, there is some plasticity among ILC groups. For instance, one subtype of ILC3s, the natural cytotoxicity receptor $(NCR)^+$ ILC3, can upregulate T-bet to express IFN-γ (138). Similarly, recent studies demonstrated that IL-13^+ ILC2s can express IFN-γ or IL-17, resulting in hybrid IL-13^+IFN-γ^+ or IL-13^+IL-17^+ ILCs (139, 140). ILCs are thus as phenotypically and functionally complex as T cells and warrant further investigation in chronic inflammatory diseases like NASH. We recently reported that under homeostatic conditions, ILC1s comprise the majority of group 1 ILCs in murine livers (Krueger, et al. Manuscript under review). These liver-resident ILC1s maintain immune tolerance by limiting the influx of NK cells during viral infection. Whether ILC1s similarly attempt to curb inflammation

during NASH will be interesting to investigate and may uncover novel targets for limiting inflammatory injury in the liver.

Compelling evidence for a protective role of ILCs in metabolic disorders include the ability of ILC2s to promote the infiltration of eosinophils and alternatively activated macrophages into adipose tissue (141, 142). The influx of these cells into adipose tissue is necessary for limiting weight gain and insulin resistance. Remarkably, activation of ILC2s follows a circadian pattern and is stimulated by food intake (143). Consequently, it is not surprising that loss of TSLP expression, which also activates ILC2 responses, was associated with an increased incidence of hypertension in obese patients, reiterating the importance of this population in metabolic syndrome-associated conditions (144). Furthermore, ILC2s were shown to promote the beiging of white adipose tissue, thus conferring protection against the development of obesity (145, 146). These findings underscore a distinct function of ILC2s in maintaining metabolic homeostasis.

ILC3s may also protect against development of obesity and liver injury. For example, loss of lymphotoxin, which is produced by the lymphoid tissue inducer subset of group 3 ILCs, renders mice resistant to diet-induced obesity by promoting an overgrowth of segmented filamentous bacteria in the gut (147). Similarly, exogenous administration of IL-22, which is produced by both Th17 cells and ILC3s, was reported to induce a remarkable reversal of insulin resistance, weight gain, and bacterial dissemination to the liver in obese mice (148). Indeed, ILC3-derived IL-22 is essential in preventing systemic inflammation as it also restricts bacterial dissemination from lymphoid compartments (149). Additionally, as discussed above, IL-22 protects against fibrosis in the liver. These findings collectively suggest that ILC3 responses may play a

critical role in limiting the loss of epithelial integrity in the gut and expression of fibrogenic markers in the liver during NASH.

Rationale

Despite the differences in their etiology, hepatitis C and fatty liver disease are both chronic liver diseases that share two features: dysregulated hepatic lipid metabolism and inflammation. I aimed to investigate these characteristics by exploring two main questions that are either unanswered or poorly defined in the field: 1) with regards to HCV infection, what is the contribution of intracellular lipids as compared to extracellular lipids (Chapter 2), and 2) what, if any, is the role of mucosal-resident ILCs in restoring tissue homeostasis during NASH (Chapter 3). Given the increase in lipogenic programs in HCV infection, I hypothesize that intracellular or *de novo* synthesized lipids play a distinct role in the life cycle of HCV that is not redundant to the contributions of extracellular lipids. I also propose that the mucosa-like nature of the liver will invite ILC3 responses that act to maintain and/or restore tissue homeostasis in NASH. These questions might at first appear disparate. However, chronic inflammatory responses exacerbate metabolic disturbances, while chronic changes in metabolism lead to tissue damage, which in turn induces inflammation. Thus, although I investigate lipid metabolism and immune responses using two different disease models, the findings from one are likely to have implications not only for the other, but also to all chronic inflammatory diseases of the liver.

Table 1.1. Role of the liver in energy metabolism in fed and fasting states.

	FED STATE	FASTING STATE
Carbohydrates	▪ Oxidized to produce ATP ▪ Stored as glycogen ▪ Converted to fatty acids via *de novo* lipogenesis ▪ Diverted to nucleotide synthesis via pentose phosphate pathway	▪ Glycogenolysis releases glucose ▪ Gluconeogenesis
Lipids	▪ Stored as triglycerides, phospholipids, and cholesterol esters ▪ Secreted as lipoproteins for delivery to extrahepatic tissues	▪ Converted to ketone bodies via β-oxidation and ketogenesis
Amino acids	▪ Synthesized into proteins ▪ Converted to glucose, acetyl-CoA, or nucleic acids ▪ Oxidized to produce ATP	▪ Diverted to gluconeogenesis and ketogenesis

Figure 1.1. Overview of hepatic lipid metabolism.

Hepatic fatty acid pools are derived from three sources: 1) Lipids delivered in chylomicrons from the gut are repackaged into VLDL for distribution to extrahepatic sites such as muscle and adipose tissue, where LPL hydrolyzes fatty acids from TAGs. The resulting IDL can be taken up by the liver or further hydrolyzed to generate LDL that returns residual cholesterol to the liver. The liver also produces HDL that scavenges excess cholesterol from extrahepatic tissues for disposal by the liver. 2) Free fatty acids released from adipose tissue are activated and esterified upon entry into the hepatocyte. 3) *De novo* synthesis of fatty acids from glycolytic products is initiated by the carboxlyation of acetyl-CoA to produce malonyl-CoA, which is subsequently converted to the 16-carbon fatty acid, palmitate. Esterified fatty acids are stored in lipid droplets as TAGs.

VLDL, very low-density lipoprotein; LPL, lipoprotein lipase; TAG, triacylglycerol; IDL, intermediate-density lipoprotein; LDL, low-density lipoprotein; HDL, high-density lipoprotein; ACC, acetyl-CoA carboxylase; FAS, fatty acid synthase.

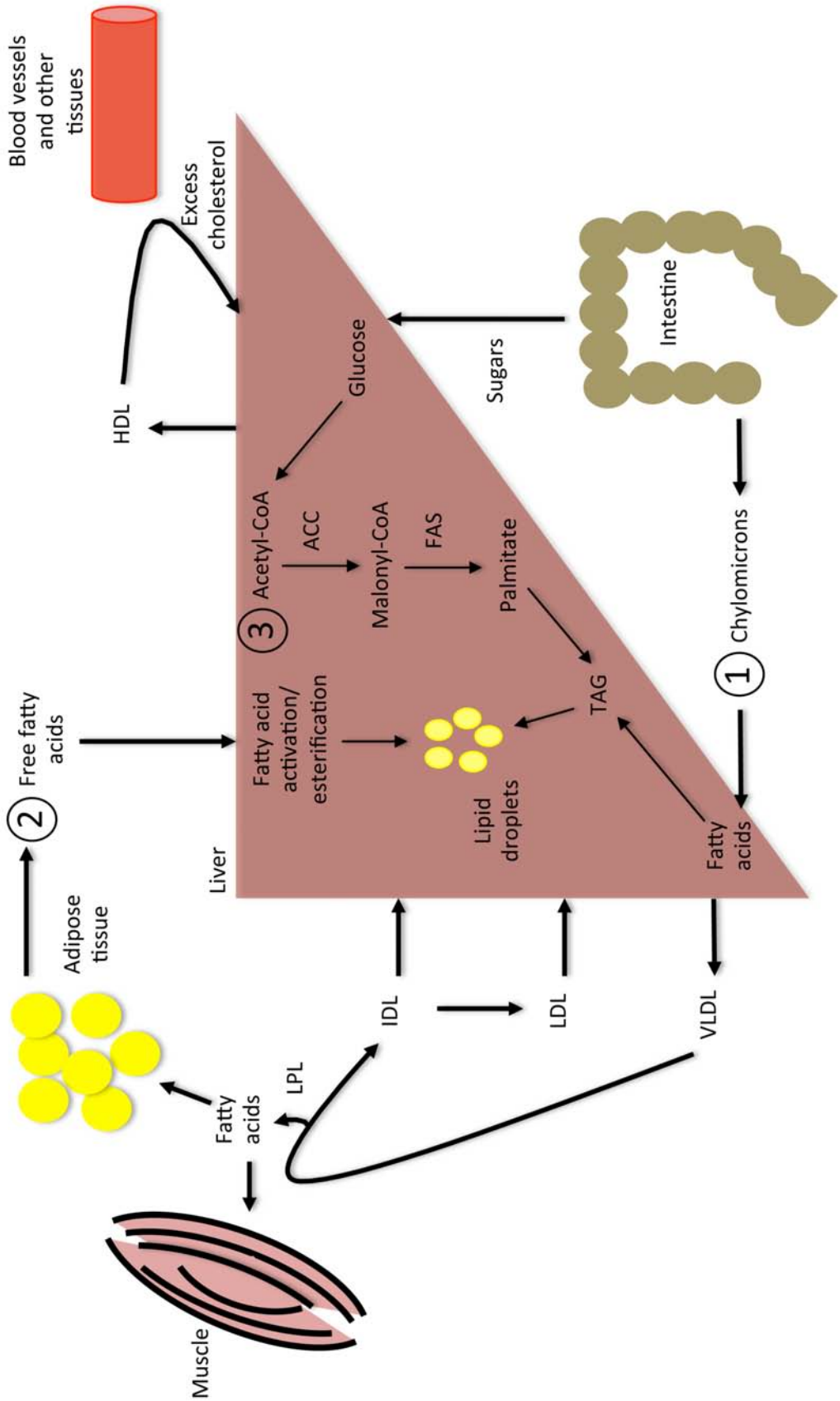
Blood vessels and other tissues
Excess cholesterol
HDL
Glucose
Sugars
Intestine
Acetyl-CoA
ACC
Malonyl-CoA
FAS
Palmitate
3
1
Chylomicrons
Free fatty acids
2
Fatty acid activation/ esterification
TAG
Lipid droplets
Liver
Fatty acids
Adipose tissue
IDL
LDL
VLDL
LPL
Fatty acids
Muscle

Figure 1.2. Uptake and processing of free fatty acids by hepatocytes.

Fatty acids are transported across the hepatocyte membrane via FATP and the scavenger receptor, CD36, expressed on the basolateral surface facing the liver sinusoids. Upon entry into the hepatocytes, fatty acids are bound by FABP and delivered to intracellular membranes such as the outer membranes of the ER and mitochondria, where they are activated by the addition of a –CoA group. Activated fatty acids can be bound by acyl-CoA binding proteins and trafficked to various sites to meet cellular demands.

FATP, fatty acid transport protein; FA, fatty acid; FABP, fatty acid binding protein; ACS, acyl-CoA synthetase; CoA, coenzyme A; FA-CoA, fatty acyl-CoA; Acyl-CoA BP, acyl-CoA binding protein.

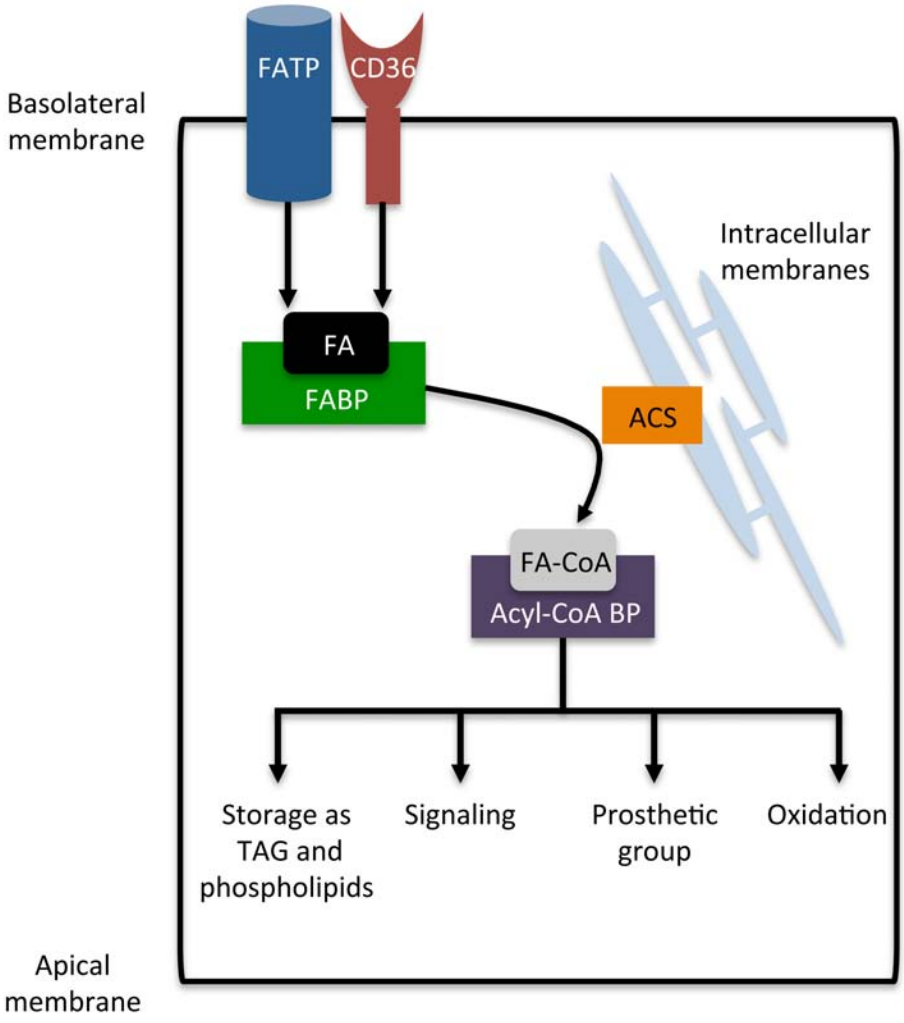
FATP
CD36
Basolateral membrane
Intracellular membranes
FA
FABP
ACS
FA-CoA
Acyl-CoA BP
Storage as TAG and phospholipids
Signaling
Prosthetic group
Oxidation
Apical membrane

Figure 1.3. *De novo* synthesis of fatty acids.

(A) Acetyl-CoA generated from pyruvate or citrate is carboxylated by ACC to form malonyl-CoA. Successive addition of malonyl-CoA to a growing acyl chain is catalyzed by FAS, using the reducing agent NADPH generated via the pentose phosphate pathway. The end product of *de novo* lipogenesis is palmitate, which can be converted to other fatty acids to generate a large repertoire of fatty acids varying in chain length and saturation. The majority of hepatic fatty acids are stored as TAG. The glycolytic intermediate G-3-P supplies the glycerol backbone for TAG synthesis. Solid arrows indicate direct conversion, while dotted arrows indicate conversion via intermediates. (B) Mechanism of action of ACC. Conversion of acetyl-CoA to malonyl-CoA proceeds via a two-step process. 1) Carboxylatin of biotin bound to the BCCP is driven by ATP hydrolysis and catalyzed by the BC domain. 2) The CT domain completes the reaction by transferring the carboxyl group from biotin to acetyl-CoA without using an additional source of energy.

G-6-P, glucose-6-phosphate; G-3-P, glyceraldehyde-3-phosphate; ACC, acetyl-CoA carboxylase; FAS, fatty acid synthase; TAG, triacylglycerol; NADPH, reduced nicotinamide adenine dinucleotide phosphate; ATP, adenosine triphosphate; BCCP, biotin carboxyl carrier protein; BC, biotin carboxylase; ADP, adenosine diphosphate; CT, carboxyltransferase.

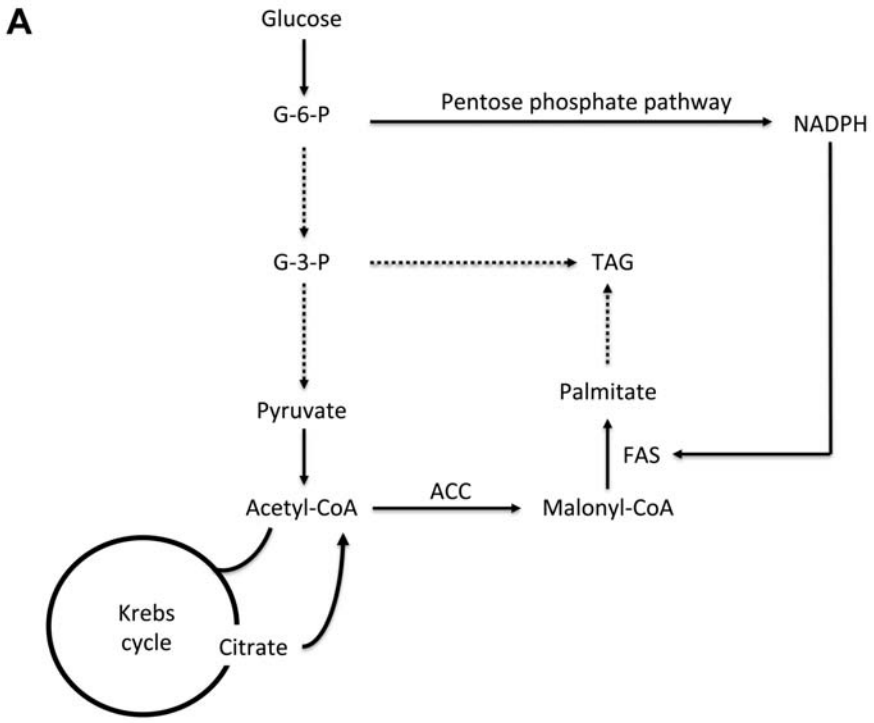

B

(1) HCO_3^- + Mg^{2+}-ATP + BCCP-Biotin ⟷ (BC) BCCP-Biotin-CO_2^- + Mg^{2+}-ADP + Pi

(2) BCCP-Biotin-CO_2 + Acetyl-CoA ⟷ (CT) BCCP-Biotin + Malonyl-CoA

Figure 1.4. Hepatitis C virus (HCV) genome and proteome.

HCV virions are comprised of structural proteins marked by white boxes. Non-structural proteins are indicated in grey boxes and function in genome replication, virion assembly, and modulation of host responses.

IRES, internal ribosomal entry site; RNA, ribonucleic acid.

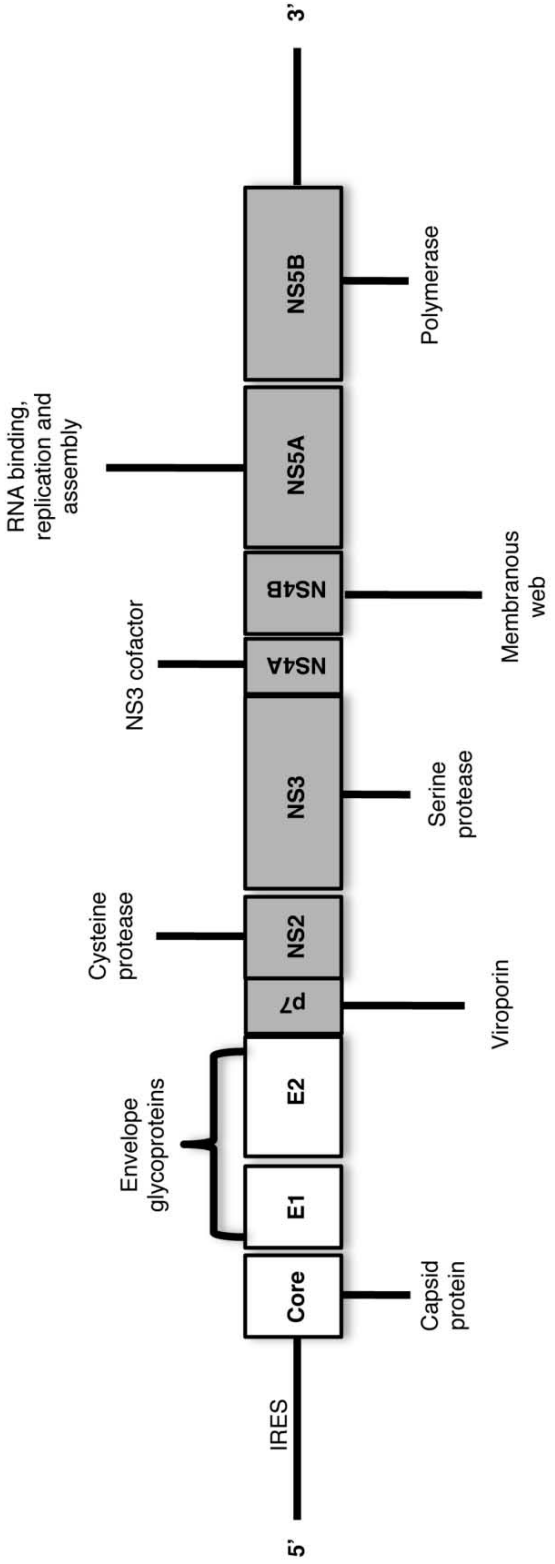
5'
IRES
Core
E1
E2
p7
NS2
NS3
NS4A
NS4B
NS5A
NS5B
3'
Capsid protein
Envelope glycoproteins
Cysteine protease
NS3 cofactor
RNA binding, replication and assembly
Serine protease
Viroporin
Membranous web
Polymerase

Figure 1.5. HCV life cycle.

HCV enters hepatocytes using a multitude of host receptors, including SRB1, CD81, CLDN1, and OCLN. Following endocytosis, the (+)-sense viral RNA is released into the cytoplasm and translated to synthesize viral proteins that replicate the RNA in specialized membrane structures on the ER. The newly synthesized viral RNA is assembled with the nucleocapsid protein that localizes to the surface of host lipid droplets. Addition of envelope glycoproteins and host-derived lipoproteins occurs as the virus moves through the secretory pathway in the Golgi. A proportion of virus is released as LVP, the most infectious form of HCV.

HCV, hepatitis C virus; SRB1, scavenger receptor B1; CD, cluster of differentiation; CLDN1, claudin-1; OCLN, occludin; LVP, lipoviroparticle.

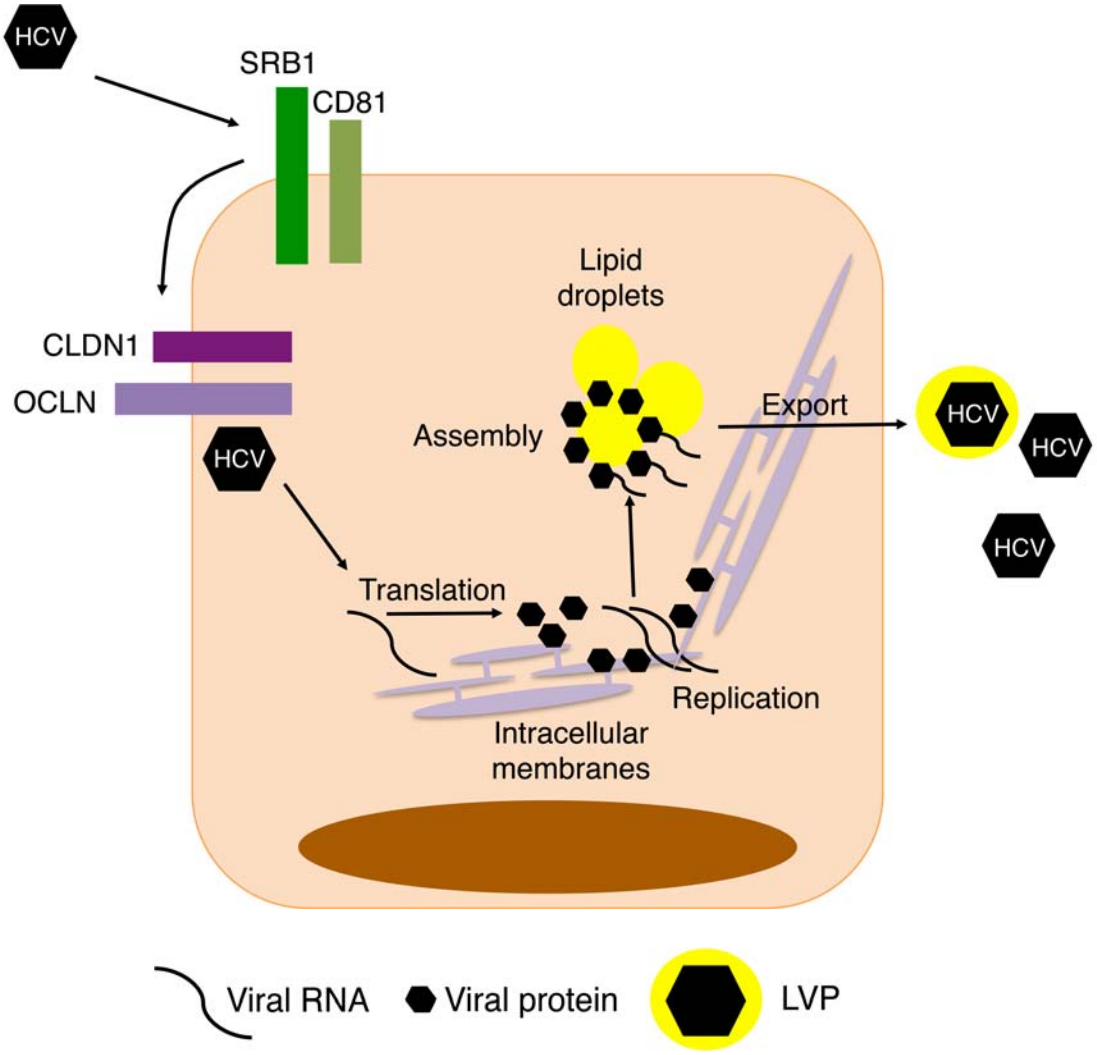
HCV
SRB1
CD81
CLDN1
OCLN
HCV
Lipid
droplets
Assembly
Export
HCV
HCV
HCV
Translation
Replication
Intracellular
membranes
Viral RNA
Viral protein
LVP

Figure 1.6. Diversity of human innate lymphoid cell (ILC) populations.

ILCs develop from a common lymphoid progenitor (CLP) that differentiates into a natural killer precursor (NKp) or a common helper innate lymphoid progenitor (CHILP). Subsequent differentiation of CHILP gives rise to ILC1s, ILC2s, and a variety of group 3 ILCs, which include natural cytotoxicity receptor (NCR) positive and negative ILC3s and lymphoid tissue induers (LTi). Intermediate precursors and additional transcription factors that contribute to ILC differentiation are not pictured. Figure adapted from Sonnenberg and Artis, *Nature Medicine* 2015 and Hazenberg and Spits, *Blood* 2014 (137, 150).

IL: interleukin; IFN, interferon; TNF, tumor necrosis factor; TSLP, thymic stromal lymphopoietin; CD, cluster of differentiation; T-bet, T-box expressed in T cells; ROR, retinoic acid receptor-related orphan receptor.

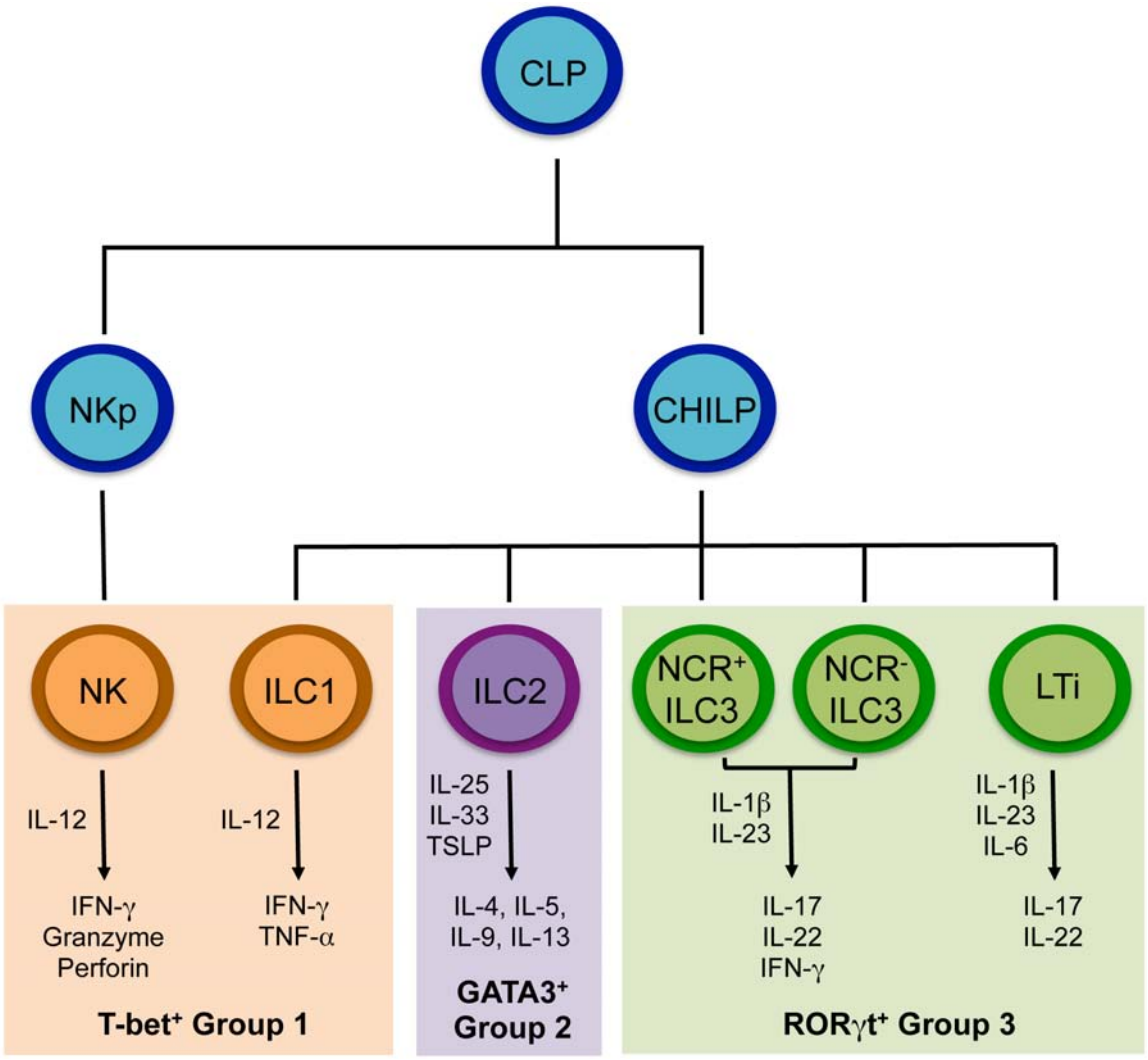
CLP
NKp
CHILP
NK
ILC1
ILC2
NCR+ ILC3
NCR- ILC3
LTi
IL-12
IL-12
IL-25
IL-33
TSLP
IL-1β
IL-23
IL-1β
IL-23
IL-6
IFN-γ
Granzyme
Perforin
IFN-γ
TNF-α
IL-4, IL-5,
IL-9, IL-13
IL-17
IL-22
IFN-γ
IL-17
IL-22
T-bet+ Group 1
GATA3+
Group 2
RORγt+ Group 3

CHAPTER 2: *De novo* lipogenesis in hepatitis C virus infection

Included in part in a "Distinct roles for intracellular and extracellular lipids in hepatitis C virus infection" (manuscript under review).

ABSTRACT

Hepatitis C is a chronic liver disease that contributes to progressive metabolic dysfunction. Infection of hepatocytes by hepatitis C virus (HCV) results in reprogramming of hepatic and serum lipids. However, the specific contribution of these distinct pools of lipids to HCV infection remains ill defined. In this study, we investigated the role of hepatic lipogenesis in HCV infection by targeting the rate-limiting step in this pathway, which is catalyzed by the acetyl-CoA carboxylase (ACC) enzymes. Using two structurally unrelated ACC inhibitors, we determined that blockade of lipogenesis resulted in reduced viral replication, assembly, and release. The effect of ACC inhibition on viral RNA levels was comparable to sofosbuvir, a viral polymerase inhibitor used in hepatitis C patients. Supplementing exogenous lipids to cells treated with ACC inhibitors rescued HCV assembly with no effect on viral replication and release. Intriguingly, loss of viral RNA was not recapitulated at the protein level and addition of 2-bromopalmitate, a competitive inhibitor of protein palmitoylation, mirrored the effects of ACC inhibitors on reduced viral RNA without a concurrent loss in protein expression. These correlative results suggest that newly synthesized lipids may have a role in protein palmitoylation during HCV infection wherein inefficient palmitoylation of viral and/or host proteins may limit their ability to function in HCV replication, thus leading to a loss in viral RNA and an accumulation of nonfunctional viral protein.

INTRODUCTION

The liver is the primary site of synthesis, storage, and oxidation of lipids and other macromolecules. As such, hepatic lipid metabolism is essential for the maintenance of systemic nutrient homeostasis. Dysregulation of hepatic lipid metabolism is a hallmark of several diseases including diabetes, alcoholic and non-alcoholic fatty liver disease, and parasitic and viral infections, including hepatitis C virus (HCV) infection (151-155). HCV infection is associated with the development of liver disease characterized by chronic hepatic inflammation leading to cirrhosis and hepatocellular carcinoma (156, 157). At present, as many as 2-3% of the world's population is infected with HCV, although the recent development of viral protease and polymerase inhibitors has made notable advancements in the treatment of the disease (158-161). However, many patients are precluded from receiving treatment due to comorbidities or infection with resistant genotypes of HCV (162). Thus, understanding the pathogenesis of HCV infection is essential for providing insights into the development of novel pan-genotypic therapeutic agents.

The life cycle of HCV relies on hepatic lipids, which results in metabolic disturbances. This manifests clinically as insulin resistance, dysregulated serum lipoproteins, and abnormal accumulation of intracellular lipids, i.e., steatosis (117, 163-168). These metabolic shifts are partly due to virus-induced increases in *de novo* lipogenesis (167, 169, 170). Despite the enhanced synthesis of lipids during HCV infection, *de novo* lipogenesis contributes to less than 5% of hepatic lipid stores, indicating that the bulk of lipids available to HCV may be derived from extracellular sources (171-174). Indeed, the lipoviroparticle, the most infectious form of HCV

consisting of virus packaged with triglyceride-rich lipoproteins, is enriched in viral RNA post-prandially when compared to fasting states (110, 111, 175, 176). These observations point to an intimate link between HCV and lipids; yet, the specific contributions of *de novo* synthesized lipids compared to those obtained from the extracellular environment have not been well elucidated in HCV infection or other viral diseases. Indeed, considering that changes in host lipid metabolism are characteristic of many positive-strand RNA viruses, understanding the contributions of *de novo* synthesized and exogenous lipids may have significant implications for the biology of formidable pathogens, such as encephalitic Togaviruses and Flaviviruses.

The acetyl-CoA carboxylase enzymes (ACC1 and ACC2) catalyze the rate-limiting step of *de novo* lipogenesis, in which acetyl-CoA is carboxylated to form malonyl-CoA. Malonyl-CoA is subsequently converted to palmitate, a 16-carbon saturated fatty acid. In addition to their role as the building blocks of most lipids, fatty acids also participate in numerous cellular processes, including post-translational modification of proteins. Covalent addition of palmitate to a cysteine residue on proteins, termed S-palmitoylation, regulates protein conformation, stability, function, trafficking to membranes, and interactions with other proteins (177-179). In addition to the indispensable role of protein palmitoylation in many cellular processes, it also has been reported to play a crucial role in regulating virion composition, infectivity, and evasion of host immune responses (180-182). In particular, palmitoylation of HCV core and NS4B was previously shown to influence the efficiency of viral assembly and replication (107, 108). Conversely, while palmitoylation of the host protein CD81 increases susceptibility to HCV, it also confers anti-viral activity to interferon-induced transmembrane proteins

(183, 184). Both exogenously derived and *de novo* synthesized lipids can be used to palmitoylate proteins; however, *de novo* lipogenesis is required for palmitoylation of specific host proteins (179). Therefore, the metabolic imbalances in *de novo* lipogenesis and extrahepatic lipids in HCV-infected patients may uniquely influence both the virus and the host through changes in protein palmitoylation.

Here, we investigated the respective roles of *de novo* lipogenesis and extracellular lipids in HCV infection using two non-competitive inhibitors of ACC enzymes, K1 and soraphen A. We found that blockade of *de novo* lipogenesis through ACC inhibition decreased HCV RNA by limiting viral replication, lipid droplets available for assembly, and viral export. Supplying ACC inhibitor-treated cells with exogenous fatty acids, the end products of *de novo* lipogenesis, selectively rescued lipid droplets, with no effect on viral replication and release; this suggests that solely repleting lipids is insufficient to overcome the effects of inhibiting *de novo* lipogenesis. Furthermore, inhibiting protein palmitoylation recapitulated the effects of ACC inhibition. These results suggest that intracellular and extracellular lipids contribute differentially to HCV infection.

MATERIALS AND METHODS

Virus, cells, and reagents.

The JFH-1 strain of HCV was kindly provided by Takaji Wakita (185). UV-inactivated virus was generated by exposing virus stocks to 2-3 minutes of UV light in a Stratalinker 3000 (Agilent Technologies). Huh7.5.1 cells were maintained in DMEM with 10% FBS, 100 U/mL penicillin/streptomycin, 2 mM L-glutamine, and 1% non-essential amino acids and infected with cell culture-derived JFH-1 at a multiplicity of

infection (MOI) of 0.1. Primary hepatocytes were obtained from Life Technologies and infected at an MOI of 0.5. Huh7.5 cells harboring the HCV subgenomic replicon (Huh7.5-SG), a gift from Charles Rice, were cultured in Huh7.5.1 media in the presence of 750 μg/mL of G418 (Invivogen) to maintain viral RNA (186). K1 and soraphen A (Figures 2.1.A and 2.1.B) were provided by Crop Solution, Inc. K1 was synthesized as described (187). Sofosbuvir, the NS5B polymerase inhibitor (PSI-7977), was purchased from MedChem Express. The inhibitor of palmitoylation, 2-bromopalmitate (2-BP), was obtained from Sigma-Aldrich.

Real-time PCR.

Cellular RNA was extracted using the GenElute Mammalian Total RNA Miniprep Kit (Sigma-Aldrich) or the RNAeasy Plus Mini Kit (Qiagen). Viral RNA in the supernatant was extracted using the QIAamp Viral RNA Mini Kit (Qiagen). As a loading control, RNA from the influenza virus strain A/PR/8/34 (kindly provided by Dr. Braciale) was added to all samples after extraction and before cDNA synthesis. Following reverse transcription with the High Capacity RNA-to-cDNA kit (Life Technologies), RT-PCR was run on the StepOnePlus Real-Time PCR System with Taqman RT-PCR assays (Life Technologies) for *ACTB* (Assay ID Hs99999903_m1), *HPRT1* (Assay ID Hs99999909_m1), HCV JFH-1 (Custom design; forward 5'-CCTTCACGGAGGCCATGA-3'; reverse 5'-ACAGGATGTTATTAGCTCCAG-GTCATA-3'; probe 5'-CCTCCTGGTGATCCC-3'; FAM reporter; MGB-NFQ quencher), and M gene of A/PR/8/34 (Custom design; forward 5'-GGACTGCAGCGTAGACGCTT-3'; reverse 5'-

CATCCTGTTGTATATGAGGCCCAT-3'; probe 5'-CTCAGTTATTCTGCTGGTGCACTTGCCA-3'; VIC reporter; TAMRA quencher) (188). Data are presented as relative fold increases in HCV RNA. *ACC1* and *ACC2* mRNA were detected using SYBR green dye (Life Technologies) using the primers *ACC1* forward, 5'- ATCCCGTACCTTCTTCTACTG-3' and reverse, 5'-CCCAAACATAAGCCTTCACTG-3', and *ACC2* forward, 5'-CGGATGCGTAACTTCGATCTG-3' and reverse, 5'-CTATGGTCCGTCACTTCCACAC-3'.

Crystal violet assay.

Huh7.5.1 cells were grown in 96-well plates at 20,000 cells/well. At the time of assessment, culture supernatants were aspirated and cells were treated with crystal violet solution (0.5% crystal violet in 50% methanol/water) for 20 minutes. The stain was solubilized with 1% SDS for 3 hours. Absorbance was read at 570 nm on a PowerWave XS spectrophotometer (BioTek).

MTT assay.

Uninfected and infected Huh7.5.1 were grown in 96-well plates at 20,000 cells/well. At three hours before reading the absorbance, the cells were incubated at 37ºC with 20 μL/well of 5 mg/mL of MTT (3-(4,5-dimethylthizaol-2-yl)-2,5-diphenyltetrazolium bromide). Precipitates were solubilized in isopropanol containing 4 mM HCl and 0.1% NP-40. Absorbance was read at 570 nm on a BioTek PowerWave XS.

Intracellular ATP quantification.

Uninfected and infected Huh7.5.1 were grown in 96-well plates at 20,000 cells/well.. Intracellular ATP content was quantified using the CellTiter-Glo® Luminescent Cell Viability Assay (Promega) according to the manufacturer's instructions.

siRNA and plasmid transfections.

siRNA pools against ACC1, ACC2, or a negative control were purchased from Dharmacon and transfected with DharmaFECT 4 Transfection reagent. pFR_HCV_xb plasmid, a gift from Phil Sharp (Addgene plasmid #11510), was transfected using Lipofectamine 2000 (Invitrogen) (189). pSGR_JFH1/GND_Fluc was a gift from Zhensheng Zhang and Jake Liang and was transfected using calcium phosphate (Invitrogen). Luciferase activity for translation assays were determined using the Dual-Luciferase® Reporter Assay System (Promega) and quantified on a GloMax®-Multi Detection System (Promega).

Mass spectrometry.

Cultured cells were trypsinized, centrifuged at 400 × g for 5 minutes at 4ºC, and resuspended in PBS. 50 μL of cell lysate was added to 1 mL acidified methanol (0.1 N HCl) containing internal standard cocktails for sphingolipids (containing 0.5 nmol each: C_{17}-ceramide, C_{12}-glucosylceramide, C_8-dihydroceramide, and C_{12}-sphingomyelin) and glycerolipids (0.1 nmol each of C_{15}-diacylglycerol and C_{17}-lysophosphatidic acid). Sphingolipids, glycerolipids, and phospholipids were extracted and measured via liquid chromatography-tandem mass spectrometry (LC/MS/MS) as previously described with

slight modifications for the measurement of phospholipids (190). Phosphatidic acids, lysophosphatidic acids, and phosphatidyl-serines were analyzed in negative mode after separation in a Discovery (Supelco) C18 column (50 mm × 2.1 mm, 5 μm bead size). Mobile phase A consisted of 60% acetonitrile, 40% H_2O, 0.1% formic acid, and 1 mM ammonium acetate. Mobile phase B consisted of 90% isopropyl alcohol, 10% acetonitrile, 0.1% formic acid, and 1 mM ammonium formate. Chromatography was run for a total of 10 min using the following gradient: 1 minute 100% solvent A; a linear gradient to 100% solvent B over 6 min; 2 min 100% solvent B; 1 min 100% solvent A. Total flow was 0.6 ml/min. Total values were normalized to protein concentration. Significance in fold change was determined by Student's *t* test ($p<0.05$) and further corrected by a false discovery rate adjustment ($p<0.1$).

Immunoblot analysis.

Cells were lysed in radioimmunoprecipitation assay (RIPA) lysis buffer, suspended in Laemmli buffer, resolved on a 4-15% Mini-PROTEAN® TGX gel (Biorad) or a 6% polyacrylamide gel (for detecting ACC), and blotted on a PVDF membrane with antibodies for ACC1 (Millipore), ACC2 (Cell Signaling), HCV core (Anogen), NS3 (Abcam), LDLR (Cayman Chemical), SRB1 (GeneTex), the ER stress makers, BiP, calnexin, IRE1α, PDI, and PERK (all from Cell Signaling Technology) and vinculin (Cell Signaling Technology).

HCV titration.

Virus stocks generated from culture supernatants of Huh7.5.1 cells following 6-8 days of infection were centrifuged to remove debris. HCV titer was determined by infecting Huh7.5.1 cells in Lab-Tek® chamber slides at various dilutions for 3 days, after which the cells were fixed in 4% paraformaldehyde/PBS. Cells were blocked in 0.3% Triton-X/5% goat serum, stained using mouse anti-HCV core antigen antibody (Thermo Scientific) and highly cross-adsorbed APC goat-anti-mouse IgG (Life Technologies), and mounted in ProLong® Gold Antifade Mountant with DAPI (Life Technologies). Images were captured on Zeiss LSM 710 Multiphoton microscope and the number of focus forming units was calculated from at least 10 fields in each experiment.

Confocal microscopy.

Cells were stained as described under "HCV titration." For assembly studies, bodipy (Life Technologies) was added along with the secondary antibody. Adjustments to brightness and contrast made in Adobe Photoshop CS were kept to a minimum and applied to all images from a given experiment. The number of pixels was quantified over 10 fields/condition in each experiment using ImageJ. In brief, each image was split into individual channels. Thresholds for each channel were kept constant within each experiment. The "measure" function was used to quantify the number of pixels in each channel. To calculate the percentage of red pixels that co-localized with green pixels, both channels were inverted, after which a selection was created for red pixels and pasted onto the green channel using the "ROI (region of interest) manager" tool.

Addition of exogenous fatty acids.

Sodium salts of palmitate, oleate, and linoleate were purchased from Sigma-Aldrich and mixed in methanol in a 1:2:1 ratio (191). The methanol was removed using nitrogen and the fatty acid mixture was reconstituted in culture media containing 0.25% fatty acid free BSA (Sigma-Aldrich) to a final concentration of 25 μM palmitate, 50 μM oleate, and 25 μM linoleate.

Electron microscopy.

Cell cultures were fixed in 4% paraformaldehyde/2.5% glutaraldehyde in PBS, post-fixed with 1% osmium tetroxide and potassium ferricyanide, dehydrated in ethanol, and embedded in Epon 812. Sections were cut on a Leica Ultracut UCT at a thickness of 60-80 nm and placed on 200 mesh copper grids for viewing in a JEOL 1010 transmission electron microscope. Images were obtained with a Hamamatsu ORCA-HR.

Protein aggregate staining.

Huh7.5.1 cells were grown in Lab-Tek® chamber slides. Protein aggregates were stained using the ProteoStat® Aggresome detection kit (Enzo Life Sciences) as per the manufacturer's instructions. Images were captured on Zeiss LSM 710 Multiphoton microscope with 5-10 fields for each condition per experiment.

Statistical analysis.

Results are the mean ± SEM. Statistical significance was determined by an unpaired *t* test, one-way analysis of variance (ANOVA) with Tukey's post-test, or two-

way ANOVA with Bonferroni post-test. Statistical analyses were performed using Prism GraphPad software v4.0c. ns: not significant, *$p<0.05$, **$p<0.01$, ***$p<0.001$.

RESULTS

ACC inhibition decreases intracellular HCV RNA.

De novo lipogenesis, the process of generating fatty acids from acetyl-CoA, is upregulated upon expression of HCV proteins (169, 192, 193); however, the specific contribution of enhanced *de novo* lipogenesis to HCV infection is not well defined. The enzymes ACC1 and ACC2 catalyze the rate-limiting step of *de novo* lipogenesis and represent a potential pharmacological target for delineating the function of *de novo* synthesized lipids in HCV infection. Utilizing a well-established *in vitro* model of HCV infection, i. e., the human hepatocyte cell line Huh7.5.1 infected with the JFH-1 strain of HCV, we treated hepatocytes at D1 post-infection with two non-competitive ACC inhibitors, K1 or soraphen A, or vehicle control (DMSO) (Figures 2.2.A, and 2.2.B) (194). While intracellular HCV RNA was notably decreased in K1 and soraphen A-treated cells compared to vehicle-treated cells beginning at D2 post-treatment (PT), this decrease was most prominent at D3 PT, and was maintained through D5 PT (Figure 2.2.B). Notably, there were no additive or synergistic effects of K1 and soraphen A on intracellular HCV RNA (Figure 2.2C). The effect on viral RNA was dose-dependent for both K1 and soraphen A, and began to plateau at doses of 1 μM K1 and 100 nM soraphen A (Figures 2.2.D and 2.2.E). All subsequent experiments were therefore conducted at D3 PT with 1 μM K1 and 100 nM soraphen A.

Next, we verified that the anti-viral effects of ACC inhibition were not limited to the Huh7.5.1 cell line. Addition of K1 or soraphen A to HCV-infected primary human hepatocytes reduced viral RNA to levels comparable to sofosbuvir, an NS5B polymerase inhibitor used in HCV patients (Figure 2.2.F). We also confirmed that the effect on viral RNA was due to specific inhibition of ACC through transient knockdown of the two ACC isoforms—ACC1 and ACC2. Viral RNA was decreased even with a partial loss of ACC1 or ACC2, verifying that inhibition of *de novo* lipogenesis leads to a loss in intracellular HCV RNA (Figures 2.2.G and 2.2.H). However, gene expression of ACC1 appeared to slightly increase upon treatment with K1 and soraphen A, while expression of ACC2 mRNA was reduced (Figures 2.2.I and 2.2.J). These findings indicate that despite differential effects on the two isoforms of ACC, the loss in intracellular viral RNA upon K1 and soraphen A treatment was likely due to the inhibition of both ACC1 and ACC2.

Importantly, inhibition of *de novo* lipogenesis did not significantly affect the viability of uninfected or infected cells, as total DNA content, redox capacity, and ATP production were similar among all treatment groups (Figure 2.3). These results indicate that inhibition of *de novo* lipogenesis via K1 and soraphen A treatment significantly decreases intracellular HCV RNA, without compromising hepatocyte viability.

ACC inhibition limits HCV replication, lipid droplets required for viral assembly, and virion production.

The decrease in HCV RNA observed upon ACC inhibition may reflect changes in one or more steps of the HCV life cycle. Therefore, we sought to identify the effects of

ACC inhibition on multiple steps of the HCV life cycle, namely entry, replication, translation, assembly, and release of infectious virions. We first examined the effects of K1 and soraphen A on viral entry. Negative-strand HCV RNA, which is an RNA intermediate during viral replication, appears within five hours of infection *in vitro* (76). In order to exclude any replicated viral RNA intermediates in our analysis, we measured the genomic viral RNA in K1 and soraphen A-treated Huh7.5.1 cells infected with HCV for one hour. Untreated HepG2 cells, which do not express CD81 and are thus less permissive to infection with JFH-1, were used as a negative control. Cells treated with either K1 or soraphen A had equivalent, if not increased, intracellular viral RNA compared to vehicle-treated cells (Figure 2.4.A), suggesting that a defect in viral entry was not contributing to the loss in intracellular HCV RNA following inhibition of *de novo* lipogenesis. Furthermore, ACC inhibition did not affect the expression of select HCV entry receptors, including LDLR and SRB1 (Figure 2.4.B).

We next evaluated the effect of ACC inhibition on viral replication using Huh7.5-SG cells, which harbor an HCV subgenomic replicon lacking structural proteins. These cells do not produce intact virus capable of initiating secondary infections, yet provide an ideal model to study the impact of inhibiting *de novo* lipogenesis on HCV replication. Similar to treatment of Huh7.5.1 cells infected with infectious virus, addition of either K1 or soraphen A significantly reduced viral RNA (Figure 2.4.C). These findings were further supported by a similar loss in viral RNA in cells treated with the polymerase inhibitor, sofosbuvir. *De novo* lipogenesis thus plays a critical role in viral RNA synthesis.

Given that the inhibition of *de novo* lipogenesis decreased replication of viral RNA, we expected to see a similar loss in viral proteins. Surprisingly, the amounts of HCV core and NS3 proteins were comparable between DMSO, K1, and soraphen A-treated cells (Figure 2.4.D). To address if the mismatch in viral RNA and protein was due to an increase in translation, we transfected cells with a bicistronic construct expressing renilla luciferase under the control of the HCV internal ribosome entry site (IRES) (189). Firefly luciferase activity is thus an indicator of transfection efficiency while renilla luciferase activity is a measure of translation directed by the HCV IRES. As seen in Figure 2.4.E, both firefly and renilla luciferase activities were also comparable among all three treatment groups. Luciferase activity was also unaffected by ACC inhibition in Huh7.5.1 cells transfected with a replication deficient subgenomic replicon, which allows the study of HCV translation in the absence of replication (Figure 2.4.F). These results suggest that the discrepancy between viral RNA and viral protein levels resulting from the inhibition of ACC was not due to enhanced translation through the HCV IRES.

We next evaluated subsequent steps of the viral life cycle. To this end, we tested the effect of ACC inhibitors on viral assembly. HCV assembly requires the co-localization of the HCV core protein with lipid droplets (90, 195, 196). As expected, DMSO-treated cells had an abundance of core protein that co-localized with lipid droplets (Figures 2.5.A-C). In contrast, K1 and soraphen A-treated cells displayed a marked loss of lipid droplets, yet retained expression of HCV core as demonstrated in the immunoblots of total lysates (Figures 2.4.2D and 2.5.A-C). The prerequisite for viral assembly, namely, the colocalization of HCV core and lipid droplets, thus appeared to be compromised in cells with reduced ACC activity. These findings indicate that *de novo*

lipogenesis plays a critical role in propagating HCV in part by supplying the scaffold for viral assembly.

Lastly, we assessed viral titer in the supernatants of cells treated with ACC inhibitors and found that the infectious titer was reduced in K1 and soraphen A-treated cells when compared to the vehicle controls (Figure 2.5.D). The decrease in intracellular RNA was matched by the loss in viral RNA in the supernatant (Figure 2.5.E). Collectively, these results demonstrate that ACC inhibition affects multiple steps of the HCV life cycle, specifically replication, assembly, and production of infectious virions.

ACC inhibition changes the hepatocyte lipidome.

Given the loss of lipid droplets in K1 and soraphen A-treated cells, we sought to identify changes in the lipidome that may be contributing to the loss of viral replication, assembly, and virion production. We used liquid chromatography tandem mass spectrometry (LC-ESI-MS/MS) to measure different lipid species in uninfected and infected hepatocytes treated with DMSO, K1, or soraphen A. Because HCV upregulates lipogenesis, it was not unexpected that several classes of lipids were increased upon infection (Figure 2.6.A-J). Importantly, the majority of lipids measured were decreased upon inhibition of ACC in both uninfected and infected hepatocytes (Figure 2.7, Appendix tables 1 and 2). In particular, phosphatidic acid, phosphatidylcholine, diacylglycerol, and ceramide species were decreased significantly in both K1 and soraphen A treated cells (based on $p<0.05$ in Appendix tables 1 and 2). Of these, the glycerophospholipids, i. e., phosphatidic acid, phosphatidylcholine, and diacylglycerol were significantly increased with infection but were returned to levels comparable to

uninfected cells upon K1 and soraphen A treatment (Figures 2.6.B, 2.6.D, and 2.6.E). These lipids are key players in maintenance of cellular membranes. Consequently, their loss upon treatment with K1 and soraphen A may be indicative of changes in the quality of intracellular membranes that facilitate viral replication.

Exogenous fatty acids restore lipid droplets but fail to rescue viral replication and virion production.

The end product of *de novo* lipogenesis is palmitate, a 16-carbon saturated fatty acid, which can then be modified to generate a diverse repertoire of lipids. Given that inhibition of *de novo* lipogenesis decreases HCV replication, cellular lipid droplets, and infectious titer, we tested whether supplementing fatty acids would rescue these defects. We added a mixture of saturated and unsaturated fatty acids including palmitate, oleate, and linoleate, at concentrations found in blood, to cells treated with ACC inhibitors (191). Notably, cells were treated with ACC inhibitors in media containing serum; as such, the addition of these fatty acids is in excess of fatty acids in the serum. Supplementing with the fatty acid mixture restored lipid droplets in K1 and soraphen A-treated cells (Figures 2.8.A, 2.8.B, and 2.8.D). Importantly, the lipid droplets co-localized with HCV core, indicating that extracellular sources of fatty acids contribute to lipid droplet formation even in the absence of *de novo* lipogenesis (Figures 2.8.A-E). However, supplementation with fatty acids did not restore intracellular or extracellular HCV RNA and did not affect the infectious virions released in culture supernatants HCV (Figures 2.8.F-H). These results indicate that viral replication is a limiting factor for the production of infectious virus. Alternatively, changes in the export of lipids through lipoproteins may also be

compromised upon ACC inhibition. Consequently, decreased export of lipids and lipid-containing viral particles may also underlie the loss in viral titer and extracellular viral RNA. Collectively, these results support the hypothesis that while *de novo* lipogenesis is necessary for viral replication and perhaps viral export, exogenous sources of lipids can supply triglycerides for the formation of lipid droplets that contribute to HCV assembly.

Changes in ER stress response and replication complex formation do not explain the link between *de novo* lipogenesis and HCV replication.

Significant changes in hepatocyte lipid metabolism activate the endoplasmic reticular (ER) stress response. The ER stress response, also known as the unfolded protein response, alleviates the translational burden in the ER by inhibiting protein translation, inducing transcription of chaperones that aid in protein folding or genes that aid in ER-associated degradation of proteins, and upregulating lipogenesis to facilitate expansion of the ER (197). Importantly, expression of HCV proteins upregulates ER stress markers, which in turn facilitate viral replication via induction of autophagy (198-203). We therefore assessed whether the ER stress response was altered by treatment of infected hepatocytes with ACC inhibitors. As seen in Figure 2.9, there were no significant changes in ER stress markers upon K1 or soraphen A treatment. Although phosphorylated forms of PERK and IRE1α are more sensitive measures of activation of the ER stress response, the lack of notable changes in the expression levels of the chaperones BiP, phosphate disulfide isomerase (PDI), and calnexin, verifies that differences in ER stress were not contributing to the loss in viral RNA upon inhibiting *de novo* lipogenesis in HCV-infected hepatocytes.

A recent study reported that soraphen A inhibits HCV replication by reducing the number and size of double-membraned vesicles where HCV replication complexes are thought to reside (204). To compare our results with these findings, we used electron microscopy to study ultrastructural features of hepatocytes treated with ACC inhibitors. Lipid droplets were completely absent in K1 and soraphen A-treated cells, confirming the results obtained by fluorescent microscopy (Figures 2.5.A-C and 2.10.A). More importantly, double-membraned vesicles were present in cells treated with DMSO and ACC inhibitors, indicating that replication complexes were not absent upon inhibition of *de novo* lipogenesis (Figure 2.10.B). In contrast to the study mentioned above, we did not evaluate the number and size of these vesicles; therefore, quantitative and qualitative differences in replication complexes may be contributing to the loss of viral RNA in K1 and soraphen A-treated cells.

Inhibiting protein palmitoylation mimics effects of ACC inhibition.

Fatty acids are essential for several cellular functions including post-translational modification of proteins by palmitoylation. Palmitoylation of HCV core and NS4B was previously shown to be required for optimal production of virions and formation of the HCV replication complex, respectively (107, 108). We therefore investigated whether inhibiting protein palmitoylation during HCV infection would produce results similar to inhibition of *de novo* lipogenesis. To test this hypothesis, HCV-infected cells were treated with 2-bromopalmitate (2-BP), a competitive inhibitor of palmitoyl acyltransferases. Our results demonstrate that addition of 2-BP to HCV-infected hepatocytes decreased viral RNA with minimal loss in viral protein, recapitulating the effects of ACC inhibitors

(Figures 2.11.A and 2.11.B). Depalmitoylation of proteins is known to alter their cellular membrane localization, function, and aggregate formation (205, 206). Previous studies had demonstrated that palmitoylation of HCV core regulated trafficking to ER membranes, while palmitoylation of NS4B was necessary for its interaction with other viral proteins (107, 108). In addition to these well-established functions of palmitoylation in HCV infection, our study investigated the function of this process in protein aggregate formation. As seen in Figure 2.11.C, protein aggregates were increased in cells treated with K1, soraphen A, or 2-BP compared to those treated with DMSO. Cells treated with a proteasome inhibitor served as the positive control. These results may be indicative of mislocalization of viral proteins, essential host factors, or both. In fact, as the requirement for palmitoylation of NS4B in HCV replication was recently challenged, our results may be more suggestive of defects in palmitoylation of host proteins (109). Nonetheless, although the similarities with 2-BP treatment are correlative and do not definitely prove a role for ACC inhibitors in regulating protein palmitoylation, they offer the possibility that *de novo* lipogenesis may facilitate palmitoylation of proteins necessary for optimal replication of HCV.

DISCUSSION

The link between lipid metabolism and HCV is a well-defined relationship that is thought to partly dictate the tropism of the virus to the liver (96, 207). HCV-induced upregulation of *de novo* lipogenesis contributes to viral replication, assembly, and packaging for export through biogenesis of membranes, lipid droplets, and lipoproteins. In this report, we define an additional role for *de novo* lipogenesis in HCV infection

where the specific inhibition of ACC activity, which catalyzes the rate-limiting step of *de novo* lipogenesis, decreases viral RNA replication without a concurrent loss in viral protein levels. Importantly, inhibition of protein palmitoylation in the infected host mirrored the effects of inhibiting the ACC enzymes, suggesting a potential role for ACC inhibitors in altering HCV replication through palmitoylation. Moreover, ACC inhibition resulted in a notable reduction in lipid droplets, which were restored by the addition of exogenous fatty acids. Collectively, our results posit distinct roles for *de novo* synthesized and extracellular lipids in HCV infection: *de novo* lipogenesis facilitates viral RNA replication potentially through palmitoylation of host and viral proteins, while exogenous lipids are trafficked to lipid droplets that act as scaffolds for viral assembly (Figure 2.12).

To dissect the roles of intracellular and extracellular pools of lipids in HCV infection, we used K1 and soraphen A, two non-competitive inhibitors of ACC, the enzyme that catalyzes the rate-limiting step of *de novo* lipogenesis. ACC is a large multi-domain enzyme that exists in two isoforms, ACC1 and ACC2, both of which are expressed in the liver (208). ACC1 is localized to the cytosol where it functions in carboxylating acetyl-CoA to malonyl-CoA for nascent fatty acid synthesis. ACC2 is targeted to the mitochondria where it inhibits β-oxidation of fatty acids. Although ACC1 is thought to be responsible for the bulk of fatty acid synthesis, previous studies have demonstrated that ACC2 can also function in *de novo* lipogenesis (209). It is likely for this reason that even partial inhibition of either ACC isoform resulted in a loss in viral RNA.

Our finding that inhibition of ACC decreases viral replication corroborates previous studies demonstrating that lipogenesis is essential for HCV replication. Specifically, previous reports identify a role for fatty acids in the formation of the membranous web, which is the site of HCV replication (204, 210, 211). Our findings do not exclude this possibility as lipidomic analysis revealed a significant loss in lipids in cells treated with K1 or soraphen A for 3 days (Figures 2.6 and 2.7 and Appendix tables 1 and 2). Surprisingly, treatment with K1 resulted in a loss of sphingomyelins in contrast to the slight increase in these lipids upon soraphen A treatment. In addition, K1 treatment produced a more pronounced loss in ceramides and glucosylceramides, with little to no effect on dihydroceramides, when compared to the effects of soraphen A. We cannot discount the possibility that these differences are due to off-target effects of the drug, which may also be contributing to the effect on HCV. Nevertheless, the concerted loss of other classes of lipids in both K1 and soraphen A-treated cells suggests that specific inhibition of ACC may be a common mechanism by which these inhibitors impact HCV infection. For example, the loss of diacylglycerols substantiated the absence of lipid droplets upon ACC inhibition, since diacylglycerols are the precursor to triacylglycerols, the predominant lipid found in lipid droplets. Notably, the striking loss of phosphatidic acids and phosphatidylcholines indicated potential changes to cellular membranes, as both classes of lipids are major membrane components (212). Therefore, in keeping with previous studies, altered cellular membranes are thus likely contributing to the loss in viral RNA seen upon inhibition of *de novo* lipogenesis (204). In addition, viral RNA in membranous webs has a longer half-life than its cytosolic counterpart (76), providing a potential explanation for the loss in viral RNA in K1 and soraphen A-treated cells.

Our findings also suggest that HCV assembly may be compromised in K1 and soraphen A-treated cells as lipid droplets were notably lost upon ACC inhibition. Historically, the association of HCV core with the surface of lipid droplets was thought to facilitate viral assembly as disrupting this association significantly reduced virus production (90, 195). In recent years, this view has been challenged by reports of the ER being the more critical site for HCV assembly (213, 214). It is therefore possible that the loss of lipid droplets in K1 and soraphen A-treated cells does not necessarily indicate a defect in viral assembly as core could contribute to assembly at the ER instead. However, these reports delineating the role of the ER in HCV assembly employed genomes of HCV isolates other than JFH-1 or assessed JFH-1 after an extended period of culture (213, 214). Our results may thus represent the impact of ACC inhibitors on HCV assembly exclusively in JFH-1 isolates early in infection. Future investigations that evaluate the effect of ACC inhibitors on other HCV genotypes may help identify a more universal function of *de novo* lipogenesis in HCV assembly.

Nonetheless, to our knowledge, this study is the one of the few reports in which viral protein does not parallel viral RNA in HCV infection. Differences in experimental systems could explain this discrepancy as previous studies investigating the role of *de novo* lipogenesis targeted pathways downstream of ACC, employed transfected HCV replicons or chimeric viruses, or infected cells with cell-culture derived HCV for longer than 24 hours before adding lipid-depleting agents (204, 210, 211, 215-217). In contrast, our studies were performed by inhibiting *de novo* lipogenesis at 24-hours post-infection with cell-culture derived HCV. As HCV RNA is exponentially increased early in infection and begins to plateau at 30-72 hours post-infection (76), the time at which

inhibition of *de novo* lipogenesis is initiated may be important. Therefore, the discrepancy in viral RNA and protein levels may reflect the early impact of *de novo* lipogenesis in HCV infection, which is compounded over time with changes in membrane lipids, and distinct from the contributions of exogenous lipids.

In particular, protein palmitoylation may be one of the events dependent on *de novo* lipogenesis early in infection. More specifically, palmitoylation of host or viral proteins necessary for HCV replication may be temporally or spatially coupled to *de novo* lipogenesis, such that the target proteins would not be palmitoylated upon the addition of ACC inhibitors. As a result, these host or viral factors would not be able to participate in viral replication, yet would continue to be translated from input viral RNA and the low levels of replicated RNA. The fates of these depalmitoylated proteins could be explained by the increased incidence of protein aggregates upon treatment of HCV-infected hepatocytes with ACC inhibitors or 2-bromopalmitate. Indeed, previous studies have established that loss of palmitoylation does not necessarily target the protein for degradation; instead, depalmitoylated proteins accumulate as stable aggregates (177, 218, 219). The diversion of proteins to these aggregates may be one explanation for the accumulation of viral protein in cells treated with ACC inhibitors. These data thus raise the possibility that inhibition of *de novo* lipogenesis results in redirection of depalmitoylated host and, potentially, viral proteins to aggregates where they cannot function in replicating the viral genome. However, addition of a mixture of exogenous fatty acids restored lipid droplets without rescuing viral replication or infectious titer. We therefore hypothesize that palmitoylation of proteins that participate in HCV replication may require *de novo* lipogenesis and be independent of exogenously derived lipids.

Alternatively, ACC inhibition could result in the deliberate diversion of exogenously derived fatty acids, or fatty acids liberated from intracellular sources, away from proteins that require palmitoylation. This phenomenon of actively directing fatty acids toward various metabolic fates is known as channeling (220). It is intriguing to speculate that inhibition of *de novo* lipogenesis during viral infection forces the cell to channel the limited supply of fatty acids towards alternative fates. Such tactics may help combat invasion by the virus by sequestering metabolites essential for viral propagation. These findings may be particularly relevant to infections with HCV genotype 3, which is characterized by extensive steatosis that corresponds to the course of infection (118, 221). Selective depletion of hepatic lipids in genotype 3 infections may be a promising alternative to direct acting anti-viral agents, especially since these treatments are ineffective against this genotype (121, 158). Moreover, as steatosis can initiate and exacerbate chronic hepatic inflammation, hypolipidemic agents like the ACC inhibitors may help reduce tissue damage caused by persistent immune responses.

Even before HCV was identified as the causative agent of hepatitis C, its link with hepatic lipid metabolism was foreshadowed by the high incidence of steatosis in patients with what was then called non-A, non-B hepatitis (112). Our results establish a putative distinction between *de novo* synthesized and exogenously derived lipids in HCV infection using a novel ACC inhibitor, K1, in comparison to an established counterpart, soraphen A. Our findings have important implications for all Flaviruses and other positive-sense RNA viruses, which rely extensively on manipulating host lipid metabolism for their propagation (222-225). Future studies examining whether host-derived metabolites in turn dictate the metabolome of invading microbes may help

identify novel points of therapeutic intervention. In addition, further investigation of the relationship between cellular metabolic processes and pathogens will help improve our understanding of the selective pressures driving the evolution of host-microbe interactions.

Figure 2.1. Structures of ACC inhibitors.

(A) Structure of the novel ACC inhibitor, K1.

(B) Structure of soraphen A (obtained from the PubChem database maintained by the National Center for Biotechnology Information).

A

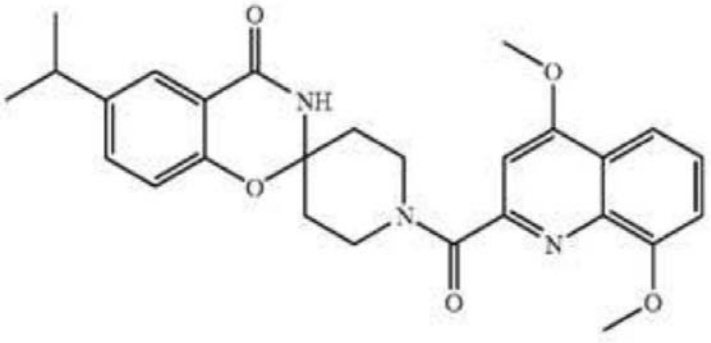

B

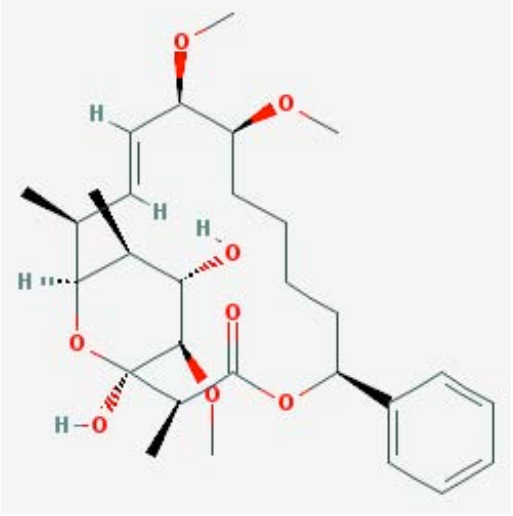

Figure 2.2. Inhibition of *de novo* lipogenesis decreases intracellular HCV RNA.

(A) Experimental setup.

(B) Kinetics of changes in HCV RNA. Infected Huh7.5.1 cells were treated with 1 μM K1 or 100 nM soraphen A. DMSO was added at an equivalent volume. The media was replaced with fresh ACC inhibitors on D3 post-treatment (PT). HCV RNA was detected by qRT-PCR. The plotted values are fold increases relative to D0 PT (1 day post-infection, before addition of ACC inhibitors). Significance was calculated relative to the DMSO controls from the same time point.

(C) Co-treatment of K1 and soraphen A. Infected Huh7.5.1 cells were treated with DMSO, 1 μM K1 or 100 nM soraphen A, both K1 and soraphen A. Cells were collected for qRT-PCR analysis on D3 PT.

(D, E) Dose response of K1 (D) and soraphen A (E). Infected Huh7.5.1 cells were treated with DMSO, K1, or soraphen A for 3 days before qRT-PCR analysis.

(F) Effect on primary cells. Infected primary hepatocytes were treated daily (D0-D2 PT) with DMSO, 2 μM K1, 200 nM soraphen A, or 500 nM of the NS5B polymerase inhibitor, sofosbuvir. Cells were collected for qRT-PCR analysis on D3 PT.

(G, H) Silencing of ACC1 and ACC2. Infected Huh7.5.1 cells were transfected with a pool of siRNA against ACC1 or ACC2 for 3 days before immunoblot (G) and qRT-PCR analysis (H).

(I, J) Infected Huh7.5.1 cells were treated with DMSO, 1 μM K1 or 100 nM soraphen A. Cells were collected for qRT-PCR analysis on D3 PT.

Results are the representative or mean ± SEM of 2 (F) or 3-5 independent experiments. Statistical significance was calculated by two-way ANOVA with Bonferroni post-tests

(B, D, E) or one-way ANOVA with Tukey's post-test (C, H-J). nd: not detected, *p<0.05, **p<0.01, ***p<0.001.

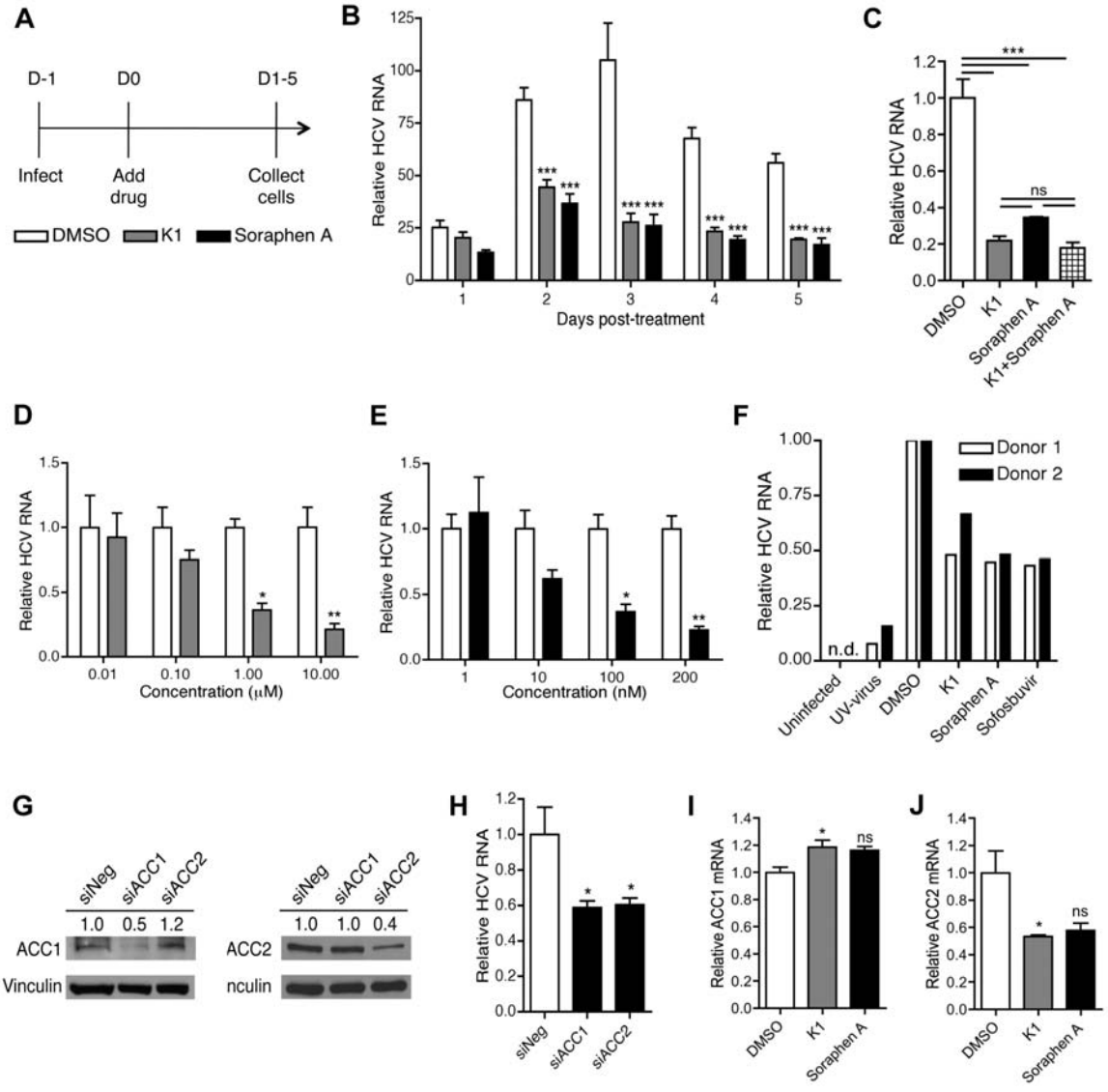
A
D-1
D0
D1-5
Infect
Add drug
Collect cells
DMSO
K1
Soraphen A
B
Relative HCV RNA
Days post-treatment
C
Relative HCV RNA
ns
DMSO
K1
Soraphen A
K1+Soraphen A
D
Relative HCV RNA
Concentration (μM)
E
Relative HCV RNA
Concentration (nM)
F
Relative HCV RNA
Donor 1
Donor 2
n.d.
Uninfected
UV-virus
DMSO
K1
Soraphen A
Sofosbuvir
G
siNeg
siACC1
siACC2
1.0 0.5 1.2
ACC1
Vinculin
1.0 1.0 0.4
ACC2
nculin
H
Relative HCV RNA
siNeg
siACC1
siACC2
I
Relative ACC1 mRNA
DMSO
K1
Soraphen A
J
Relative ACC2 mRNA
DMSO
K1
Soraphen A

Figure 2.3. Inhibition of *de novo* lipogenesis does not significantly alter cell viability.

(A) Cell viability upon treatment with K1 and soraphen A. Uninfected and infected Huh7.5.1 were treated with media, DMSO, 1 μM K1, or 100 nM soraphen A for 3 days. Viability was determined by crystal violet staining.

(B) Redox capacity upon K1 and soraphen A treatment was determined by MTT assay using the setup described in (A).

(C) Intracellular ATP content was quantified in DMSO, K1, and soraphen A-treated cells using the setup described in (A).

Results are the mean ± SEM of 3 independent experiments.

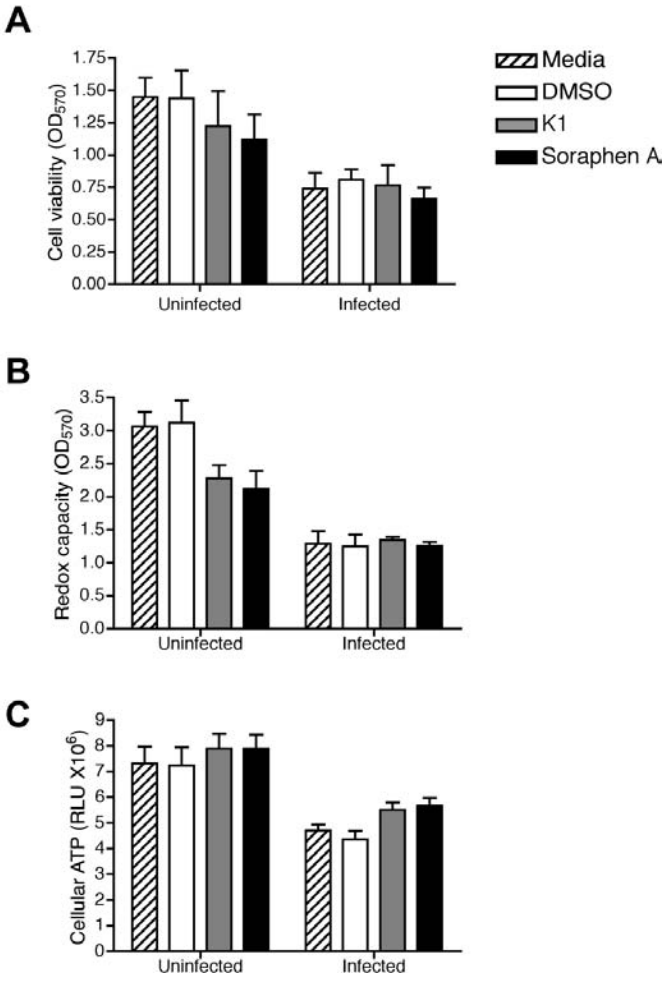
A
Cell viability (OD570)
1.75
1.50
1.25
1.00
0.75
0.50
0.25
0.00
Uninfected
Infected
Media
DMSO
K1
Soraphen A
B
Redox capacity (OD570)
3.5
3.0
2.5
2.0
1.5
1.0
0.5
0.0
Uninfected
Infected
C
Cellular ATP (RLU X10^6)
9
8
7
6
5
4
3
2
1
0
Uninfected
Infected

Figure 2.4. *De novo* lipogenesis is required for HCV replication, but does not contribute to translation of viral genome or viral protein expression.

(A) Effect on entry. Huh7.5.1 cells were treated with DMSO, 1 μM K1, or 100 nM soraphen A for 3 days after which the media was replaced with JFH-1 (MOI 0.1). HepG2 cells were used as a negative control. Cells were collected for qRT-PCR analysis at 1 hour post-infection.

(B) Effect on expression of viral entry factors. Huh7.5.1 cells were treated with DMSO, 1 μM K1, or 100 nM soraphen A for 3 days. Protein was assessed by immunoblotting. Densities of LDLR and SRB1 staining were calculated relative to vinculin and then normalized to DMSO in each experiment.

(C) Effect on replication. Huh7.5 cells harboring HCV subgenomic replicons were treated with DMSO, 1 μM K1, 100 nM soraphen A, or 250 nM of the NS5B polymerase inhibitor, sofosbuvir, for 3 days. HCV RNA was detected by qRT-PCR.

(D) Effect on viral protein. Infected Huh7.5.1 cells were treated with DMSO, 1 μM K1, or 100 nM soraphen A for 3 days. Intracellular viral protein was assessed by immunoblotting. Densities of NS3 and core staining were calculated relative to vinculin and then normalized to DMSO in each experiment.

(E) Effect on translation. Huh7.5.1 cells were transfected with the bicistronic pFR_HCV_xb construct in which the HCV IRES regulated translation of renilla luciferase. Mock transfected cells served as controls. Twenty-four hours post-transfection, the media was replaced with DMSO, 1 μM K1, or 100 nM soraphen A for 3 days. Cellular lysates were assessed for both firefly and renilla luciferase activity.

(F) Effect on translation of a replication deficient replicon. Huh7.5.1 cells were transfected with the pSGR_JFH1/GND_Fluc construct, which expresses HCV NS3-NS5B, but is unable to replicate due to a point mutation in NS5B. pUC19 vector transfected cells served as controls. Twenty-four hours post-transfection, the media was replaced with DMSO, 1 μM K1, or 100 nM soraphen A for 3 days. Cellular lysates were assessed for firefly luciferase activity.

Results are the representative or mean ± SEM of 2-6 independent experiments. Statistical significance was calculated relative to the DMSO treated cells by one-way ANOVA with Tukey's post-test. ns: not significant, $^{**}p<0.01$, $^{***}p<0.001$.

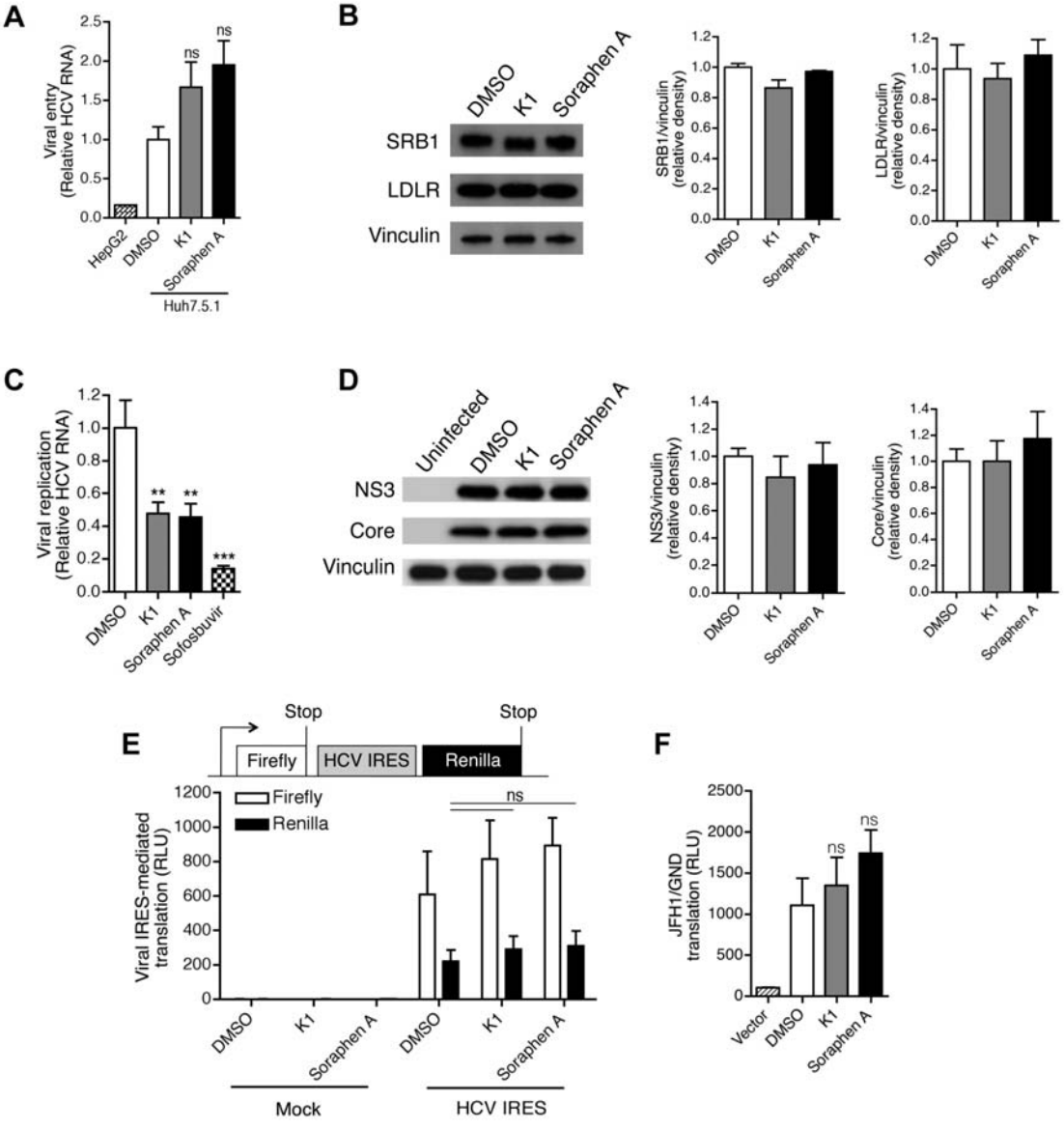
A
Viral entry (Relative HCV RNA)
ns
ns
HepG2
DMSO
K1
Soraphen A
Huh7.5.1
B
DMSO
K1
Soraphen A
SRB1
LDLR
Vinculin
SRB1/vinculin (relative density)
LDLR/vinculin (relative density)
C
Viral replication (Relative HCV RNA)
**
**
***
DMSO
K1
Soraphen A
Sofosbuvir
D
Uninfected
DMSO
K1
Soraphen A
NS3
Core
Vinculin
NS3/vinculin (relative density)
Core/vinculin (relative density)
E
Stop
Stop
Firefly
HCV IRES
Renilla
Firefly
Renilla
ns
Viral IRES-mediated translation (RLU)
DMSO
K1
Soraphen A
Mock
HCV IRES
F
JFH1/GND translation (RLU)
ns
ns
Vector
DMSO
K1
Soraphen A

Figure 2.5. *De novo* lipogenesis provides the platform for viral assembly and contributes to infectious virion production.

(A-C) Effect on assembly. Infected Huh7.5.1 cells were treated with DMSO, 1 μM K1 or 100 nM soraphen A for 3 days and stained for the nucleocapsid core protein and lipid droplets. Number of red (HCV core, F) and green (lipid droplets, G) was quantified over 10 fields in each experiment. Scale bar is equivalent to 20 μm.

(D) Effect on infectious titer. Huh7.5.1 were infected with serially diluted supernatants of infected Huh7.5.1 cells that had been treated with DMSO, 1 μM K1, or 100 nM soraphen A for 3 days. The number of HCV-core positive focus forming units (FFU) was quantified 3 days post-infection.

(E) Effect on extracellular RNA. HCV RNA was detected by qRT-PCR in supernatants of infected Huh7.5.1 cells that had been treated with DMSO, 1 μM K1, or 100 nM soraphen A for 3 days.

Results are the representative or mean ± SEM of 3-4 independent experiments. Statistical significance was calculated by one-way ANOVA with Tukey's post-test. ns: not significant, $**p<0.01$, $***p<0.001$.

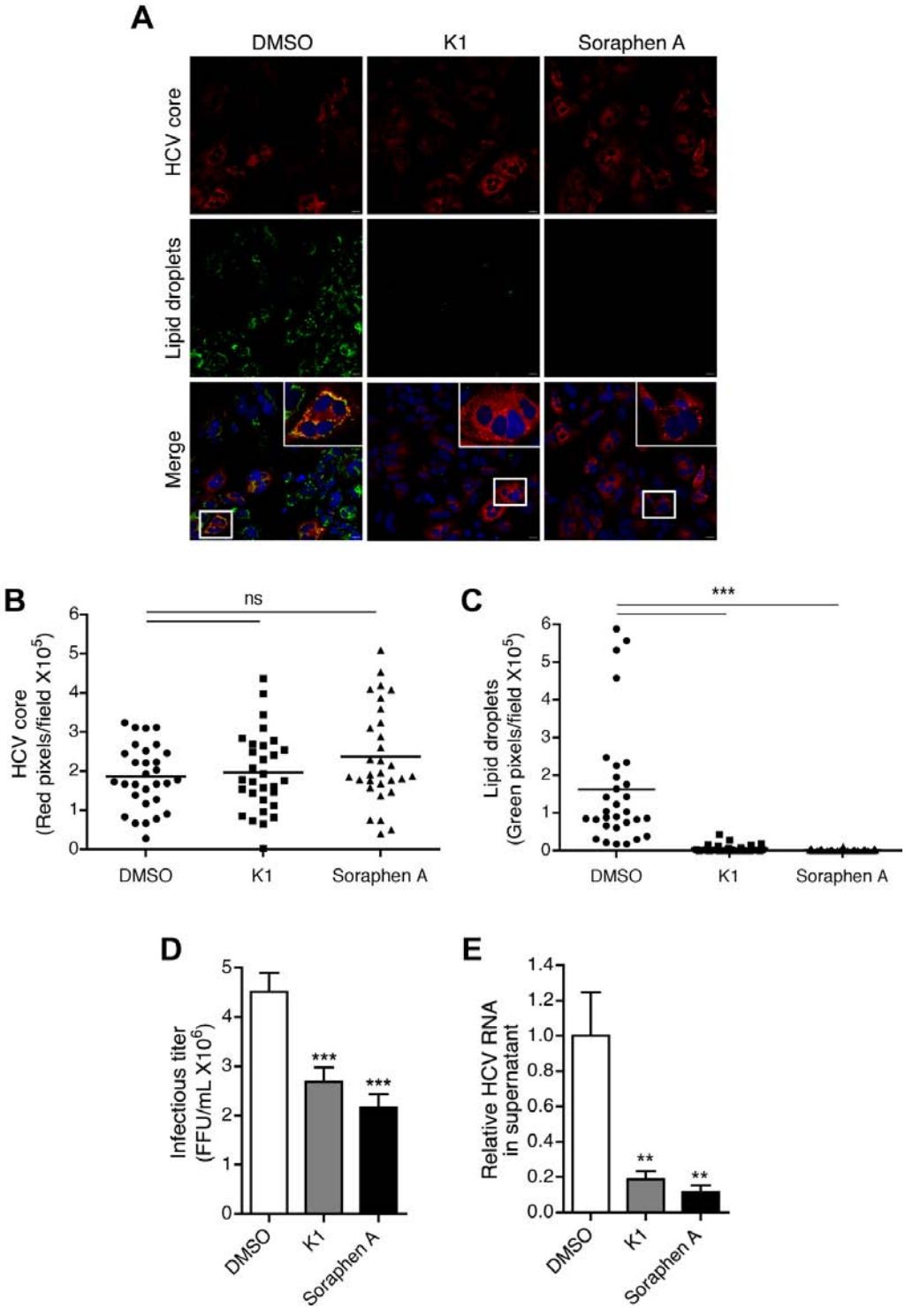
A
DMSO
K1
Soraphen A
HCV core
Lipid droplets
Merge
B
ns
HCV core
(Red pixels/field X10^5)
DMSO
K1
Soraphen A
C
***
Lipid droplets
(Green pixels/field X10^5)
DMSO
K1
Soraphen A
D
Infectious titer
(FFU/mL X10^6)
***
***
DMSO
K1
Soraphen A
E
Relative HCV RNA
in supernatant
**
**
DMSO
K1
Soraphen A

Figure 2.6. Inhibiting *de novo* lipogenesis changes the lipid repertoire in uninfected and HCV-infected hepatocytes.

(A-J) Uninfected and infected Huh7.5.1 cells were treated with DMSO, 1 μM K1, or 100 nM soraphen A for 3 days. The relative abundance of (A) phosphatidylserine, (B) phosphatidic acid, (C) phosphatidylethanolamine, (D) phosphatidylcholine, (E) diacylglyercol, (F) lysophosphatidic acid, (G) sphingomyelin, (H) glucosylceramide, (I) dihydroceramide, and (J) ceramide was calculated by mass spectrometry.

Results are from 3-4 independent experiments. Statistical significance was calculated by two-way ANOVA with Bonferroni post-tests. ns: not significant, *p<0.05, **p<0.01, ***p<0.001.

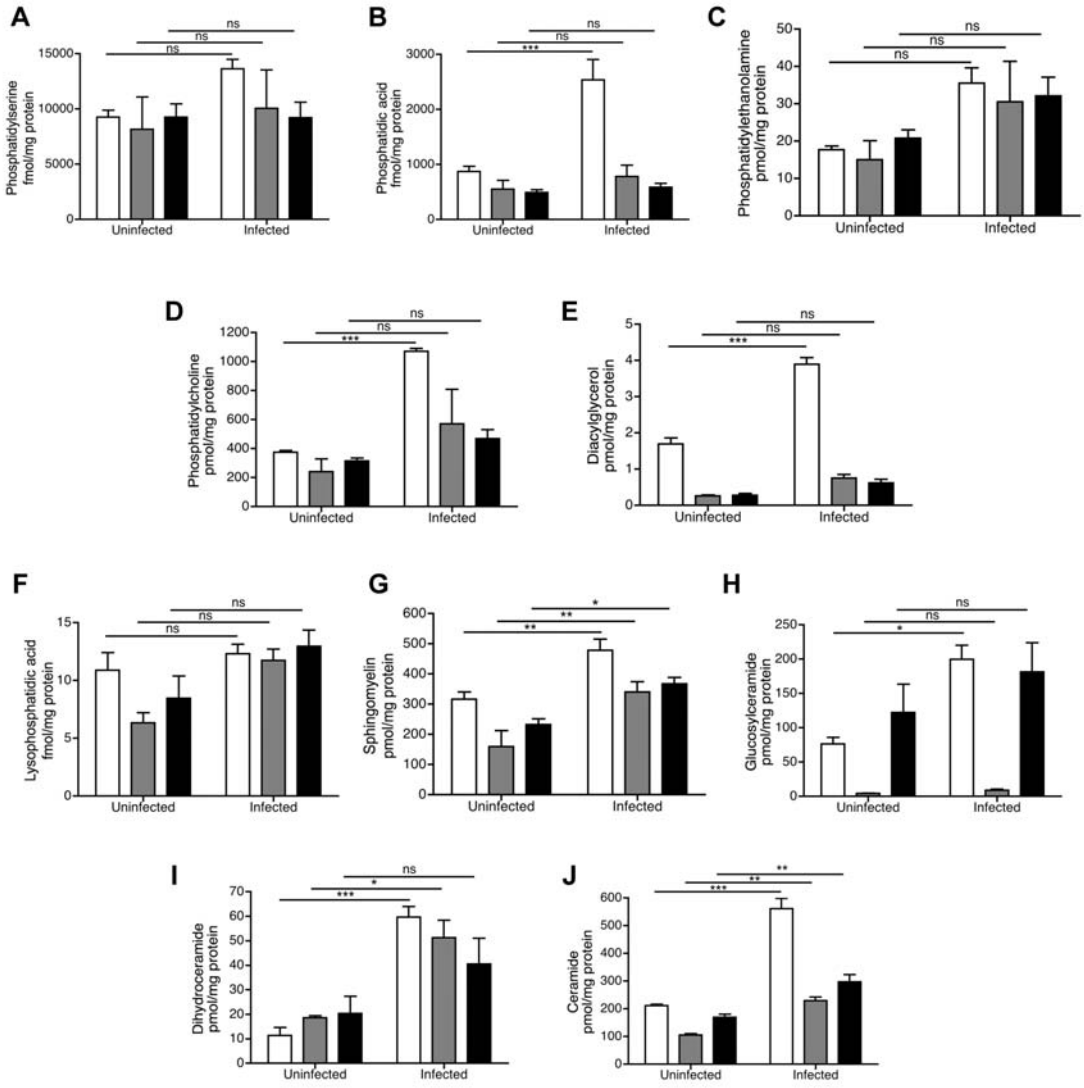
A
Phosphatidylserine fmol/mg protein
15000
10000
5000
0
ns
ns
ns
Uninfected
Infected
B
Phosphatidic acid fmol/mg protein
3000
2000
1000
0
ns
ns
***
Uninfected
Infected
C
Phosphatidylethanolamine pmol/mg protein
50
40
30
20
10
0
ns
ns
ns
Uninfected
Infected
D
Phosphatidylcholine pmol/mg protein
1200
1000
800
600
400
200
0
ns
ns
***
Uninfected
Infected
E
Diacylglycerol pmol/mg protein
5
4
3
2
1
0
ns
ns
***
Uninfected
Infected
F
Lysophosphatidic acid fmol/mg protein
15
10
5
0
ns
ns
ns
Uninfected
Infected
G
Sphingomyelin pmol/mg protein
600
500
400
300
200
100
0
*
**
**
Uninfected
Infected
H
Glucosylceramide pmol/mg protein
250
200
150
100
50
0
ns
ns
*
Uninfected
Infected
I
Dihydroceramide pmol/mg protein
70
60
50
40
30
20
10
0
ns
*
***
Uninfected
Infected
J
Ceramide pmol/mg protein
600
500
400
300
200
100
0
**
**
***
Uninfected
Infected

Figure 2.7. Inhibiting *de novo* lipogenesis leads to broad changes in the hepatocyte lipidome.

(A, B) Uninfected (A) and infected (B) Huh7.5.1 cells were treated with DMSO, 1 μM K1, or 100 nM soraphen A for 3 days. Indicated lipids were quantified by mass spectrometry and are plotted as normalized values relative to the average in DMSO treated cells. Fatty acid chain length and degree of saturation are indicated on the left. Hashed gray boxes represent replicates that were not detected by the spectrometer. Results are from 3-4 independent experiments.

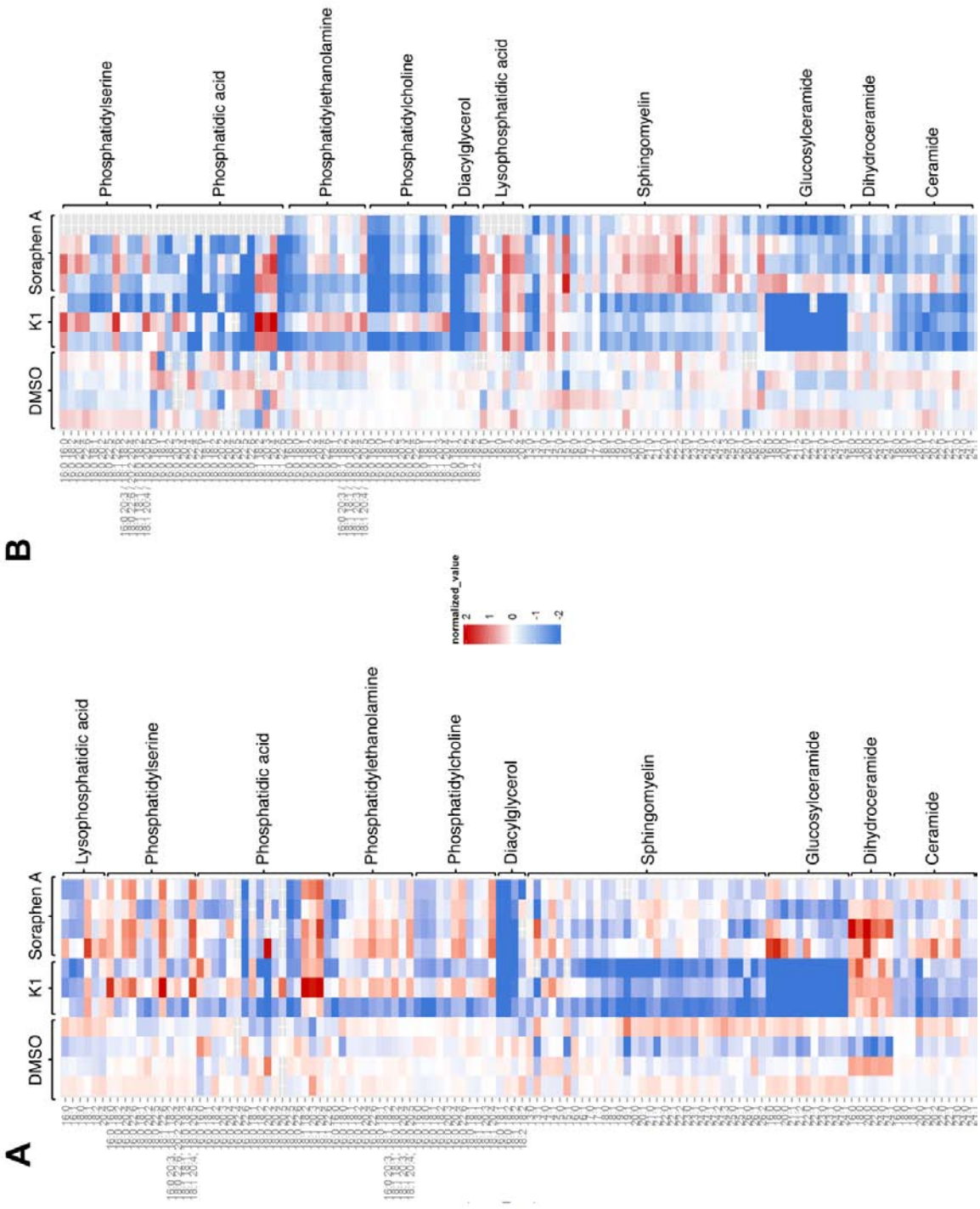
A
B
DMSO
K1
Soraphen A
Lysophosphatidic acid
Phosphatidylserine
Phosphatidic acid
Phosphatidylethanolamine
Phosphatidylcholine
Diacylglycerol
Sphingomyelin
Glucosylceramide
Dihydroceramide
Ceramide
normalized_value
2
1
0
-1
-2

Figure 2.8. Exogenous lipids contribute to HCV assembly via lipid droplet formation but are dispensable for replication and release.

(A-E) Infected Huh7.5.1 cells were treated with 1 μM K1, 100 nM soraphen A, or an equivalent volume of DMSO in media containing BSA (A) only or BSA + fatty acids (palmitate, oleate, and linoleate) (B). At D3 of treatment, cells were stained for the HCV nucleocapsid core protein and lipid droplets. Nuclei are indicated in blue. Areas of co-localization are indicative of assembly of infectious virions. Scale bar is equivalent to 20 μm. Number of red (HCV core, C) pixels and green (lipid droplets, D) pixels were quantified over 10 fields in each experiment. E, Percentage of red pixels that colocalized with green pixels.

(F) Infected Huh7.5.1 cells were treated as described in A-E. Intracellular HCV RNA was detected by qRT-PCR.

(G) Supernatants of cells treated as described in A-E were used to infect Huh7.5.1 cells for 3 days after which the number of core positive foci was quantified.

(H) Effect on extracellular RNA. HCV RNA was detected by qRT-PCR in supernatants of cells treated as described in A-E.

Results are the representative or mean ± SEM of 3-5 independent experiments. Statistical significance was calculated by one-way ANOVA with Tukey's post-test. ns: not significant, *$p<0.05$, **$p<0.01$, ***$p<0.001$.

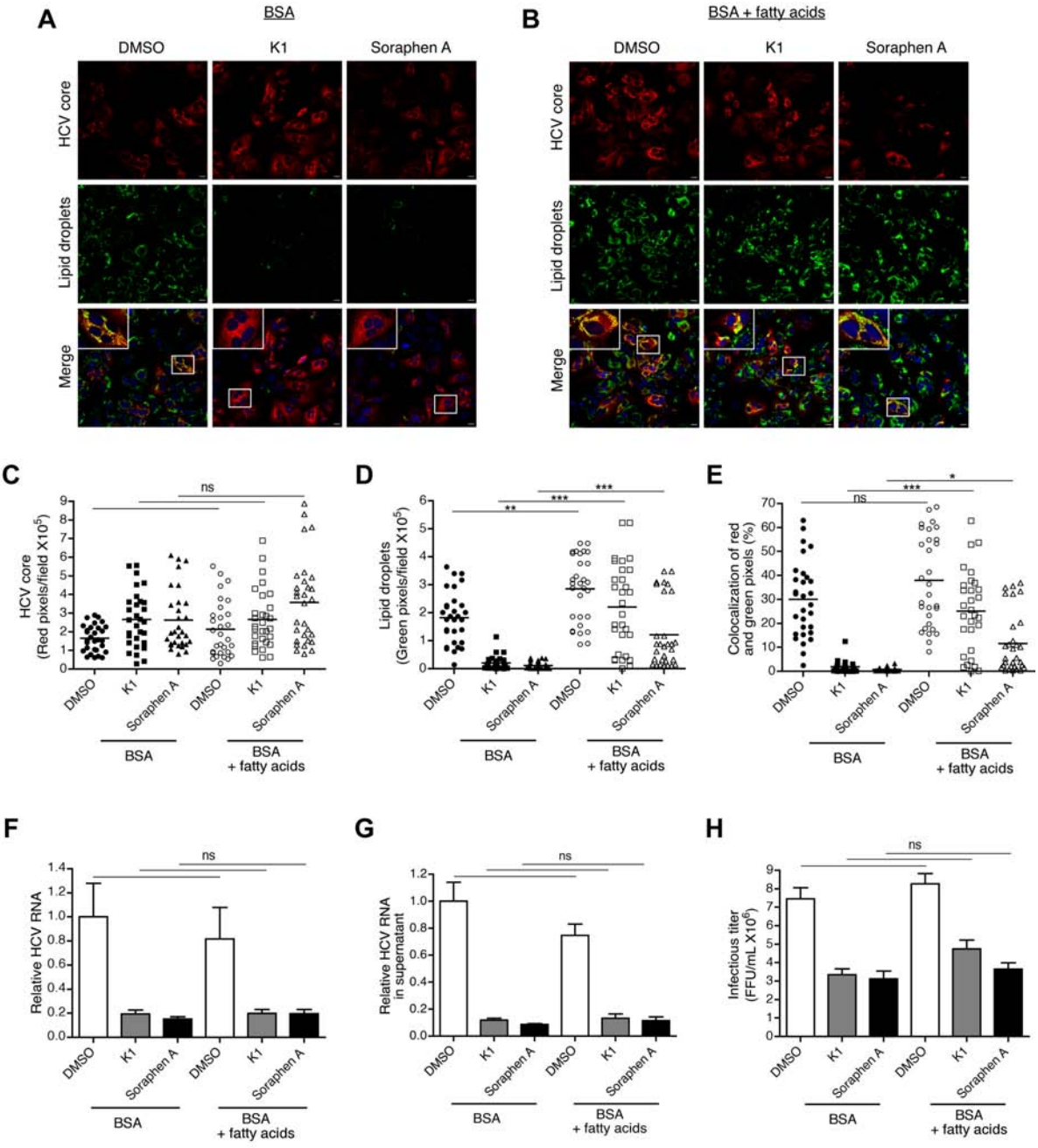
A
BSA
DMSO
K1
Soraphen A
HCV core
Lipid droplets
Merge
B
BSA + fatty acids
DMSO
K1
Soraphen A
HCV core
Lipid droplets
Merge
C
HCV core
(Red pixels/field X10^5)
ns
DMSO
K1
Soraphen A
DMSO
K1
Soraphen A
BSA
BSA
+ fatty acids
D
Lipid droplets
(Green pixels/field X10^5)
**
***
***
DMSO
K1
Soraphen A
DMSO
K1
Soraphen A
BSA
BSA
+ fatty acids
E
Colocalization of red
and green pixels (%)
ns
***
*
DMSO
K1
Soraphen A
DMSO
K1
Soraphen A
BSA
BSA
+ fatty acids
F
Relative HCV RNA
ns
DMSO
K1
Soraphen A
DMSO
K1
Soraphen A
BSA
BSA
+ fatty acids
G
Relative HCV RNA
in supernatant
ns
DMSO
K1
Soraphen A
DMSO
K1
Soraphen A
BSA
BSA
+ fatty acids
H
Infectious titer
(FFU/mL X10^6)
ns
DMSO
K1
Soraphen A
DMSO
K1
Soraphen A
BSA
BSA
+ fatty acids

Figure 2.9. ACC inhibition does not induce ER stress.

Huh7.5.1 cells were treated with DMSO, 1 μM K1, or 100 nM soraphen A for 3 days. Protein was assessed by immunoblotting. Densities of total proteins were calculated relative to vinculin and then normalized to DMSO.

Results are the representative of 3 independent experiments.

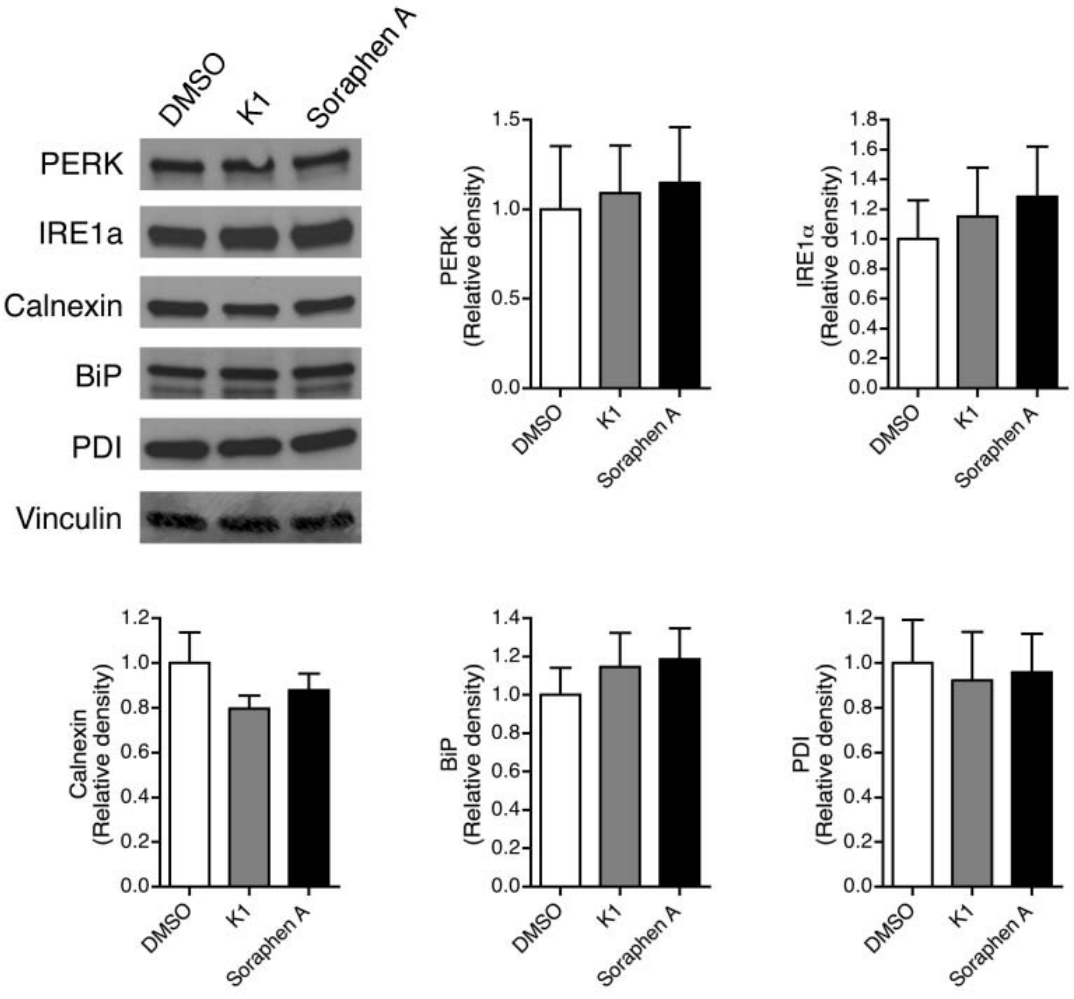
DMSO
K1
Soraphen A
PERK
IRE1a
Calnexin
BiP
PDI
Vinculin
PERK (Relative density)
IRE1α (Relative density)
Calnexin (Relative density)
BiP (Relative density)
PDI (Relative density)
DMSO
K1
Soraphen A

Figure 2.10. Inhibition of *de novo* lipogenesis leads to a loss of lipid droplets but retains replication complexes.

(A) Uninfected and infected Huh7.5.1 cells were treated with DMSO, K1, and Soraphen A for 3 days. Lipid droplets are indicated by the arrowheads. Scale bar is equivalent to 2 μm.

(B) Higher magnification images of infected Huh7.5.1 cells were treated with DMSO, K1, and Soraphen A for 3 days. Arrows indicate double membrane vesicles that are thought to be sites of HCV replication. Scale bar is equivalent to 500 nm for DMSO and K1 and 100 nm for soraphen A.

Images are representative of 2-3 independent experiments.

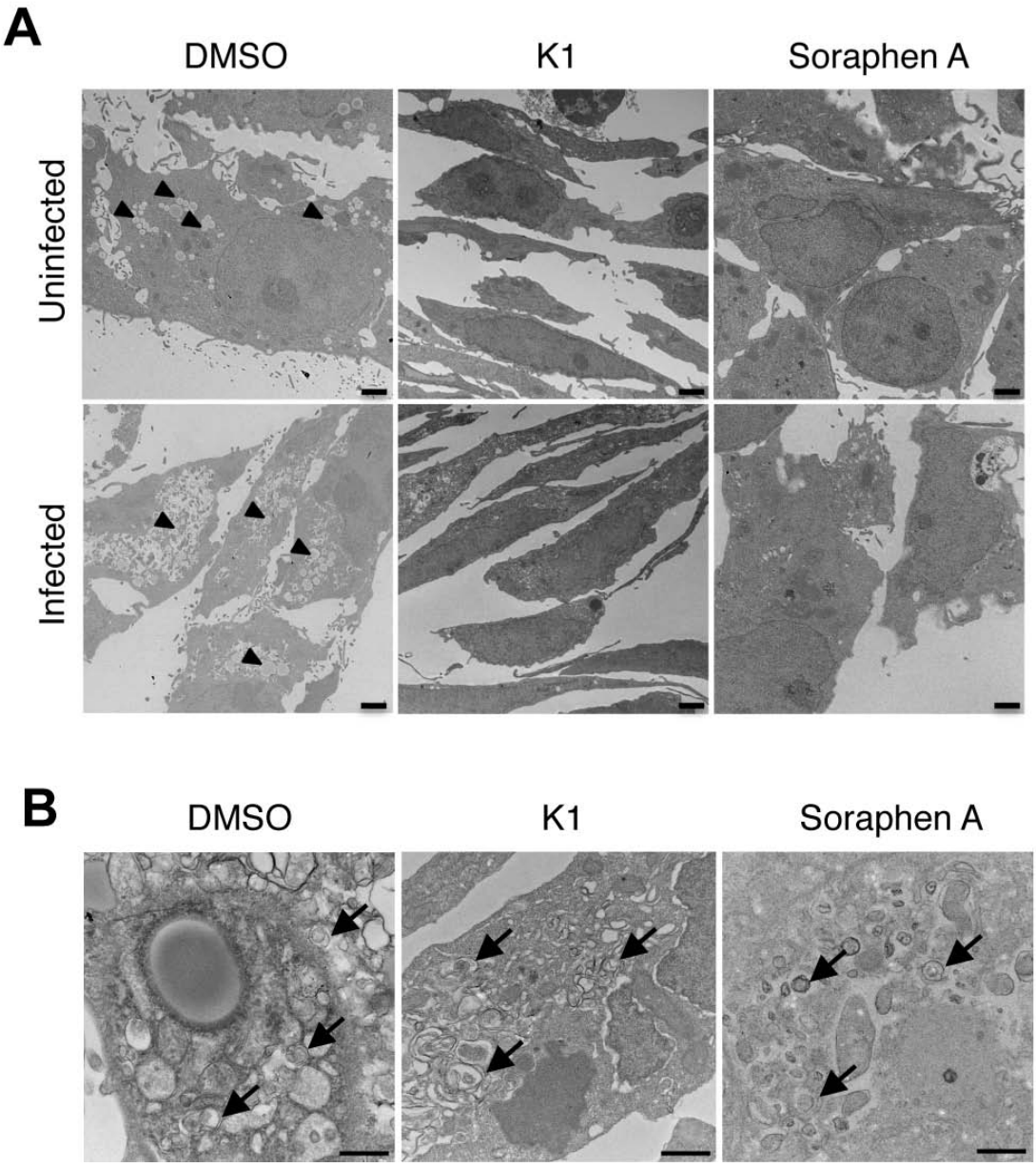
A
DMSO
K1
Soraphen A
Uninfected
Infected
B
DMSO
K1
Soraphen A

Figure 2.11. Inhibition of protein palmitoylation also leads to a loss in viral RNA without a concurrent loss in viral protein.

(A, B) Infected Huh7.5.1 cells were treated with 60 μM 2-bromopalmitate (2-BP) or an equivalent volume of DMSO for 3 days. A, Intracellular HCV RNA was detected by qRT-PCR. B, Intracellular viral protein was assessed by immunoblotting. Densities of NS3 and core were calculated relative to vinculin and then normalized to DMSO.

(C) Infected Huh7.5.1 cells were treated with DMSO, 1 μM K1, 100 nM soraphen A, or 60 μM 2-BP for 3 days and stained for protein aggregates. Cells treated for 6 hours with 5 μM MG-132, a proteosome inhibitor, served as the positive control.

Results are the representative or mean ± SEM of 3-4 independent experiments. Statistical significance was calculated by an unpaired *t* test. ns: not significant, $^{**}p<0.01$.

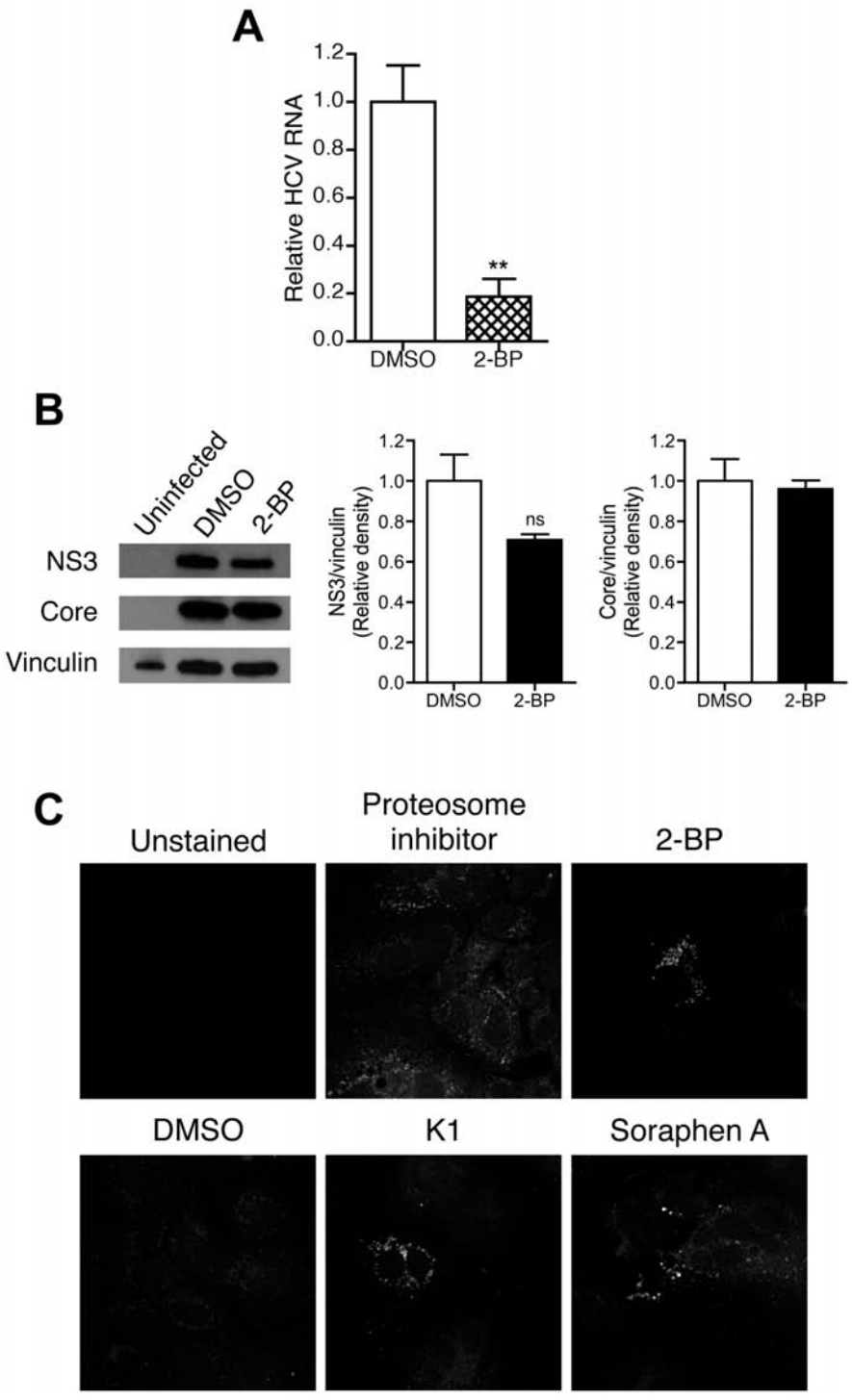
A
Relative HCV RNA
1.2
1.0
0.8
0.6
0.4
0.2
0.0
**
DMSO
2-BP
B
Uninfected
DMSO
2-BP
NS3
Core
Vinculin
NS3/vinculin (Relative density)
ns
Core/vinculin (Relative density)
C
Unstained
Proteosome inhibitor
2-BP
DMSO
K1
Soraphen A

Figure 2.12. Working model of the roles of intracellular and extracellular lipids in HCV infection.

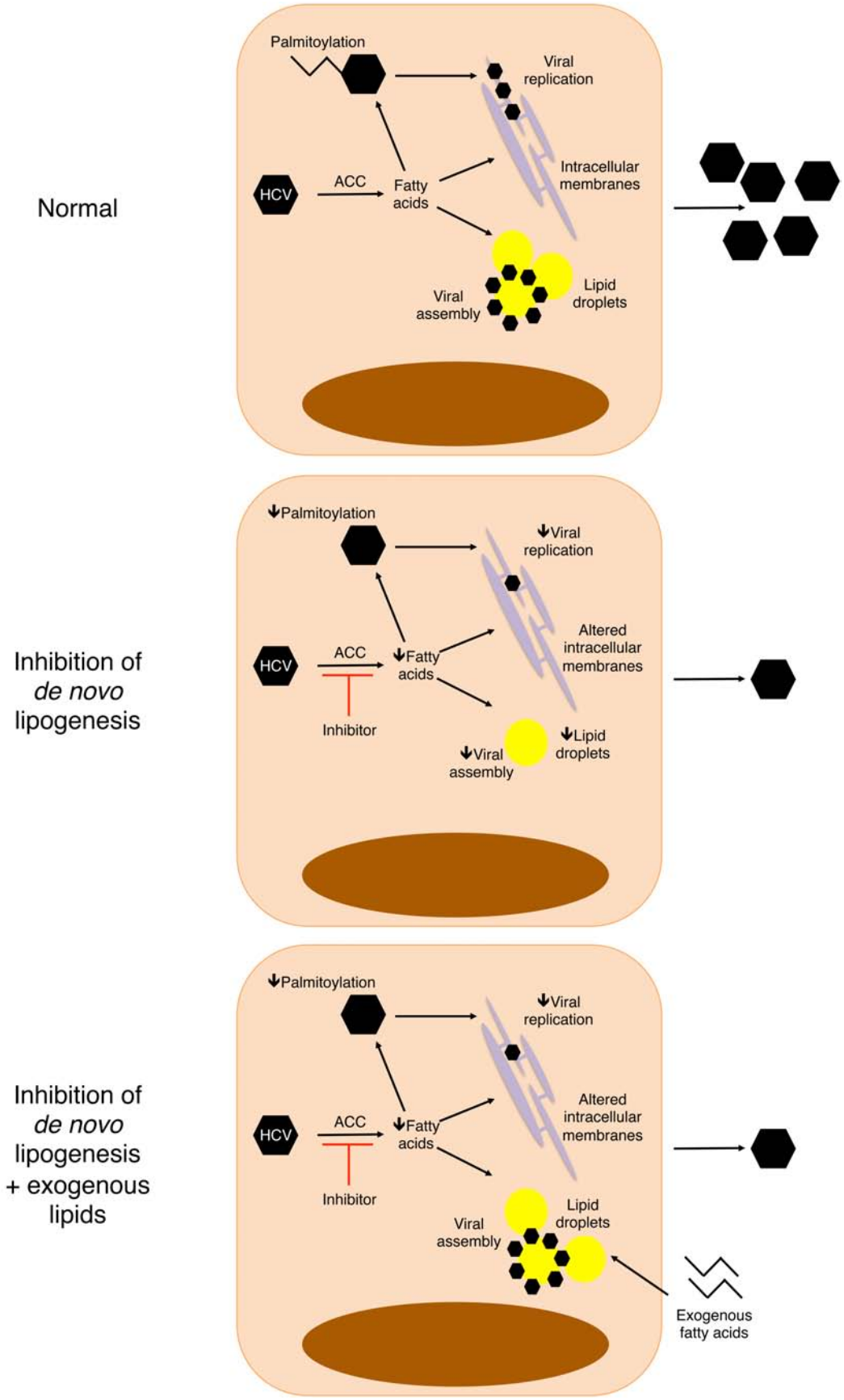
Normal
Palmitoylation
Viral replication
HCV
ACC
Fatty acids
Intracellular membranes
Viral assembly
Lipid droplets
Inhibition of de novo lipogenesis
↓Palmitoylation
↓Viral replication
HCV
ACC
↓Fatty acids
Altered intracellular membranes
Inhibitor
↓Viral assembly
↓Lipid droplets
Inhibition of de novo lipogenesis + exogenous lipids
↓Palmitoylation
↓Viral replication
HCV
ACC
↓Fatty acids
Altered intracellular membranes
Inhibitor
Viral assembly
Lipid droplets
Exogenous fatty acids

CHAPTER 3: Group 3 innate lymphoid cells in nonalcoholic steatohepatitis

ABSTRACT

Innate lymphoid cells (ILCs) are a recently discovered group of immune cells that initiate and regulate responses, often at mucosal surfaces. The hepatic microenvironment is partially mucosal in nature: similar to conventional epithelial surfaces, the liver is continually exposed to potentially foreign drug and food products in addition to a high burden of bacterial components draining from the gut. Considering the similarities between mucosal surfaces and the liver, we hypothesized that ILCs will play a significant role in liver diseases. Specifically, we proposed that group 3 ILCs (ILC3s) play a beneficial role in the pathogenesis of nonalcoholic steatohepatitis (NASH), a chronic inflammatory disease characterized by dysregulated hepatic lipid metabolism. To test our hypothesis, we have established a novel method to enrich ILCs from human blood and tonsils. In addition, we developed an *in vitro* model of NASH in which the human heptoma cells HepG2 are treated with fatty acids and LPS to mimic the steatotic and inflammatory environment of NASH livers, respectively. Culturing hepatocytes with fatty acids increased expression of TGF-β, which induces fibrosis in hepatic stellate cells (HSCs), and the chemokine CCL20, which is known to recruit ILC3s. Importantly, ILC3s produce IL-22, which is known to promote tissue repair, supporting a model wherein ILC3s are recruited to the liver during NASH to produce IL-22 in an effort to restore homeostasis. Collectively, our results are a promising start to investigate ILCs in the pathogenesis of chronic inflammatory diseases of the liver.

INTRODUCTION

The increased incidence of obesity worldwide is accompanied by a number of systemic diseases, including nonalcoholic fatty liver disease (NAFLD). NAFLD is marked by extensive steatosis, or the accumulation and enlargement of hepatic lipid droplets, which results from the increased uptake of fatty acids by the liver and elevated rates of hepatic *de novo* lipogenesis. Although steatosis is not pathological, undefined cellular and molecular triggers can propel this benign condition to a chronic inflammatory disease called nonalcoholic steatohepatitis (NASH). Importantly, NASH can lead to significant clinical sequelae, including cirrhosis, malignancy, and cardiovascular events (126). Development of these end-stage diseases is preceded by fibrosis of the liver, which is the deposition of scar tissue in response to chronic inflammatory injury. Importantly, fibrosis is thought to be reversible and therefore presents an ideal target to limit the development of more significant liver and systemic pathologies.

The immune response in NASH presents several potential diagnostic and therapeutic avenues as it regulates fibrogenesis and disease outcome (Chapter 1, pp. 18-35). Specifically, the cytokine IL-22 has emerged as a critical regulator of metabolic diseases as administration of exogenous IL-22 reverses weight gain, insulin resistance, and translocation of gut bacteria to the liver in mouse models of obesity (148). Furthermore, IL-22 administration was also protective against fibrosis in a biliary cirrhosis model, underscoring its universal role in regulating fibrogenesis in the liver (226). The beneficial effects of IL-22 in liver fibrosis are in part due to its ability to inhibit proliferation and induce senescence in hepatic stellate cells (HSCs), which secrete

copious amounts of extracellular matrix components upon activation (227). Additionally, IL-22 protects hepatocytes from immune-mediated damage and promotes their proliferation and survival, thus aiding in tissue regeneration (228, 229). IL-22 also has extrahepatic roles that contribute to its favorable role in NASH and other liver pathologies. Similar to its role in promoting tissue repair in hepatocytes, IL-22 preserves colonic epithelial integrity that is necessary to contain commensal bacteria within the gut (149). As leakiness in the gut barrier is characteristic of NASH patients, IL-22's role in extrahepatic tissues may also regulate the extent of injury in the liver (230).

IL-22 belongs to the IL-10 family of cytokines and signals through a heterodimeric receptor consisting of the IL-10R2 and IL-22R1 subunits (231, 232). Expression of the IL-22R is restricted to cells of nonhematopoetic origin, verifying its importance in mediating protection of host tissues during inflammatory responses (233). Conversely, production of IL-22 is limited to T cells and innate lymphoid cells (ILCs). T cell subsets that produce IL-22 include Th17, Th22, γδ T cells, and a subset of CD8 T cells (234-239). Although the contribution of these T cell subsets to the pathogenesis of NASH is only partially explored, several of them have been shown to play a pathogenic role in NASH (Chapter 1, pp. 30-33). Consequently, amplifying responses of non-T cell sources of IL-22 may be beneficial in regulating disease progression in NASH.

ILCs are a recently discovered subset of immune cells that are emerging as critical regulators of metabolic diseases (Chapter 1, pp. 33-35). Specifically, group 3 ILCs (ILC3s) produce copious amounts of IL-22 and may therefore be an important player in mediating protection against inflammatory injury in NASH. However, while ILC responses have begun to be characterized in adipose tissue, their role in regulating

hepatic inflammation in the liver during NASH is yet to be described. We hypothesized that the hepatic injury combined with loss of epithelial integrity in the gut of NASH patients will mobilize ILCs, specifically ILC3s, to the liver, where they will promote hepatocyte regeneration and inhibit stellate cell-induced fibrogenesis through production of IL-22. Here, we report the establishment of a novel *in vitro* model of NASH and a customized technique to enrich ILC populations from human peripheral blood and tonsils. These methodological advancements will be further developed to test the hypothesis that ILC3s are necessary to maintain and/or restore tissue homeostasis in the chronic inflammatory environment of NASH livers.

MATERIALS AND METHODS

Cells and fatty acids.

HepG2 cells were maintained in low glucose MEM (Gibco 11095080) with 10% FBS and 10 U/mL penicillin/streptomycin. PBMCs were maintained in RPMI with 10% FBS, 2 mM L-glutamine, 1 mM sodium pyruvate, 10 mM HEPES, and 10 U/mL penicillin/streptomycin. Sodium salts of palmitate and oleate were purchased from Sigma-Aldrich and mixed in methanol in a 1:2 ratio (240). The methanol was removed using nitrogen and the fatty acid mixture was reconstituted in culture media containing 1% fatty acid free BSA (Sigma-Aldrich) to a final concentration of 333.3 μM palmitate and 666.6 μM oleate. LPS (Sigma-Aldrich) was added at 200 ng/mL. LX2 cells were a gift from Dr. Lucy Golden-Mason (University of Colorado-Denver). Recombinant human TGF-β was purchased from Peprotech.

Flow cytometry for neutral lipids.

HepG2 cells were plated in 12-well plates at 0.3 X 10^6 cells/well. At 12 h post-seeding, the media was replaced with BSA ± oleate/palmitate ± LPS for 24 h at which time the monolayer was rinsed in PBS and the cells were collected by treatment with trypsin + EDTA (Gibco) and spun down. Cells were fixed in 4% PFA/PBS for 15 minutes, washed in PBS, and stained for 30' at room temperature in PBS containing 1:1000 HCS LipidTOX™ Deep Red neutral lipid stain (Invitrogen). Cells were then pelleted again by centrifugation, washed 1X in PBS, and run on a BD FACS Canto II (BD Biosciences) and analyzed using FlowJo software version 10.1 (TreeStar).

Crystal violet assay.

HepG2 cells were plated in 96-well plates at 40,000 cells/well. At the time of assessment, culture supernatants were aspirated and cells were treated with crystal violet solution (0.5% crystal violet in 50% methanol/water) for 20 minutes. The stain was solubilized with 1% SDS for 2-3 hours. Absorbance was read at 570 nm on a PowerWave XS spectrophotometer (BioTek).

Quantitative RT-PCR.

RNA was extracted using the RNeasy Plus Kit (Qiagen) and reverse transcribed using the high-capacity RNA-to-cDNA kit (Life Technologies). qRT-PCR was run on a StepOnePlus RT-PCR system (Applied Biosystems) with SYBR green dye (Life Technologies) using the following primers: *TGFB1* forward, 5'-CTGGCGATACCTCAGCAACC-3' and reverse, 5'-

CCGGTAGTGAACCCGTTGATGT-3', *Col1A1* (Collagen I) forward, 5'-CGGCTCCTGCTCCTCTT-3' and reverse, 5'- GGGGCAGTTCTTGGTCTC-3', *ACTA2* (αSMA) forward, 5'- CGTGGCTATTCCTTCGTTAC-3' and reverse, 5'-TGCCAGCAGACTCCATCC-3', *TIMP2* forward, 5'-AGAGGATCCAGTATGAGATCAAGCAG-3' and reverse, 5'-TGGTACCTGTGGTTCAGGCTCTTC-3', and *HPRT1* forward, 5'-GAAAAGGACCCCACGAAGTG-3' and reverse, 5'-AGTCAAGGGCATATCCTACAAC-3'. Expression levels of each gene were first calculated relative to *HPRT1* and then normalized to the average of the control group.

ILC enrichment by magnetic selection.

Approximately 60-80 X 10^6 mononuclear cells from peripheral blood (PBMCs) or tonsils from healthy donors were depleted of T cells, B cells, monocytes, and NK cells using a custom designed magnetic selection kit (StemCell Technologies). Although the markers for depleting T cells, B cells, and monocytes were proprietary, NK cells were depleted using antibodies against CD94. The remaining cells were cultured at 0.05-0.15 X 10^6 cells/200 μL of PBMC media in 96-well plates for 72 hours. In the experiment assessing the impact of TGF-β on ILC cytokine production, 2.5 ng/mL TGF-β was added to half of the enriched tonsillar cells for the last 48 hours of culture.

Flow cytometry for ILCs.

Cells were stained for 20' on ice with the following surface antibodies: FITC conjugated anti-CD3, CD5, and CD14 (all from Tonbo Biosciences) and CD19 and CD94

(both from eBioscience) were added at 0.5 μL/test; PE-CD161 (Tonbo biosciences) or PerCP-Cy5.5-CD161, APC-eF780-CD127, PE-Cy7-cKit, and eF450-NKp44 (all from eBioscience) were added at 1 μL/test. APC-CRTH2 (eBioscience) was added at 5 μL/test. Live cells were distinguished by fixable viability dye eFluor-506 (eBioscience). For intracellular IL-22 staining, cells were treated with 100 ng/mL PMA and 1 μg/mL ionomycin with 1:1000 dilutions each of Golgi Stop and Golgi Plug (both from BD biosciences) for the last 5 hours of culture. Cells were fixed in Cytofix/Cytoperm (BD biosciences) and stained with PE-conjugated anti-IL-22 at 5 μL/test for 30' on ice (eBioscience). All samples were run on a CytoFLEX flow cytometer (Beckman Coulter) and analyzed using FlowJo software version 10.1 (TreeStar).

Luminex assay.

Cytokines in culture supernatants of HepG2 cells ± oleate:palmitate ± LPS were quantified using the Luminex MAGPIX bead-based multiplex analyzer at the University of Virginia Flow Cytometry Core Facility.

Statistical analysis

Results are the mean ± SEM. Statistical significance was determined by one-way analysis of variance (ANOVA) with Tukey's post-test. Statistical analyses were performed using Prism GraphPad software v4.0c. ns: not significant, *p<0.05.

RESULTS

Addition of fatty acids and LPS to HepG2 cells is an *in vitro* model of NASH.

Current *in vitro* models of NAFLD use a combination of fatty acids to induce lipotoxic injury in primary hepatocytes or hepatoma cell lines (241, 242). However, these models do not account for the loss of gut integrity in NASH patients, which increases hepatic concentrations of immunogenic stimuli, such as lipopolysaccharide (LPS). We therefore modified a previously established model of benign steatosis, in which the human hepatocellular carcinoma line HepG2 is treated with an excess of the fatty acids oleate and palmitate in a 2:1 ratio (240). Specifically, we added 200 ng/mL of LPS to HepG2 cells treated with albumin or albumin complexed with 1 mM oleate:palmitate at a 2:1 ratio. As expected, addition of fatty acids increased the neutral lipid content of HepG2 cells when compared to cells treated with BSA ± LPS (Figures 3.1.A). LPS treatment further enhanced lipid accumulation in fatty acid loaded cells, although this increase did not reach statistical significance; interestingly, this trend was not seen in cells loaded with the vehicle BSA (Figures 3.1.A). In addition, treatment with an excess of oleate:palmitate or LPS did not reduce cell viability (Figure 3.1.B).

To further verify that these *in vitro* conditions mimic the fibrogenic microenvironment of NASH livers, we evaluated gene expression levels of TGF-β, which is a potent stimulator of fibrogenesis in hepatic stellate cells (HSCs). Upregulation of TGF-β was most prominent in HepG2 cells loaded with fatty acids (Figure 3.1.C). It is surprising that treatment of steatotic hepatocytes with LPS reduces the production of TGF-β, as it is a well-known inducer of TGF-β production (243). Nonetheless, we confirmed the profibrogenic effects of TGF-β by assessing the expression of fibrogenic genes in the human HSC line, LX2, treated with increasing concentrations of TGF-β. As seen in Figure 3.1.D, gene expression of type I collagen increased proportionally to the

dose of TGF-β. Surprisingly, additional markers of fibrogenesis, namely the myofibroblast marker α-SMA and the matrix metalloproteinase inhibitor TIMP-2 did not appreciably change in response to TGF-β (Figure 3.1.D). Thus, some of our initial observations are at odds with reported findings. However, our findings indicate that culturing HepG2 cells with fatty acids is a model of simple steatosis while the addition of LPS may be a model of NASH.

ILC3s are found in nonmucosal sites and produce IL-22 upon stimulation.

Liver fibrosis is initiated by the activation and proliferation of HSCs. Previous studies have reported that while TGF-β activates HSCs, the cytokine IL-22 and its downstream signals counter the effects of TGF-β and limit expression of fibrogenic genes in HSCs (226, 227, 244). This was of interest to our hypothesis as IL-22 is produced by ILC3s. Cellular sources of IL-22 include T cells and ILC3s. As T cells are known to play pathogenic roles in NASH, ILC3s may be a more beneficial source of IL-22 during disease development. We therefore sought to establish a system that would allow investigation of human ILC subsets in conjunction with our *in vitro* model of NASH. All 3 groups of ILCs have been reported in human blood and tonsils (150). However, ILCs are a rare population in both tissues; we therefore used negative selection to magnetically enrich for ILCs by depleting T cells, B cells, monocytes, and NK cells (Figure 3.2.A). Following 72 hours of culture, cells were assessed by flow cytometry for surface expression of ILCs defined as $Lin^{-}CD127^{+}CD161^{+}$ cells, which were further divided into the 3 subsets: $cKit^{-}CRTH2^{-}NKp44^{-}$ ILC1s, $CRTH2^{+}$ ILC2s, and $cKit^{+}CRTH2^{-}NKp44^{-}$ natural cytotoxicity receptor negative (NCR^{-}) ILC3s or $cKit^{+}CRTH2^{-}NKp44^{+}$ NCR^{+}

ILC3s. The enrichment process resulted in ~40% lineage$^-$ cells compared to <1% of lineage$^-$ cells present in total PBMCs (Figure 3.2.B). Additionally, in agreement with previously published reports, ILC3 populations in PBMCs were limited to NCR$^-$ ILC3s (150).

While the presence of ILC3s in PBMCs is encouraging, the lack of NCR$^+$ ILC3s limits functional assessment of these cells, as only NKp44$^+$ ILC3s were shown to produce IL-22 (245, 246). In contrast to blood, human tonsils are reported to harbor a notable population of NCR$^+$ ILC3s (150). We therefore enriched for ILCs in human tonsils using the same strategy as we did for blood-derived ILCs (Figure 3.3.A). Compared to ~9% lineage$^-$ cells from the total mononuclear population, enrichment resulted in 68% lineage$^-$ tonsillar cells (Figures 3.3.B and 3.3.C). As described in previous studies, ILC3s in the tonsils included both NCR$^-$ and NCR$^+$ subsets (Figure 3.3.C)(150). Importantly, these NCR$^+$ ILC3s produced IL-22 upon stimulation with PMA/ionomycin (Figure 3.3.D). These observations indicate that tonsil-derived ILCs are a reliable cellular source of IL-22 that could be used to investigate the role of these cells in NASH.

Recently, TGF-β was shown to impair the development of NCR$^+$ ILC3s in mice (247). Seeing as gene expression of TGF-β was upregulated in HepG2 cells loaded with fatty acids, and that NCR$^+$ ILC3s are the sole ILC population capable of producing IL-22, we investigated the possibility that TGF-β could directly impair NCR$^+$ ILC3s' ability to produce IL-22. To test this idea, we cultured enriched tonsillar ILCs in 2.5 ng/mL of TGF-β for the last 48 hours of the 72 hour culture. Cells were stimulated with PMA/ionomycin 5 hours before collection for analysis by flow cytometry. Surprisingly, addition of TGF-β increased the mean fluorescence intensity (MFI) of IL-22$^+$NCR$^+$ILC3s

(Figure 3.3.D). Collectively, these data identify IL-22 production by NCR^{+}ILC3s as a potential target of immune modulation in the fibrogenic microenvironment of NASH.

CCL20 is an ILC3 chemotactic factor that is upregulated during NASH *in vitro*.

As ILCs are conventionally mucosal-resident populations, we investigated whether it would be possible for them to migrate to the liver during NASH. To this end, we quantified cytokines and chemokines released in supernatants of HepG2 cells cultured with fatty acids ± LPS for 24 hours. The chemokine CCL20, which binds the ligand CCR6, trended towards an increase in hepatocytes treated with fatty acids and LPS (Figure 3.4). CCR6 is expressed on all subsets of human ILC3s (248). These preliminary results thus indicate that the molecular signals driving infiltration of ILC3s to the liver are present in the inflammatory milieu in NASH.

DISCUSSION

To identify novel cellular and molecular factors that contribute to the inflammatory environment in NASH, we aimed to establish a novel *in vitro* model of the disease that accurately reflected both hepatic steatosis and heightened inflammation. Surprisingly, the addition of LPS did not result in notable upregulation of TNF-α or IL-1β at the transcriptional or translational level (data not shown, Figure 3.4), initially suggesting that TLR4 was insufficiently activated in the conditions used. However, the conditions used to grow the HepG2 cells were optimized to promote growth as a monolayer in contrast to the spheroids in which this cell line usually grows. These growth conditions facilitated visualization of neutral lipid accumulation and consistency in

cellularity between experiments. Unfortunately, spheroid HepG2 cultures were shown to respond more robustly to LPS as they express higher levels of CD14, the co-receptor for TLR4, which binds LPS on the cell surface (249). Thus, while the trend towards increased steatotis and elevated levels of CCL20 in HepG2 cells treated with fatty acids and LPS is thus a promising start to an *in vitro* model of NASH, these experiments need to be replicated in spheroid HepG2 cultures to accurately model the inflammatory environment in NASH.

We further aimed to investigate the role of ILCs in an *in vitro* model of NASH. Enrichment for lineage$^-$ cells identified a clear population of ILC1s, ILC2s, and NCR$^-$ ILC3s in PBMCs. Use of the same magnetic enrichment strategy on tonsil mononuclear cells also demarcated populations of tonsillar ILCs and that included NCR$^+$ILC3s, which produced IL-22 upon stimulation. These findings corroborate previous reports of NCR$^+$ILC3s ability to produce IL-22 and suggest that if ILC3s were to migrate to the liver during NASH, then they have the capacity to regulate the extent of local inflammation by dampening the damage to non-immune cells. Interestingly, addition of TGF-β increased the production of IL-22 by NCR$^+$ILC3s on a per cell basis. Of course, as these findings are very preliminary and from a very small population of cells, they will need to be confirmed in subsequent experiments. If true, however, the finding that TGF-β amplifies the responses of ILC3s is intriguing for multiple reasons. Firstly, as mentioned above, TGF-β was recently shown to hinder the development of NCR$^+$ILC3s in mice. Therefore, if TGF-β instead strengthens the functional responses of fully developed NCR$^+$ILC3s in humans, it would identify a dichotomous, developmentally distinct effect of this cytokine on ILC3 function. Secondly, Th17 cells are known to promote TGF-β

signaling on hepatic stellate cells (250). Our current experimental strategy excludes other sources of IL-22, including Th17 cells, which can also produce copious amounts of IL-17. These observations prompt the possibility that Th17 cells, which are known to aggravate disease progression in NASH, upregulate TGF-β-mediated production of IL-22 in ILC3s, thus initiating a compensatory response to the local pro-inflammatory milieu in NASH livers. Upon defining a role for ILC3s in NASH, it will therefore be beneficial to include other immune cells *in vitro* experiments in order to identify additional cellular networks that regulate the quality and quantity of inflammation in NASH livers. Nonetheless, our current findings give support to the hypothesis that damage to hepatocytes in NASH releases chemotactic factors that recruit ILC3s, which in turn participate in tissue repair through production of IL-22, and may be additionally regulated by immunoregulatory factors such as TGF-β (Figure 3.5).

Figure 3.1. Treatment of HepG2 cells with fatty acids±LPS may model the fibrogenic NASH microenvironment.

(A) Representative flow plot of neutral lipids in HepG2 cells were treated with 1 mM fatty acids (oleate:palmitate at a 2:1 ratio) for 24 hours in the presence or absence of 200 ng/mL LPS. Mean fluorescence intensity (MFI) is presented as relative to the BSA control in each experiment.

(B) Cell viability of HepG2 cells upon treatment with fatty acids ± LPS for 24 hours. Viability was determined by crystal violet staining.

(C) Gene expression of TGF-β in HepG2 cells loaded with fatty acids ± LPS for 24 hours. mRNA levels were first normalized to *HPRT1* and then to the average of cells treated with BSA alone.

(D) Fibrogenic gene expression in response to TGF-β. LX2 cells were plated in 12-well plates at 0.25 X 10^6 cells/well. At 12 hours post-plating, the media was replaced with media containing increasing concentrations of TGF-β. Cells were collected for qRT-PCR analysis at 48 h post-treatment. mRNA levels were first normalized to *HPRT1* and then to the average of untreated cells.

Results are the representative or mean of 3-4 independent experiments. Statistical significance was calculated by a one-way ANOVA with Tukey's post-test. *p* values are relative to cells treated with BSA alone. ns: not significant, *$p<0.05$.

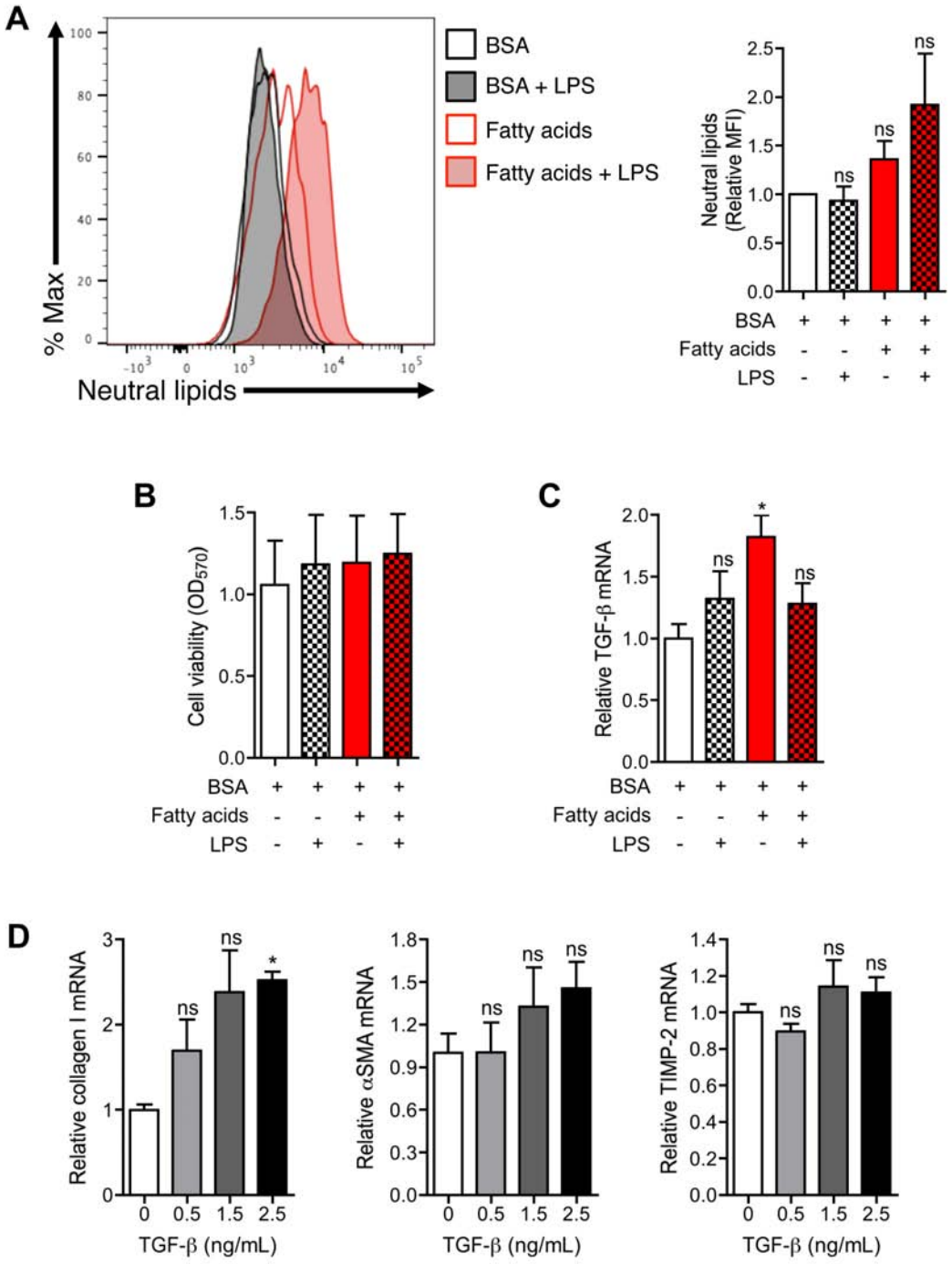
A
% Max
Neutral lipids
BSA
BSA + LPS
Fatty acids
Fatty acids + LPS
Neutral lipids (Relative MFI)
ns
BSA
Fatty acids
LPS
B
Cell viability (OD570)
C
Relative TGF-β mRNA
*
D
Relative collagen I mRNA
Relative αSMA mRNA
Relative TIMP-2 mRNA
TGF-β (ng/mL)

Figure 3.2. ILC3s are the predominant ILC population in PBMCs.

(A) Experimental setup for enrichment of ILCs from human PBMCs.

(B) Flow plots and gating strategy for all 3 groups of ILCs in human PBMCs. Population gates were based on fluorescence minus one (FMO) of freshly thawed, unenriched PBMCs from the same donor. Lineage markers included CD3, CD5, CD14, CD19, and CD94.

Results are representative of 1-3 independent experiments.

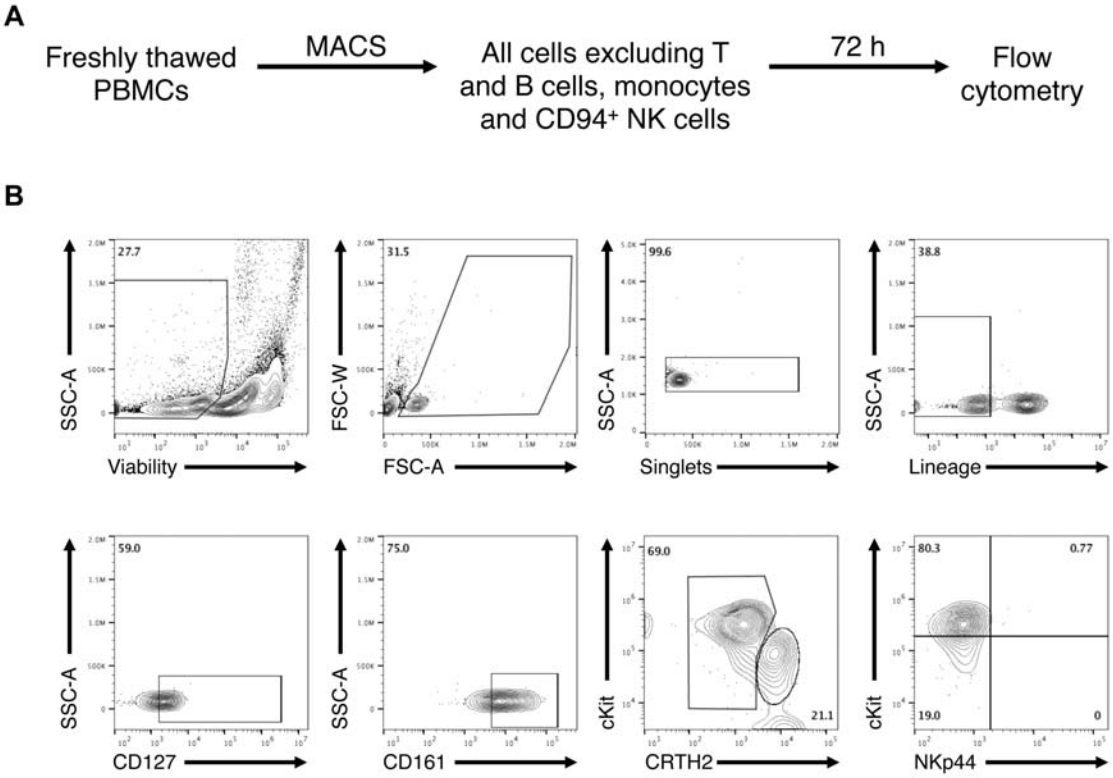
A
Freshly thawed PBMCs
MACS
All cells excluding T and B cells, monocytes and CD94+ NK cells
72 h
Flow cytometry
B
SSC-A
Viability
27.7
FSC-W
FSC-A
31.5
SSC-A
Singlets
99.6
SSC-A
Lineage
38.8
SSC-A
CD127
59.0
SSC-A
CD161
75.0
cKit
CRTH2
69.0
21.1
cKit
NKp44
80.3
0.77
19.0
0

Figure 3.3. Tonsillar ILC3s produce IL-22 upon stimulation.

(A) Experimental setup for enrichment of ILCs from human tonsils.

(B) Gating strategy and frequency of lineage- cells in total mononuclear cells from human tonsils. Flow plots and gating strategy for all 3 groups of ILCs in human tonsils. Population gates were based on fluorescence minus one (FMO) of freshly thawed, unenriched PBMCs from the same donor. Lineage markers included CD3, CD5, CD14, CD19, and CD94.

(C) Gating strategy for all three subsets of ILCs in ILC-enriched cells from human tonsils. Population gates were based on fluorescence minus one (FMO) of unenriched tonsils (B) from the autologous donor cultured for the same length of time as enriched cells. Lineage markers included CD3, CD5, CD14, CD19, and CD94.

(D) Histogram of IL-22 production by NCR^{+}ILC3s in tonsillar ILCs described in (C). TGF-β was added at 2.5 ng/mL for the last 48 hours of culture. Mean fluorescence intensities (MFI) of the $IL\text{-}22^{+}$ population is noted in black for untreated cells and red for cells that were cultured with TGF-β.

Results are from one experiment.

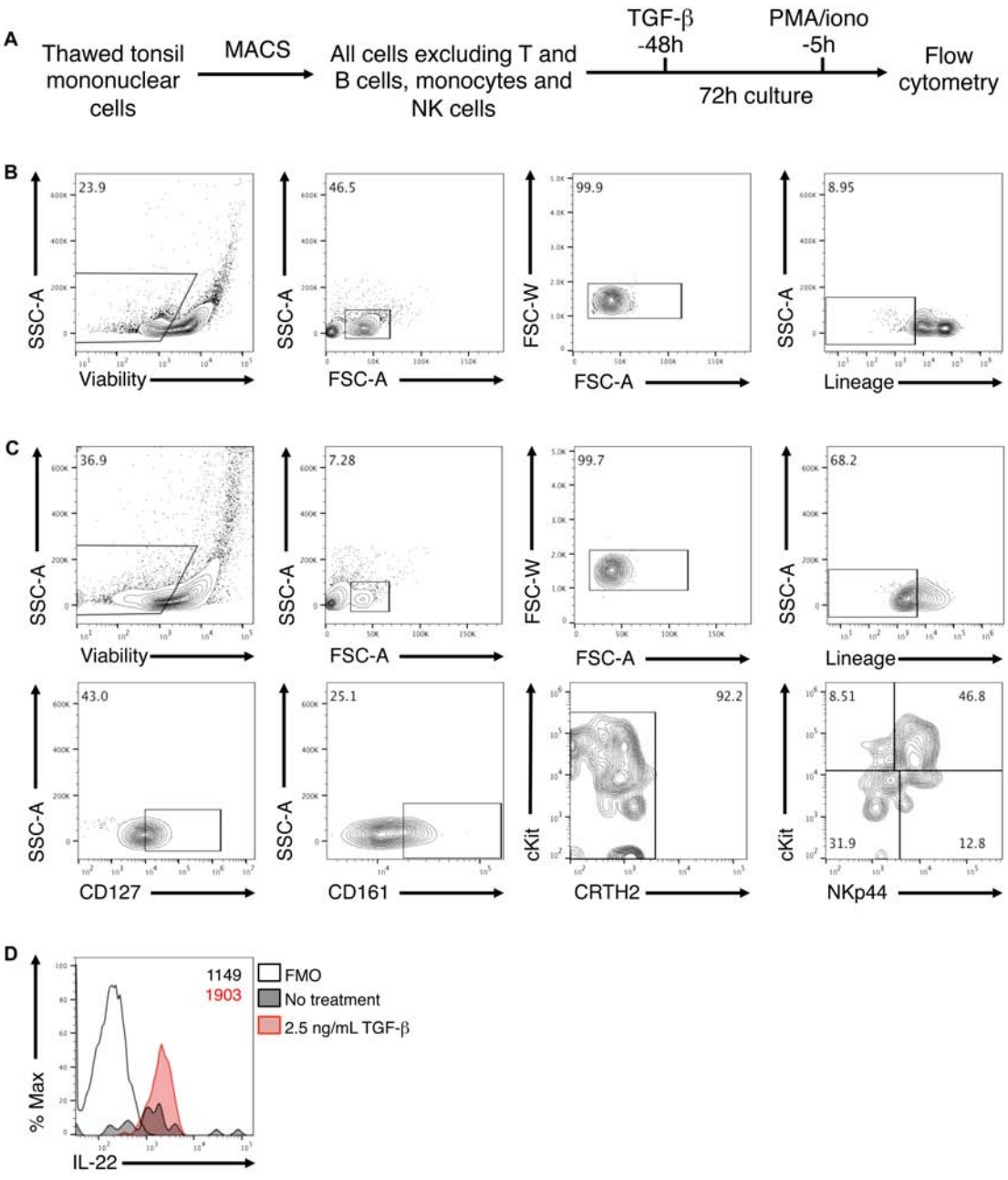
A
Thawed tonsil mononuclear cells
MACS
All cells excluding T and B cells, monocytes and NK cells
TGF-β -48h
PMA/iono -5h
72h culture
Flow cytometry
B
23.9
SSC-A
Viability
46.5
SSC-A
FSC-A
99.9
FSC-W
FSC-A
8.95
SSC-A
Lineage
C
36.9
SSC-A
Viability
7.28
SSC-A
FSC-A
99.7
FSC-W
FSC-A
68.2
SSC-A
Lineage
43.0
SSC-A
CD127
25.1
SSC-A
CD161
92.2
cKit
CRTH2
8.51
46.8
31.9
12.8
cKit
NKp44
D
1149
1903
FMO
No treatment
2.5 ng/mL TGF-β
% Max
IL-22

Figure 3.4. The ILC3 chemotactic factor CCL20 is elevated in NASH *in vitro*.

Cytokines and chemokines were quantified in supernatants from HepG2 cells treated with fatty acids ± LPS for 24 hours by multiplex analysis. The following cytokines were below the limit of detection: IL-1β, -2, -4, -5, -6, -9, -10, -12p70, -13, -15, -17A, -17E, -17F, -21, -22, 23, -27, -28A, -31, -33, GM-CSF, IFNγ, TNF-α, and -β.

Results are the mean of 2 independent experiments.

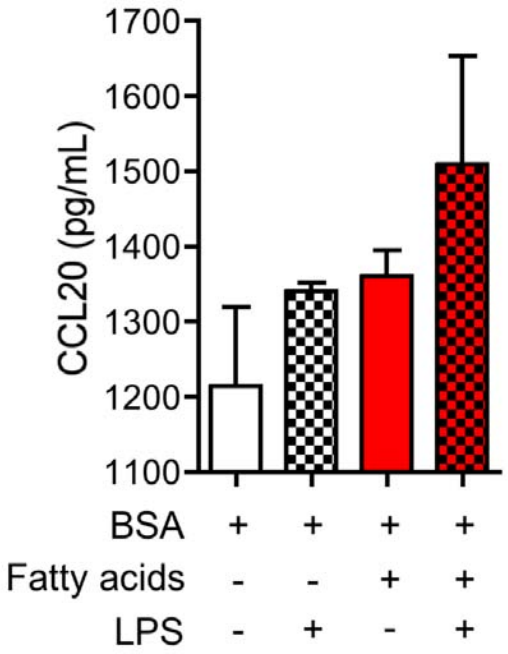
1700
1600
1500
1400
1300
1200
1100
CCL20 (pg/mL)
BSA + + + +
Fatty acids - - + +
LPS - + - +

Figure 3.5. Working model of the interplay between steatotic hepatocytes, HSCs, and ILC3s in NASH.

Hepatocyte injury in NASH is initiated by dysregulated lipid metabolism, which is in part due to increased uptake of free fatty acids from adipose tissue. Damage to the liver is accompanied by loss of epithelial integrity in the gut. We hypothesize that increased translocation of gut contents combined with production of chemotactic factors will recruit ILC3s to the liver, where they will produce IL-22 in an effort to limit hepatocyte death and fibrogenesis by HSCs. Production of TGF-β by steatotic hepatocytes may further enhance ILC3 responses. Solid lines indicate observations from published studies. Dotted lines are hypotheses that require further validation.

CCL: C-C motif chemokine ligand; ILC, innate lymphoid cell; IL, interleukin; TGF-β, transforming growth factor β; HSC, hepatic stellate cell.

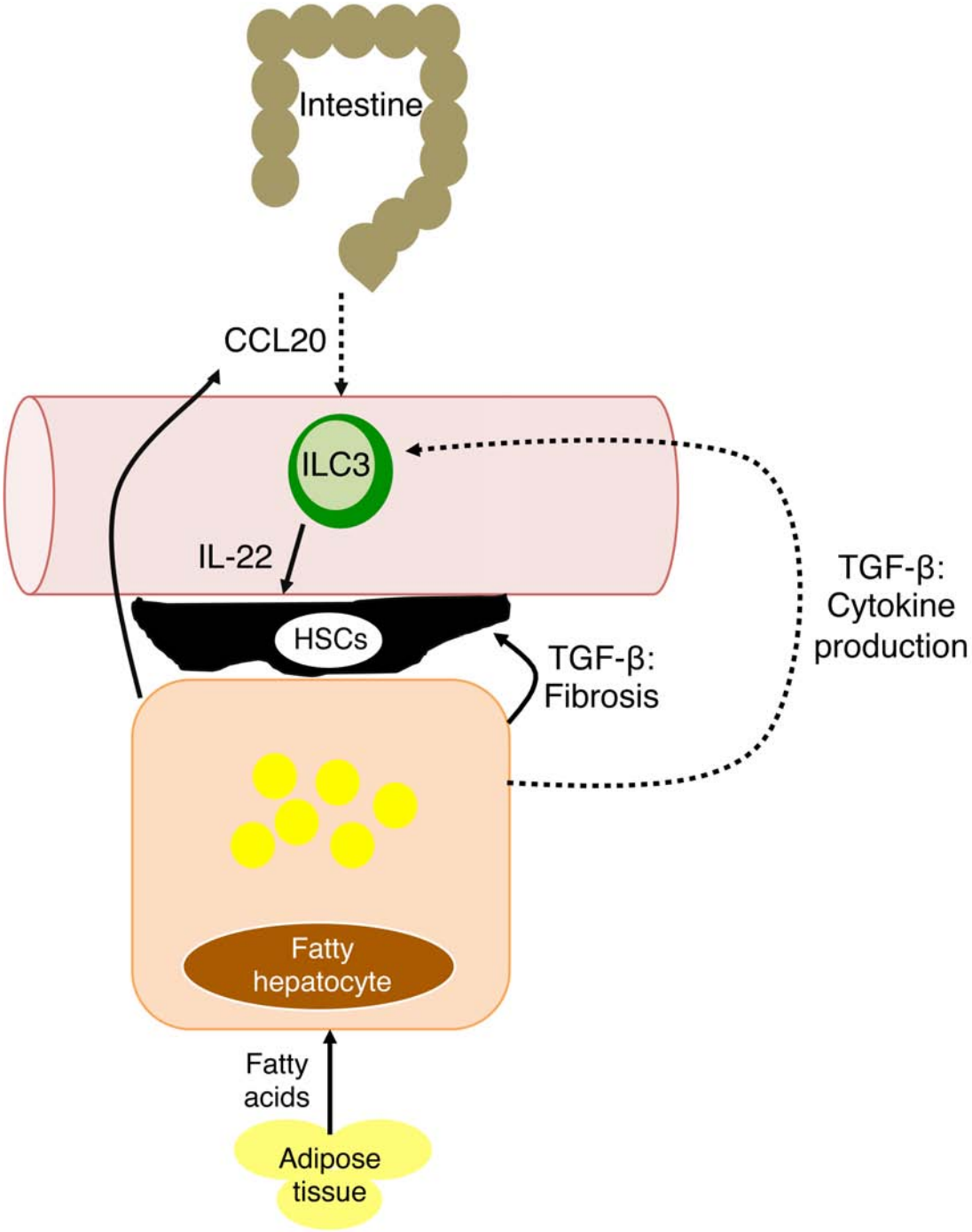
Intestine
CCL20
ILC3
IL-22
HSCs
TGF-β:
Fibrosis
TGF-β:
Cytokine
production
Fatty
hepatocyte
Fatty
acids
Adipose
tissue

CHAPTER 4: Conclusions and future directions

In contrast to skin or conventional mucosal sites, which serve as the first line of defense against potential pathogens in our environments, the liver acts as a secondary, internal firewall, shielding the body from perceived or true molecular and cellular threats that breach our initial safeguards. Yet, it is surprising that the organ that has evolved to detoxify blood of inflammatory contents, and as a result maintains a high level of tolerance to immunogenic insults, is the site of production of acute-phase reactants that trigger systemic alarms. This paradoxical immune response occurs within a microenvironment that is constantly undergoing a high rate of metabolic flux. As a result, it is not surprising that immune responses in the liver alter local and systemic metabolism; in turn, changes in nutrient homeostasis in the liver can induce cellular stress that mounts immune responses. To understand how metabolic changes influence host immunity and inflammation, I explored facets of hepatic lipid metabolism either independently (Chapter 2) or in confluence with the immune response (Chapter 3).

Chronic hepatitis C and NASH are two chronic inflammatory liver diseases that intersect in their reliance on lipid metabolism and the immune response. Despite the similarities in their pathogenesis, chronic hepatitis C and NASH differ not only in their etiology, but also in their evolutionary history. HCV is a hepacivirus whose origins are as yet unresolved. The present genetic diversity of the virus is thought to have grown from two endemic genotypes in Central Africa and South East Asia that have been in existence for 100-200 years (251). Zoonotic transmission is a plausible mode by which the virus was introduced into human populations; however, non-HCV hepaciviruses have only

been reported in horses and dogs, making them unusual zoonotic reservoirs, as most viral infections that arise endemically are transmitted from non-human primates (251-253). Advances in medicine that allowed access to parental routes and increased worldwide travel facilitated the more recent dispersion of the virus. In contrast to HCV, NASH is a very young disease, one that has paralleled the rise of western diet and sendentary lifestyles. Alarmingly, the frequency of pediatric patients with fatty liver disease is on the rise, prompting the question of whether NASH will act as a selective pressure on liver homeostasis in coming generations. Such possibilities give pause to our understanding of the liver and would certainly be fascinating to explore. In this dissertation, I investigated liver biology through more specific lenses of the impact of hepatic lipogenesis on a hepatotropic pathogen and the characteristics of the immune response to dysregulated hepatic lipid metabolism (Figure 4.1).

De novo lipogenesis in HCV infection

To explore the role of *de novo* synthesized lipids in HCV infection, I used two non-competitive inhibitors of ACC, K1 and soraphen A. Soraphen A was first described in 1994 as an antifungal compound isolated from the soil bacterium *Sorangium cellulosum* (254). Given the potency with which soraphen A inhibited eukaryotic ACC, the idea of using it to control HCV infection was patented in 2012 (WO 2012139028 A2). Soraphen A is a macrolide and therefore has poor solubility in water and low bioavailability when administered orally. Therefore, I investigated its effects on HCV in comparison to a novel spiro compound, K1. The maximal reduction in intracellular HCV RNA was ~70% of the DMSO control upon treatment with both ACC inhibitors (Figure

2.2.B, p. 77). Given that the inhibitors are added at 24 hours post-infection, it is possible that the 30% of intracellular viral RNA that persists regardless of the dose or duration of infection is sequestered in areas that are not exposed to cellular factors that degrade RNA. A previous study reported that soraphen A reduced the number and size of double-membraned vesicles that are the site of HCV RNA sequestration and replication (204). Consequently, HCV RNA may be retained in previously unidentified areas of the cell upon ACC inhibitor treatment; identifying these sites may help define novel cellular factors that contribute to HCV infection. Furthermore, the functionality of the residual RNA can be determined by quantifying viral RNA and titers upon replacing the media on cells previously treated with ACC inhibitors.

Interestingly, the loss in viral RNA was partially replicated in siRNA knockdown of both ACC1 and ACC2 (Figure 2.2.H, p. 77). As mentioned above, previous studies suggest redundancy in the two isoforms with regards to *de novo* fatty acid synthesis (209). However, I was still surprised that the reduction in viral RNA was comparable between knockdown of both isoforms, especially since transcript levels of ACC1 were unaffected by K1 and soraphen A, while ACC2 mRNA was partially reduced (Figure 2.2.I and 2.2.J, p. 77). Instead, I had hypothesized that if ACC1 and ACC2 were indeed functionally redundant, then the expression of both isoforms would be upregulated upon K1 or soraphen A treatment in an attempt to restore lipid homeostasis. Therefore, interpreting the relative contributions of ACC isoforms to HCV infection requires further experimentation, including quantifying relative expression levels of ACC1 and ACC2 proteins in infected hepatocytes, evaluating enzyme activation through changes in

phosphorylation, and identifying whether lipogenic functional redundancy of the isoforms is preserved upon K1 and soraphen A treatment.

In addition to its canonical role in *de novo* lipogenesis, ACC is also known to affect histone acetylation and has been detected in the nucleus of human hepatocytes (17, 255). It would be interesting if inhibiting *de novo* lipogenesis induces epigenetic changes that either act to limit propagation of HCV in infected hepatocytes or confer resistance to viral infection in uninfected hepatocytes. This possibility is further supported by the reduction in membrane phospholipids and diacylglycerols upon inhibition of ACC in uninfected and infected hepatocytes, as they may be indicative of changes in the activities of master transcription factors involved in the synthesis of these lipids. Evaluating epigenetic marks at genes that participate in lipid metabolism or genomic occupation by transcription factors such as SREBPs will be useful in testing the possibility that inhibiting ACC activity regulates lipogenic and perhaps other transcription programs that contribute to HCV infection.

Regardless of the mechanism by which inhibition of *de novo* lipogenesis mediates changes in the hepatocyte lipidome, it is remarkable that a process that typically contributes <5% of the hepatic fatty acid supply is essential to the cell. As an example, despite being cultured in complete media, which contains fatty acids, both uninfected and infected hepatocytes displayed a marked loss in lipid droplets upon K1 and soraphen A treatment (Figure 2.10.A, p. 94). The near complete absence of lipid droplets suggests that ACC inhibition stimulates a state of starvation in the cell, such that all intracellular depots of lipids are depleted and the supply of lipids from extracellular sources is insufficient to replete these depots. Only when fatty acids are supplied in excess do the

lipid droplets return (Figure 2.8.A, 2.8.B and 2.8.D, p. 90). Furthermore, the addition of exogenous fatty acids restores lipid droplets only when the fatty acids are added in a specific ratio. Indeed, my attempts to load various hepatoma cell lines with just palmitate did not produce any changes in the neutral lipid content as measured by lipid droplets (data not shown). These observations suggest that while both *de novo* synthesized lipids and exogenous lipids can supply lipid droplets, inhibition of *de novo* lipogenesis reprograms the uptake and/or channeling of extracellular fatty acids away from lipid droplets under unsaturated conditions.

It is intriguing to speculate on the fate of fatty acids in this starved state: the easiest explanation is that these fatty acids are oxidized to provide fuel for the cell. In fact, given that ACC2 mRNA is decreased upon K1 and soraphen A treatment, it is possible that the functions of ACC2, which include inhibiting β-oxidation, are compromised, resulting in accelerated breakdown of fatty acids in lipid droplets and those taken up from extracellular sources. Alternately, *de novo* synthesized lipids may be unique, perhaps in their intracellular trafficking patterns, making them an essential source of fatty acids for processes such as palmitoylation. HCV proteins are produced in excess of what is required for the formation of the replication complex (78). Yet, the inability of excess viral protein to replicate viral RNA indicates a functional defect resulting from reduced *de novo* lipogenesis, which might include deficiencies in protein palmitoylation. Admittedly, my data on changes in palmitoylation upon ACC inhibition are merely correlative. However, formation of protein aggregates, which have been reported to accumulate depalmitoylated proteins, was increased upon treatment of HCV-infected hepatocytes with ACC inhibitors or 2-bromopalmitate (Figure 2.11, p. 96).

Unfortunately, the spectral range of the aggregate stain precluded their co-localization with HCV proteins. Furthermore, the aggregated proteins likely include unidentified host proteins that may be essential for viral replication. Identifying the contents of these aggregates by subcellular fractionation followed by proteomic analysis may provide compelling evidence for palmitoylation of viral and host proteins in HCV infection.

Indeed, palmitoylation of HCV core was previously shown to be important in targeting it to ER membranes near lipid droplets (107). Conversely, palmitoylation of NS4B was thought to be necessary for the formation of the replication complex and the interaction of NS4B with other viral proteins (108). However, more recent evidence negated these findings as artifacts of overexpression as NS4B produced in a replicating virus (as opposed to a subgenomic replicon or transfection of NS4B alone) did not require palmitoylation to function in HCV replication (109). Nonetheless, even if changes in palmitoylation were the mechanism by which K1 and soraphen A decrease HCV RNA, the question of whether *de novo* synthesized fatty acids themselves are necessary to palmitoylate viral or host proteins remains unknown. Inhibition of *de novo* lipogenesis has been shown to reduce palmitoylation of eNOS through direct loss of *de novo* synthesized fatty acids, leading to redistribution of eNOS from the membrane to the cytoplasm (179). Importantly, addition of exogenous fatty acids failed to reverse the mislocalization of eNOS, suggesting that exogenous fatty acid may not be sufficient to restore palmitoylation (179). These findings provide additional support for the hypothesis that *de novo* synthesized lipids play a unique role in HCV infection.

Loss of protein palmitoylation could also result from changes in localization of the DHHC family of protein acyltransferases. The specificity of DHHC enzymes is partly

dependent on their co-localization with the substrate (206). Expression, localization, and function of DHHC enzymes during HCV infection have not been explored and may prove to be an exciting means of altering the course of disease. In contrast, expression of depalmitoylating proteins, namely palmitoyl-protein thioesterases (PPTs), may also be altered in HCV infection. In fact, if K1 and soraphen A treatment simulates a state of starvation in the cell, enhanced activity of PPTs may be a means to recycle the limited supply of fatty acids. Similar to DHHC proteins, the role of PPTs in HCV infection has not been reported and may provide interesting insights into the pathogenesis of HCV infection, even if it is independent of *de novo* lipogenesis.

De novo **lipogenesis: beyond the pathogenesis of hepatitis C**

The inhibition of *de novo* lipogenesis resulted in a marked loss in HCV replication. These findings have critical implications for other positive-sense RNA viruses, which also replicate within intracellular membranes, producing characteristic ultrastructural changes that resemble double-membranes vesicles seen in HCV-infected hepatocytes (256). Furthermore, the C protein of the liver-tropic dengue virus is analogous to HCV core in that it associates with lipid droplets and the ER to facilitate viral assembly (257, 258). In fact, the genome of all hepatotropic flaviviruses is near identical to HCV in that it consists of structural proteins and nonstructural proteins, which include helicases, proteases, and polymerases that serve identical functions to their HCV counterparts. It is therefore likely that inhibition of *de novo* lipogenesis would hinder the replication of other positive-sense RNA viruses using the same mechanisms as HCV infection. If so, inhibiting *de novo* lipogenesis may have some therapeutic value, for

while the idea of limiting *de novo* lipogenesis *in vivo* seems too drastic for *Flaviviridae* viruses that can be treated with less adverse measures, it may be an option for infections with encephalitic members of the *Togaviridae*, for which there are no existing treatments.

In addition to its potential role in the life cycles of other viruses, *de novo* lipogenesis is also necessary for inducing optimal responses in non-hepatocyte host cells. Since 2011, the use of direct-acting antivirals has revolutionized the treatment of hepatitis C and has been hailed as a cure for over 95% of patients infected with genotype 1. Although genotypic limitations and emergence of resistant strains continue to be a cause for concern, the newest frontier in hepatitis C research is a renewed effort at generating prophylactic or therapeutic vaccines. In parallel, studies in the past 5 years have identified specific metabolic requirements for optimal immune responses. Unfortunately, I did not find any measurable differences in the innate immune responses of hepatocytes upon ACC inhibition. However, the lessons learned from the hypolipidemic state of hepatocytes upon ACC inhibition may be applicable to immune cells as well. Indeed, treatment of T cells with soraphen A was shown to inhibit differentiation of CD4 T cells toward Th17 fates (259). In contrast, Tregs do not depend on *de novo* lipogenesis for lipid synthesis and instead meet their metabolic requirements using exogenous fatty acids (259). We previously showed that both Th17 cells and Tregs are increased during HCV infection at the cost of Th1 responses, which are necessary for generating effective anti-viral responses (260-262). Modulating *de novo* lipogenesis in immune cells may thus be an effective way of generating effective anti-viral CD4 T cell and likely other immune responses.

ILCs: newcomers to liver diseases

The recent discovery of ILCs has opened new avenues of investigation in several immune-mediated pathologies. In the liver, non-NK cell ILCs are only beginning to be understood as significant cellular players that can ameliorate or aggravate tissue injury in viral or chemical hepatitis, biliary disease, or hepatatectomy (263-269). However, there are no reports of the contributions of ILCs to NAFLD or its progression to NASH. Furthermore, several of these studies use mouse models; murine ILCs are not always phenotypically or functionally comparable to human ILCs. The preliminary experiments described in Chapter 3 are therefore a promising start to fill the niche for the role of human ILCs in the pathogenesis of NASH.

Blood or tonsil derived cells present a unique opportunity to identify and monitor molecular triggers that regulate ILC responses at various stages of NASH. However, as ILCs are typically mucosal-resident cells, results obtained from blood and lymphoid organs must be interpreted with caution. In particular, expression of transcription factors that define each ILC subset, namely T-bet for ILC1s, GATA3 for ILC2s, and RORγt for ILC3s, must first be demonstrated in these cells. Furthermore, although I have preliminary data demonstrating production of IL-22 by ILC3s upon stimulation with PMA/ionomycin, it would be useful to verify these findings upon cytokine stimulation with IL-23 and/or IL-1β. Similarly, production of cytokines such as IFN-γ by ILC1s and classic Th2 cytokines by ILC2s may help confirm that these blood and tonsil-derived ILCs are identical in phenotype and function to their mucosal counterparts. Lastly, while blood derived ILCs may have opportunities to encounter steatotic hepatocytes *in vivo*, tonsillar ILCs may be representative of those found in liver draining lymph nodes.

Despite the differences in murine and human ILCs, it may be necessary to employ mouse models to at least identify if these lymphoid-resident ILCs are able to circulate to the liver. Alternatively, evaluating the expression of chemokines in NASH livers and associated chemokine receptors on ILCs will help establish if these cells are capable of migrating to the inflamed liver. If these peripheral ILCs are proven to be bona fide ILCs, they present innumerable possibilities for studying ILC responses in humans under healthy and pathological conditions. However, with regards to NAFLD or NASH, identification of healthy controls presents an interesting challenge, as estimates of NAFLD are as high as 30% of adults in the U.S. Comparing ILC distributions across various liver pathologies may better inform ILC changes that are unique to NASH.

Assuming that the caveats of using non-mucosal sources of ILCs to study quasi-mucosal responses in the liver are adequately addressed, there are several interesting biological outcomes that could be investigated with regards to ILCs in NASH. I hypothesize that ILC3s responses will predominate in NASH livers, given that these cells will migrate from the gut to the liver due to the loss of epithelial integrity and increased translocation of bacterial products. However, as studies in other models of liver injury have described pathogenic and beneficial roles for ILC1s and ILC2s, it is highly possible that all three subsets of ILCs will participate in the progression of NASH. Identifying the respective contributions of ILC1s, ILC2s, and ILC3s to NASH pathogenesis will provide a more thorough understanding of the complexity of the disease. Similarly, the experimental setup I have used thus far eliminates the majority of immune cells in both blood and tonsil-derived ILC cultures. Determining the interactions between ILCs, other

immune cells, and non-immune cells such as hepatocytes, liver sinusoidal endothelial cells, and stellate cells are sure to provide intriguing insights into liver biology.

The existence of various types of ILCs has also prompted inquiries into the plasticity between subsets. Thus far, reversible plasticity has been established between ILC1s and ILC3s, while ILC2s have been reported to adopt ILC1-like features (139, 270-274). Given the inflammatory environment in NASH, it is possible that ILC populations that are initially recruited to restore tissue homeostasis convert to more proinflammatory and pathogenic phenotypes. Tracking expression of T-bet, GATA3, and RORγt in enriched ILCs cultured with supernatants of steatotic hepatocytes will help determine if functional plasticity of ILCs can also occur in NASH. Furthermore, I was captivated by the recent report of the contrasting effects of Notch signaling and TGF-β on development of NCR^{+}ILC3s (247). I had expected TGF-β to similarly impede ILC3 function by decreasing the production of IL-22. However, the MFI of IL-22 was elevated in cells that were cultured in the presence of TGF-β, indicating that TGF-β's role in ILC3 function may differ from its role in development (Figures 3.3.D, p. 117 and 3.5, p.121). Alternately, these differences may also reflect divergent effects of TGF-β on human and mouse ILC3s. Importantly, as TGF-β is known pathogenic factor in all chronic liver diseases, my preliminary findings regarding its effect on ILC3 function may have significant implications for NASH and other equally challenging hepatic diseases.

Chronic liver diseases

The contributions of hepatitis C and NASH to chronic liver diseases are predicted to diverge in the upcoming years. The development of highly effective direct-acting

antivirals, improved testing of blood products, and decline of the baby-boomer generation is predicted to significantly reduce the burden of hepatitis C both in the U.S. and worldwide. In contrast, the continued spread of the obesity epidemic and Western lifestyles forecast fatty liver disease as the leading cause of liver transplants. Hepatitis C stands as a remarkable example of how scientific inquiry can go from identifying a virus to developing agents that combat it in nearly 95% of infected individuals in just over 25 years. Meanwhile, our understanding of the pathogenesis of fatty liver disease presents a challenge greater than combating a foreign pathogen—changing human behavior. Researching these highly convoluted pathologies at such critical epidemiological junctures provides a rare opportunity to participate in understanding how molecular and cellular elements inform the evolution of human society.

Specifically, the following concepts in the pathogenesis of chronic liver diseases warrant further investigation regardless of the etiology: 1) metabolic flux among parenchymal (e.g. hepatocytes) and non-parenchymal cells (e.g. sinusoidal cells, stellate cells, hematopoietic stem cells, and immune cells); 2) changes in the immune responses of non-immune and resident and infiltrating hematopoietic cells as a result of disease-induced metabolic flux; 3) conversion of the hepatic microenvironment to a mucosal site due to alterations in the gut-liver axis through migration of immune cells from extrahepatic tissues or proliferation and differentiation from liver-resident progenitors. A deeper understanding of these processes will help identify pathogenic mechanisms that can be manipulated to restore homeostasis.

Figure 4.1. Lipid metabolism and inflammation in the pathogenesis of chronic liver diseases.

Chronic liver diseases are marked by dysregulated lipid synthesis that initiates inflammatory responses that further aggravate disease. Such changes in hepatic lipid metabolism can be caused by pathogens such as the hepatitis C virus (HCV) or by consumption of lipid-rich foods. Pathogeneses of these diseases are further complicated by the influx of lipids from extracellular sources and immune cells from extrahepatic sites. Green arrows mark lines of investigation undertaken in this dissertation.

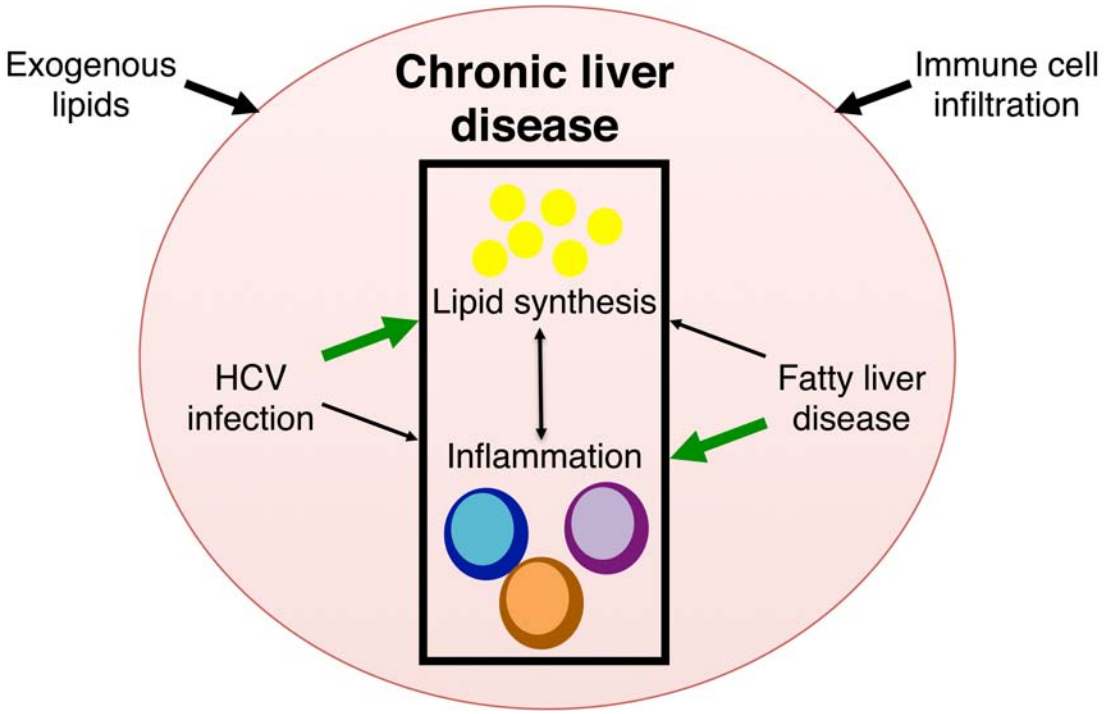
Exogenous lipids
Chronic liver disease
Immune cell infiltration
Lipid synthesis
HCV infection
Fatty liver disease
Inflammation

LITERATURE CITED

1. Xu J, Murphy SL, Kochanek KD, Bastian BA. 2016. *Deaths: Final Data for 2013*, U.S. Department of Health and Human Services, Hyattsville, MD
2. Neff GW, Duncan CW, Schiff ER. 2011. The current economic burden of cirrhosis. *Gastroenterology & hepatology* 7: 661-71
3. 2016. *Donors recovered in the U.S. by donor type*, Organ Procurement and Transplantation Network
4. 2016. *Overall by Organ: Current U.S. Waiting List*, Organ Procurement and Transplantation Network
5. Barrows BR, Parks EJ. 2006. Contributions of different fatty acid sources to very low-density lipoprotein-triacylglycerol in the fasted and fed states. *The Journal of clinical endocrinology and metabolism* 91: 1446-52
6. Coburn CT, Knapp FF, Jr., Febbraio M, Beets AL, Silverstein RL, Abumrad NA. 2000. Defective uptake and utilization of long chain fatty acids in muscle and adipose tissues of CD36 knockout mice. *The Journal of biological chemistry* 275: 32523-9
7. Koonen DP, Jacobs RL, Febbraio M, Young ME, Soltys CL, Ong H, Vance DE, Dyck JR. 2007. Increased hepatic CD36 expression contributes to dyslipidemia associated with diet-induced obesity. *Diabetes* 56: 2863-71
8. Falcon A, Doege H, Fluitt A, Tsang B, Watson N, Kay MA, Stahl A. 2010. FATP2 is a hepatic fatty acid transporter and peroxisomal very long-chain acyl-CoA synthetase. *American journal of physiology. Endocrinology and metabolism* 299: E384-93
9. Doege H, Baillie RA, Ortegon AM, Tsang B, Wu Q, Punreddy S, Hirsch D, Watson N, Gimeno RE, Stahl A. 2006. Targeted deletion of FATP5 reveals multiple functions in liver metabolism: alterations in hepatic lipid homeostasis. *Gastroenterology* 130: 1245-58
10. Bass NM. 1990. Fatty acid-binding protein expression in the liver: its regulation and relationship to the zonation of fatty acid metabolism. *Molecular and cellular biochemistry* 98: 167-76
11. Klein K, Steinberg R, Fiethen B, Overath P. 1971. Fatty acid degradation in Escherichia coli. An inducible system for the uptake of fatty acids and further characterization of old mutants. *European journal of biochemistry / FEBS* 19: 442-50
12. Knudsen J, Jensen MV, Hansen JK, Faergeman NJ, Neergaard TB, Gaigg B. 1999. Role of acylCoA binding protein in acylCoA transport, metabolism and cell signaling. *Molecular and cellular biochemistry* 192: 95-103
13. Mashek DG. 2013. Hepatic fatty acid trafficking: multiple forks in the road. *Advances in nutrition* 4: 697-710
14. Hardie DG. 1989. Regulation of fatty acid synthesis via phosphorylation of acetyl-CoA carboxylase. *Progress in lipid research* 28: 117-46
15. Tong L. 2005. Acetyl-coenzyme A carboxylase: crucial metabolic enzyme and attractive target for drug discovery. *Cellular and molecular life sciences : CMLS* 62: 1784-803

16. Wakil SJ, Stoops JK, Joshi VC. 1983. Fatty acid synthesis and its regulation. *Annual review of biochemistry* 52: 537-79
17. Abu-Elheiga L, Brinkley WR, Zhong L, Chirala SS, Woldegiorgis G, Wakil SJ. 2000. The subcellular localization of acetyl-CoA carboxylase 2. *Proceedings of the National Academy of Sciences of the United States of America* 97: 1444-9
18. Iverson AJ, Bianchi A, Nordlund AC, Witters LA. 1990. Immunological analysis of acetyl-CoA carboxylase mass, tissue distribution and subunit composition. *The Biochemical journal* 269: 365-71
19. Abu-Elheiga L, Matzuk MM, Abo-Hashema KA, Wakil SJ. 2001. Continuous fatty acid oxidation and reduced fat storage in mice lacking acetyl-CoA carboxylase 2. *Science* 291: 2613-6
20. Averhoff FM, Glass N, Holtzman D. 2012. Global burden of hepatitis C: considerations for healthcare providers in the United States. *Clinical infectious diseases : an official publication of the Infectious Diseases Society of America* 55 Suppl 1: S10-5
21. Feinstone SM, Kapikian AZ, Purcell RH, Alter HJ, Holland PV. 1975. Transfusion-associated hepatitis not due to viral hepatitis type A or B. *The New England journal of medicine* 292: 767-70
22. Tsoulfas G, Goulis I, Giakoustidis D, Akriviadis E, Agorastou P, Imvrios G, Papanikolaou V. 2009. Hepatitis C and liver transplantation. *Hippokratia* 13: 211-5
23. Beste LA, Ioannou GN. 2015. Prevalence and treatment of chronic hepatitis C virus infection in the US Department of Veterans Affairs. *Epidemiologic reviews* 37: 131-43
24. Berenguer M. 2008. Treatment of chronic hepatitis C in hemodialysis patients. *Hepatology* 48: 1690-9
25. Hezode C, Fontaine H, Dorival C, Larrey D, Zoulim F, Canva V, de Ledinghen V, Poynard T, Samuel D, Bourliere M, Zarski JP, Raabe JJ, Alric L, Marcellin P, Riachi G, Bernard PH, Loustaud-Ratti V, Metivier S, Tran A, Serfaty L, Abergel A, Causse X, Di Martino V, Guyader D, Lucidarme D, Grando-Lemaire V, Hillon P, Feray C, Dao T, Cacoub P, Rosa I, Attali P, Petrov-Sanchez V, Barthe Y, Pawlotsky JM, Pol S, Carrat F, Bronowicki JP. 2013. Triple therapy in treatment-experienced patients with HCV-cirrhosis in a multicentre cohort of the French Early Access Programme (ANRS CO20-CUPIC) - NCT01514890. *Journal of hepatology* 59: 434-41
26. Jacobson IM, McHutchison JG, Dusheiko G, Di Bisceglie AM, Reddy KR, Bzowej NH, Marcellin P, Muir AJ, Ferenci P, Flisiak R, George J, Rizzetto M, Shouval D, Sola R, Terg RA, Yoshida EM, Adda N, Bengtsson L, Sankoh AJ, Kieffer TL, George S, Kauffman RS, Zeuzem S. 2011. Telaprevir for previously untreated chronic hepatitis C virus infection. *The New England journal of medicine* 364: 2405-16
27. Poordad F, McCone J, Jr., Bacon BR, Bruno S, Manns MP, Sulkowski MS, Jacobson IM, Reddy KR, Goodman ZD, Boparai N, DiNubile MJ, Sniukiene V, Brass CA, Albrecht JK, Bronowicki JP. 2011. Boceprevir for untreated chronic HCV genotype 1 infection. *The New England journal of medicine* 364: 1195-206

28. Afdhal N, Zeuzem S, Kwo P, Chojkier M, Gitlin N, Puoti M, Romero-Gomez M, Zarski JP, Agarwal K, Buggisch P, Foster GR, Brau N, Buti M, Jacobson IM, Subramanian GM, Ding X, Mo H, Yang JC, Pang PS, Symonds WT, McHutchison JG, Muir AJ, Mangia A, Marcellin P. 2014. Ledipasvir and sofosbuvir for untreated HCV genotype 1 infection. *The New England journal of medicine* 370: 1889-98
29. Afdhal N, Reddy KR, Nelson DR, Lawitz E, Gordon SC, Schiff E, Nahass R, Ghalib R, Gitlin N, Herring R, Lalezari J, Younes ZH, Pockros PJ, Di Bisceglie AM, Arora S, Subramanian GM, Zhu Y, Dvory-Sobol H, Yang JC, Pang PS, Symonds WT, McHutchison JG, Muir AJ, Sulkowski M, Kwo P. 2014. Ledipasvir and sofosbuvir for previously treated HCV genotype 1 infection. *The New England journal of medicine* 370: 1483-93
30. Kowdley KV, Gordon SC, Reddy KR, Rossaro L, Bernstein DE, Lawitz E, Shiffman ML, Schiff E, Ghalib R, Ryan M, Rustgi V, Chojkier M, Herring R, Di Bisceglie AM, Pockros PJ, Subramanian GM, An D, Svarovskaia E, Hyland RH, Pang PS, Symonds WT, McHutchison JG, Muir AJ, Pound D, Fried MW. 2014. Ledipasvir and sofosbuvir for 8 or 12 weeks for chronic HCV without cirrhosis. *The New England journal of medicine* 370: 1879-88
31. Hagan LM, Sulkowski MS, Schinazi RF. 2014. Cost analysis of sofosbuvir/ribavirin versus sofosbuvir/simeprevir for genotype 1 hepatitis C virus in interferon-ineligible/intolerant individuals. *Hepatology* 60: 37-45
32. Klevens RM, Hu DJ, Jiles R, Holmberg SD. 2012. Evolving epidemiology of hepatitis C virus in the United States. *Clinical infectious diseases : an official publication of the Infectious Diseases Society of America* 55 Suppl 1: S3-9
33. Choo QL, Kuo G, Weiner AJ, Overby LR, Bradley DW, Houghton M. 1989. Isolation of a cDNA clone derived from a blood-borne non-A, non-B viral hepatitis genome. *Science* 244: 359-62
34. Feinstone SM, Alter HJ, Dienes HP, Shimizu Y, Popper H, Blackmore D, Sly D, London WT, Purcell RH. 1981. Non-A, non-B hepatitis in chimpanzees and marmosets. *The Journal of infectious diseases* 144: 588-98
35. Bradley DW, Maynard JE, Popper H, Ebert JW, Cook EH, Fields HA, Kemler BJ. 1981. Persistent non-A, non-B hepatitis in experimentally infected chimpanzees. *The Journal of infectious diseases* 143: 210-8
36. He LF, Alling D, Popkin T, Shapiro M, Alter HJ, Purcell RH. 1987. Determining the size of non-A, non-B hepatitis virus by filtration. *The Journal of infectious diseases* 156: 636-40
37. Bradley DW, Maynard JE, Popper H, Cook EH, Ebert JW, McCaustland KA, Schable CA, Fields HA. 1983. Posttransfusion non-A, non-B hepatitis: physicochemical properties of two distinct agents. *The Journal of infectious diseases* 148: 254-65
38. Feinstone SM, Mihalik KB, Kamimura T, Alter HJ, London WT, Purcell RH. 1983. Inactivation of hepatitis B virus and non-A, non-B hepatitis by chloroform. *Infection and immunity* 41: 816-21
39. Smith DB, Bukh J, Kuiken C, Muerhoff AS, Rice CM, Stapleton JT, Simmonds P. 2014. Expanded classification of hepatitis C virus into 7 genotypes and 67

subtypes: updated criteria and genotype assignment web resource. *Hepatology* 59: 318-27
40. Zein NN. 2000. Clinical significance of hepatitis C virus genotypes. *Clinical microbiology reviews* 13: 223-35
41. Lindenbach BD, Rice CM. 2013. The ins and outs of hepatitis C virus entry and assembly. *Nature reviews. Microbiology* 11: 688-700
42. Agnello V, Abel G, Elfahal M, Knight GB, Zhang QX. 1999. Hepatitis C virus and other flaviviridae viruses enter cells via low density lipoprotein receptor. *Proceedings of the National Academy of Sciences of the United States of America* 96: 12766-71
43. Monazahian M, Bohme I, Bonk S, Koch A, Scholz C, Grethe S, Thomssen R. 1999. Low density lipoprotein receptor as a candidate receptor for hepatitis C virus. *Journal of medical virology* 57: 223-9
44. Germi R, Crance JM, Garin D, Guimet J, Lortat-Jacob H, Ruigrok RW, Zarski JP, Drouet E. 2002. Cellular glycosaminoglycans and low density lipoprotein receptor are involved in hepatitis C virus adsorption. *Journal of medical virology* 68: 206-15
45. Scarselli E, Ansuini H, Cerino R, Roccasecca RM, Acali S, Filocamo G, Traboni C, Nicosia A, Cortese R, Vitelli A. 2002. The human scavenger receptor class B type I is a novel candidate receptor for the hepatitis C virus. *The EMBO journal* 21: 5017-25
46. Dao Thi VL, Granier C, Zeisel MB, Guerin M, Mancip J, Granio O, Penin F, Lavillette D, Bartenschlager R, Baumert TF, Cosset FL, Dreux M. 2012. Characterization of hepatitis C virus particle subpopulations reveals multiple usage of the scavenger receptor BI for entry steps. *The Journal of biological chemistry* 287: 31242-57
47. Bankwitz D, Steinmann E, Bitzegeio J, Ciesek S, Friesland M, Herrmann E, Zeisel MB, Baumert TF, Keck ZY, Foung SK, Pecheur EI, Pietschmann T. 2010. Hepatitis C virus hypervariable region 1 modulates receptor interactions, conceals the CD81 binding site, and protects conserved neutralizing epitopes. *Journal of virology* 84: 5751-63
48. Brazzoli M, Bianchi A, Filippini S, Weiner A, Zhu Q, Pizza M, Crotta S. 2008. CD81 is a central regulator of cellular events required for hepatitis C virus infection of human hepatocytes. *Journal of virology* 82: 8316-29
49. Evans MJ, von Hahn T, Tscherne DM, Syder AJ, Panis M, Wolk B, Hatziioannou T, McKeating JA, Bieniasz PD, Rice CM. 2007. Claudin-1 is a hepatitis C virus co-receptor required for a late step in entry. *Nature* 446: 801-5
50. Harris HJ, Davis C, Mullins JG, Hu K, Goodall M, Farquhar MJ, Mee CJ, McCaffrey K, Young S, Drummer H, Balfe P, McKeating JA. 2010. Claudin association with CD81 defines hepatitis C virus entry. *The Journal of biological chemistry* 285: 21092-102
51. Sourisseau M, Michta ML, Zony C, Israelow B, Hopcraft SE, Narbus CM, Parra Martin A, Evans MJ. 2013. Temporal analysis of hepatitis C virus cell entry with occludin directed blocking antibodies. *PLoS pathogens* 9: e1003244
52. Benedicto I, Molina-Jimenez F, Bartosch B, Cosset FL, Lavillette D, Prieto J, Moreno-Otero R, Valenzuela-Fernandez A, Aldabe R, Lopez-Cabrera M,

Majano PL. 2009. The tight junction-associated protein occludin is required for a postbinding step in hepatitis C virus entry and infection. *Journal of virology* 83: 8012-20

53. Ploss A, Evans MJ, Gaysinskaya VA, Panis M, You H, de Jong YP, Rice CM. 2009. Human occludin is a hepatitis C virus entry factor required for infection of mouse cells. *Nature* 457: 882-6
54. Dorner M, Horwitz JA, Robbins JB, Barry WT, Feng Q, Mu K, Jones CT, Schoggins JW, Catanese MT, Burton DR, Law M, Rice CM, Ploss A. 2011. A genetically humanized mouse model for hepatitis C virus infection. *Nature* 474: 208-11
55. Dorner M, Horwitz JA, Donovan BM, Labitt RN, Budell WC, Friling T, Vogt A, Catanese MT, Satoh T, Kawai T, Akira S, Law M, Rice CM, Ploss A. 2013. Completion of the entire hepatitis C virus life cycle in genetically humanized mice. *Nature* 501: 237-41
56. Martin DN, Uprichard SL. 2013. Identification of transferrin receptor 1 as a hepatitis C virus entry factor. *Proceedings of the National Academy of Sciences of the United States of America* 110: 10777-82
57. Sainz B, Jr., Barretto N, Martin DN, Hiraga N, Imamura M, Hussain S, Marsh KA, Yu X, Chayama K, Alrefai WA, Uprichard SL. 2012. Identification of the Niemann-Pick C1-like 1 cholesterol absorption receptor as a new hepatitis C virus entry factor. *Nature medicine* 18: 281-5
58. Farquhar MJ, Hu K, Harris HJ, Davis C, Brimacombe CL, Fletcher SJ, Baumert TF, Rappoport JZ, Balfe P, McKeating JA. 2012. Hepatitis C virus induces CD81 and claudin-1 endocytosis. *Journal of virology* 86: 4305-16
59. Lavillette D, Bartosch B, Nourrisson D, Verney G, Cosset FL, Penin F, Pecheur EI. 2006. Hepatitis C virus glycoproteins mediate low pH-dependent membrane fusion with liposomes. *The Journal of biological chemistry* 281: 3909-17
60. Lavillette D, Pecheur EI, Donot P, Fresquet J, Molle J, Corbau R, Dreux M, Penin F, Cosset FL. 2007. Characterization of fusion determinants points to the involvement of three discrete regions of both E1 and E2 glycoproteins in the membrane fusion process of hepatitis C virus. *Journal of virology* 81: 8752-65
61. Perez-Berna AJ, Bernabeu A, Moreno MR, Guillen J, Villalain J. 2008. The pre-transmembrane region of the HCV E1 envelope glycoprotein: interaction with model membranes. *Biochimica et biophysica acta* 1778: 2069-80
62. Drummer HE, Boo I, Poumbourios P. 2007. Mutagenesis of a conserved fusion peptide-like motif and membrane-proximal heptad-repeat region of hepatitis C virus glycoprotein E1. *The Journal of general virology* 88: 1144-8
63. Wang C, Sarnow P, Siddiqui A. 1993. Translation of human hepatitis C virus RNA in cultured cells is mediated by an internal ribosome-binding mechanism. *Journal of virology* 67: 3338-44
64. Niepmann M. 2013. Hepatitis C virus RNA translation. *Current topics in microbiology and immunology* 369: 143-66

65. Grakoui A, Wychowski C, Lin C, Feinstone SM, Rice CM. 1993. Expression and identification of hepatitis C virus polyprotein cleavage products. *Journal of virology* 67: 1385-95
66. Lin C, Lindenbach BD, Pragai BM, McCourt DW, Rice CM. 1994. Processing in the hepatitis C virus E2-NS2 region: identification of p7 and two distinct E2-specific products with different C termini. *Journal of virology* 68: 5063-73
67. Hijikata M, Kato N, Ootsuyama Y, Nakagawa M, Shimotohno K. 1991. Gene mapping of the putative structural region of the hepatitis C virus genome by in vitro processing analysis. *Proceedings of the National Academy of Sciences of the United States of America* 88: 5547-51
68. Hussy P, Langen H, Mous J, Jacobsen H. 1996. Hepatitis C virus core protein: carboxy-terminal boundaries of two processed species suggest cleavage by a signal peptide peptidase. *Virology* 224: 93-104
69. McLauchlan J, Lemberg MK, Hope G, Martoglio B. 2002. Intramembrane proteolysis promotes trafficking of hepatitis C virus core protein to lipid droplets. *The EMBO journal* 21: 3980-8
70. Grakoui A, McCourt DW, Wychowski C, Feinstone SM, Rice CM. 1993. A second hepatitis C virus-encoded proteinase. *Proceedings of the National Academy of Sciences of the United States of America* 90: 10583-7
71. Failla C, Tomei L, De Francesco R. 1994. Both NS3 and NS4A are required for proteolytic processing of hepatitis C virus nonstructural proteins. *Journal of virology* 68: 3753-60
72. Hijikata M, Mizushima H, Akagi T, Mori S, Kakiuchi N, Kato N, Tanaka T, Kimura K, Shimotohno K. 1993. Two distinct proteinase activities required for the processing of a putative nonstructural precursor protein of hepatitis C virus. *Journal of virology* 67: 4665-75
73. Bartenschlager R, Ahlborn-Laake L, Mous J, Jacobsen H. 1994. Kinetic and structural analyses of hepatitis C virus polyprotein processing. *Journal of virology* 68: 5045-55
74. Romero-Brey I, Merz A, Chiramel A, Lee JY, Chlanda P, Haselman U, Santarella-Mellwig R, Habermann A, Hoppe S, Kallis S, Walther P, Antony C, Krijnse-Locker J, Bartenschlager R. 2012. Three-dimensional architecture and biogenesis of membrane structures associated with hepatitis C virus replication. *PLoS pathogens* 8: e1003056
75. Li Y, Yamane D, Masaki T, Lemon SM. 2015. The yin and yang of hepatitis C: synthesis and decay of hepatitis C virus RNA. *Nature reviews. Microbiology* 13: 544-58
76. Binder M, Sulaimanov N, Clausznitzer D, Schulze M, Huber CM, Lenz SM, Schloder JP, Trippler M, Bartenschlager R, Lohmann V, Kaderali L. 2013. Replication vesicles are load- and choke-points in the hepatitis C virus lifecycle. *PLoS pathogens* 9: e1003561
77. Chang M, Williams O, Mittler J, Quintanilla A, Carithers RL, Jr., Perkins J, Corey L, Gretch DR. 2003. Dynamics of hepatitis C virus replication in human liver. *The American journal of pathology* 163: 433-44
78. Quinkert D, Bartenschlager R, Lohmann V. 2005. Quantitative analysis of the hepatitis C virus replication complex. *Journal of virology* 79: 13594-605

79. Dahari H, Ribeiro RM, Rice CM, Perelson AS. 2007. Mathematical modeling of subgenomic hepatitis C virus replication in Huh-7 cells. *Journal of virology* 81: 750-60
80. Kim DW, Gwack Y, Han JH, Choe J. 1995. C-terminal domain of the hepatitis C virus NS3 protein contains an RNA helicase activity. *Biochemical and biophysical research communications* 215: 160-6
81. Suzich JA, Tamura JK, Palmer-Hill F, Warrener P, Grakoui A, Rice CM, Feinstone SM, Collett MS. 1993. Hepatitis C virus NS3 protein polynucleotide-stimulated nucleoside triphosphatase and comparison with the related pestivirus and flavivirus enzymes. *Journal of virology* 67: 6152-8
82. Huang L, Hwang J, Sharma SD, Hargittai MR, Chen Y, Arnold JJ, Raney KD, Cameron CE. 2005. Hepatitis C virus nonstructural protein 5A (NS5A) is an RNA-binding protein. *The Journal of biological chemistry* 280: 36417-28
83. Tellinghuisen TL, Foss KL, Treadaway JC, Rice CM. 2008. Identification of residues required for RNA replication in domains II and III of the hepatitis C virus NS5A protein. *Journal of virology* 82: 1073-83
84. Appel N, Zayas M, Miller S, Krijnse-Locker J, Schaller T, Friebe P, Kallis S, Engel U, Bartenschlager R. 2008. Essential role of domain III of nonstructural protein 5A for hepatitis C virus infectious particle assembly. *PLoS pathogens* 4: e1000035
85. Masaki T, Suzuki R, Murakami K, Aizaki H, Ishii K, Murayama A, Date T, Matsuura Y, Miyamura T, Wakita T, Suzuki T. 2008. Interaction of hepatitis C virus nonstructural protein 5A with core protein is critical for the production of infectious virus particles. *Journal of virology* 82: 7964-76
86. Behrens SE, Tomei L, De Francesco R. 1996. Identification and properties of the RNA-dependent RNA polymerase of hepatitis C virus. *The EMBO journal* 15: 12-22
87. Yuan ZH, Kumar U, Thomas HC, Wen YM, Monjardino J. 1997. Expression, purification, and partial characterization of HCV RNA polymerase. *Biochemical and biophysical research communications* 232: 231-5
88. Appleby TC, Perry JK, Murakami E, Barauskas O, Feng J, Cho A, Fox D, 3rd, Wetmore DR, McGrath ME, Ray AS, Sofia MJ, Swaminathan S, Edwards TE. 2015. Viral replication. Structural basis for RNA replication by the hepatitis C virus polymerase. *Science* 347: 771-5
89. Moradpour D, Englert C, Wakita T, Wands JR. 1996. Characterization of cell lines allowing tightly regulated expression of hepatitis C virus core protein. *Virology* 222: 51-63
90. Miyanari Y, Atsuzawa K, Usuda N, Watashi K, Hishiki T, Zayas M, Bartenschlager R, Wakita T, Hijikata M, Shimotohno K. 2007. The lipid droplet is an important organelle for hepatitis C virus production. *Nature cell biology* 9: 1089-97
91. Bartenschlager R, Penin F, Lohmann V, Andre P. 2011. Assembly of infectious hepatitis C virus particles. *Trends in microbiology* 19: 95-103
92. Dubuisson J, Hsu HH, Cheung RC, Greenberg HB, Russell DG, Rice CM. 1994. Formation and intracellular localization of hepatitis C virus envelope

glycoprotein complexes expressed by recombinant vaccinia and Sindbis viruses. *Journal of virology* 68: 6147-60

93. Cocquerel L, Duvet S, Meunier JC, Pillez A, Cacan R, Wychowski C, Dubuisson J. 1999. The transmembrane domain of hepatitis C virus glycoprotein E1 is a signal for static retention in the endoplasmic reticulum. *Journal of virology* 73: 2641-9
94. Cocquerel L, Meunier JC, Pillez A, Wychowski C, Dubuisson J. 1998. A retention signal necessary and sufficient for endoplasmic reticulum localization maps to the transmembrane domain of hepatitis C virus glycoprotein E2. *Journal of virology* 72: 2183-91
95. Huang H, Sun F, Owen DM, Li W, Chen Y, Gale M, Jr., Ye J. 2007. Hepatitis C virus production by human hepatocytes dependent on assembly and secretion of very low-density lipoproteins. *Proceedings of the National Academy of Sciences of the United States of America* 104: 5848-53
96. Gastaminza P, Cheng G, Wieland S, Zhong J, Liao W, Chisari FV. 2008. Cellular determinants of hepatitis C virus assembly, maturation, degradation, and secretion. *Journal of virology* 82: 2120-9
97. Bradley D, McCaustland K, Krawczynski K, Spelbring J, Humphrey C, Cook EH. 1991. Hepatitis C virus: buoyant density of the factor VIII-derived isolate in sucrose. *Journal of medical virology* 34: 206-8
98. Nielsen SU, Bassendine MF, Burt AD, Martin C, Pumeechockchai W, Toms GL. 2006. Association between hepatitis C virus and very-low-density lipoprotein (VLDL)/LDL analyzed in iodixanol density gradients. *Journal of virology* 80: 2418-28
99. Thomssen R, Bonk S, Propfe C, Heermann KH, Kochel HG, Uy A. 1992. Association of hepatitis C virus in human sera with beta-lipoprotein. *Medical microbiology and immunology* 181: 293-300
100. Hijikata M, Shimizu YK, Kato H, Iwamoto A, Shih JW, Alter HJ, Purcell RH, Yoshikura H. 1993. Equilibrium centrifugation studies of hepatitis C virus: evidence for circulating immune complexes. *Journal of virology* 67: 1953-8
101. Andre P, Komurian-Pradel F, Deforges S, Perret M, Berland JL, Sodoyer M, Pol S, Brechot C, Paranhos-Baccala G, Lotteau V. 2002. Characterization of low- and very-low-density hepatitis C virus RNA-containing particles. *Journal of virology* 76: 6919-28
102. Maillard P, Huby T, Andreo U, Moreau M, Chapman J, Budkowska A. 2006. The interaction of natural hepatitis C virus with human scavenger receptor SR-BI/Cla1 is mediated by ApoB-containing lipoproteins. *FASEB journal : official publication of the Federation of American Societies for Experimental Biology* 20: 735-7
103. von Hahn T, Yoon JC, Alter H, Rice CM, Rehermann B, Balfe P, McKeating JA. 2007. Hepatitis C virus continuously escapes from neutralizing antibody and T-cell responses during chronic infection in vivo. *Gastroenterology* 132: 667-78
104. Shi ST, Lee KJ, Aizaki H, Hwang SB, Lai MM. 2003. Hepatitis C virus RNA replication occurs on a detergent-resistant membrane that cofractionates with caveolin-2. *Journal of virology* 77: 4160-8

105. Aizaki H, Lee KJ, Sung VM, Ishiko H, Lai MM. 2004. Characterization of the hepatitis C virus RNA replication complex associated with lipid rafts. *Virology* 324: 450-61
106. Wang C, Gale M, Jr., Keller BC, Huang H, Brown MS, Goldstein JL, Ye J. 2005. Identification of FBL2 as a geranylgeranylated cellular protein required for hepatitis C virus RNA replication. *Molecular cell* 18: 425-34
107. Majeau N, Fromentin R, Savard C, Duval M, Tremblay MJ, Leclerc D. 2009. Palmitoylation of hepatitis C virus core protein is important for virion production. *The Journal of biological chemistry* 284: 33915-25
108. Yu GY, Lee KJ, Gao L, Lai MM. 2006. Palmitoylation and polymerization of hepatitis C virus NS4B protein. *Journal of virology* 80: 6013-23
109. Paul D, Bartenschlager R, McCormick C. 2015. The predominant species of nonstructural protein 4B in hepatitis C virus-replicating cells is not palmitoylated. *The Journal of general virology* 96: 1696-701
110. Felmlee DJ, Sheridan DA, Bridge SH, Nielsen SU, Milne RW, Packard CJ, Caslake MJ, McLauchlan J, Toms GL, Neely RD, Bassendine MF. 2010. Intravascular transfer contributes to postprandial increase in numbers of very-low-density hepatitis C virus particles. *Gastroenterology* 139: 1774-83, 83 e1-6
111. Diaz O, Delers F, Maynard M, Demignot S, Zoulim F, Chambaz J, Trepo C, Lotteau V, Andre P. 2006. Preferential association of Hepatitis C virus with apolipoprotein B48-containing lipoproteins. *The Journal of general virology* 87: 2983-91
112. Dienes HP, Popper H, Arnold W, Lobeck H. 1982. Histologic observations in human hepatitis non-A, non-B. *Hepatology* 2: 562-71
113. Asselah T, Rubbia-Brandt L, Marcellin P, Negro F. 2006. Steatosis in chronic hepatitis C: why does it really matter? *Gut* 55: 123-30
114. Czaja AJ, Carpenter HA, Santrach PJ, Moore SB. 1998. Host- and disease-specific factors affecting steatosis in chronic hepatitis C. *Journal of hepatology* 29: 198-206
115. Adinolfi LE, Gambardella M, Andreana A, Tripodi MF, Utili R, Ruggiero G. 2001. Steatosis accelerates the progression of liver damage of chronic hepatitis C patients and correlates with specific HCV genotype and visceral obesity. *Hepatology* 33: 1358-64
116. Mihm S, Fayyazi A, Hartmann H, Ramadori G. 1997. Analysis of histopathological manifestations of chronic hepatitis C virus infection with respect to virus genotype. *Hepatology* 25: 735-9
117. Negro F. 2010. Abnormalities of lipid metabolism in hepatitis C virus infection. *Gut* 59: 1279-87
118. Rubbia-Brandt L, Quadri R, Abid K, Giostra E, Male PJ, Mentha G, Spahr L, Zarski JP, Borisch B, Hadengue A, Negro F. 2000. Hepatocyte steatosis is a cytopathic effect of hepatitis C virus genotype 3. *Journal of hepatology* 33: 106-15
119. Poynard T, Ratziu V, McHutchison J, Manns M, Goodman Z, Zeuzem S, Younossi Z, Albrecht J. 2003. Effect of treatment with peginterferon or

interferon alfa-2b and ribavirin on steatosis in patients infected with hepatitis C. *Hepatology* 38: 75-85

120. Browning JD, Horton JD. 2004. Molecular mediators of hepatic steatosis and liver injury. *The Journal of clinical investigation* 114: 147-52
121. Jacobson IM, Gordon SC, Kowdley KV, Yoshida EM, Rodriguez-Torres M, Sulkowski MS, Shiffman ML, Lawitz E, Everson G, Bennett M, Schiff E, Al-Assi MT, Subramanian GM, An D, Lin M, McNally J, Brainard D, Symonds WT, McHutchison JG, Patel K, Feld J, Pianko S, Nelson DR. 2013. Sofosbuvir for hepatitis C genotype 2 or 3 in patients without treatment options. *The New England journal of medicine* 368: 1867-77
122. Charlton MR, Burns JM, Pedersen RA, Watt KD, Heimbach JK, Dierkhising RA. 2011. Frequency and outcomes of liver transplantation for nonalcoholic steatohepatitis in the United States. *Gastroenterology* 141: 1249-53
123. Lambert JE, Ramos-Roman MA, Browning JD, Parks EJ. 2014. Increased de novo lipogenesis is a distinct characteristic of individuals with nonalcoholic fatty liver disease. *Gastroenterology* 146: 726-35
124. Romeo S, Kozlitina J, Xing C, Pertsemlidis A, Cox D, Pennacchio LA, Boerwinkle E, Cohen JC, Hobbs HH. 2008. Genetic variation in PNPLA3 confers susceptibility to nonalcoholic fatty liver disease. *Nature genetics* 40: 1461-5
125. Kozlitina J, Smagris E, Stender S, Nordestgaard BG, Zhou HH, Tybjaerg-Hansen A, Vogt TF, Hobbs HH, Cohen JC. 2014. Exome-wide association study identifies a TM6SF2 variant that confers susceptibility to nonalcoholic fatty liver disease. *Nature genetics* 46: 352-6
126. Adams LA, Lymp JF, St Sauver J, Sanderson SO, Lindor KD, Feldstein A, Angulo P. 2005. The natural history of nonalcoholic fatty liver disease: a population-based cohort study. *Gastroenterology* 129: 113-21
127. Bhattacharjee J, Kumar JM, Arindkar S, Das B, Pramod U, Juyal RC, Majumdar SS, Nagarajan P. 2014. Role of immunodeficient animal models in the development of fructose induced NAFLD. *The Journal of nutritional biochemistry* 25: 219-26
128. Tosello-Trampont AC, Landes SG, Nguyen V, Novobrantseva TI, Hahn YS. 2012. Kuppfer cells trigger nonalcoholic steatohepatitis development in diet-induced mouse model through tumor necrosis factor-alpha production. *The Journal of biological chemistry* 287: 40161-72
129. Lassen MG, Lukens JR, Dolina JS, Brown MG, Hahn YS. 2010. Intrahepatic IL-10 maintains NKG2A+Ly49- liver NK cells in a functionally hyporesponsive state. *Journal of immunology* 184: 2693-701
130. Knolle PA, Uhrig A, Hegenbarth S, Loser E, Schmitt E, Gerken G, Lohse AW. 1998. IL-10 down-regulates T cell activation by antigen-presenting liver sinusoidal endothelial cells through decreased antigen uptake via the mannose receptor and lowered surface expression of accessory molecules. *Clinical and experimental immunology* 114: 427-33
131. Norris S, Collins C, Doherty DG, Smith F, McEntee G, Traynor O, Nolan N, Hegarty J, O'Farrelly C. 1998. Resident human hepatic lymphocytes are

phenotypically different from circulating lymphocytes. *Journal of hepatology* 28: 84-90

132. Waggoner SN, Taniguchi RT, Mathew PA, Kumar V, Welsh RM. 2010. Absence of mouse 2B4 promotes NK cell-mediated killing of activated CD8+ T cells, leading to prolonged viral persistence and altered pathogenesis. *The Journal of clinical investigation* 120: 1925-38
133. Hegde S, Lockridge JL, Becker YA, Ma S, Kenney SC, Gumperz JE. 2011. Human NKT cells direct the differentiation of myeloid APCs that regulate T cell responses via expression of programmed cell death ligands. *Journal of autoimmunity* 37: 28-38
134. Limmer A, Ohl J, Kurts C, Ljunggren HG, Reiss Y, Groettrup M, Momburg F, Arnold B, Knolle PA. 2000. Efficient presentation of exogenous antigen by liver endothelial cells to CD8+ T cells results in antigen-specific T-cell tolerance. *Nature medicine* 6: 1348-54
135. Schildberg FA, Wojtalla A, Siegmund SV, Endl E, Diehl L, Abdullah Z, Kurts C, Knolle PA. 2011. Murine hepatic stellate cells veto CD8 T cell activation by a CD54-dependent mechanism. *Hepatology* 54: 262-72
136. Bertolino P, Trescol-Biemont MC, Rabourdin-Combe C. 1998. Hepatocytes induce functional activation of naive CD8+ T lymphocytes but fail to promote survival. *European journal of immunology* 28: 221-36
137. Sonnenberg GF, Artis D. 2015. Innate lymphoid cells in the initiation, regulation and resolution of inflammation. *Nature medicine* 21: 698-708
138. Klose CS, Kiss EA, Schwierzeck V, Ebert K, Hoyler T, d'Hargues Y, Goppert N, Croxford AL, Waisman A, Tanriver Y, Diefenbach A. 2013. A T-bet gradient controls the fate and function of CCR6-RORgammat+ innate lymphoid cells. *Nature* 494: 261-5
139. Lim AI, Menegatti S, Bustamante J, Le Bourhis L, Allez M, Rogge L, Casanova JL, Yssel H, Di Santo JP. 2016. IL-12 drives functional plasticity of human group 2 innate lymphoid cells. *The Journal of experimental medicine* 213: 569-83
140. Huang Y, Guo L, Qiu J, Chen X, Hu-Li J, Siebenlist U, Williamson PR, Urban JF, Jr., Paul WE. 2015. IL-25-responsive, lineage-negative KLRG1(hi) cells are multipotential 'inflammatory' type 2 innate lymphoid cells. *Nature immunology* 16: 161-9
141. Molofsky AB, Nussbaum JC, Liang HE, Van Dyken SJ, Cheng LE, Mohapatra A, Chawla A, Locksley RM. 2013. Innate lymphoid type 2 cells sustain visceral adipose tissue eosinophils and alternatively activated macrophages. *The Journal of experimental medicine* 210: 535-49
142. Hams E, Locksley RM, McKenzie AN, Fallon PG. 2013. Cutting edge: IL-25 elicits innate lymphoid type 2 and type II NKT cells that regulate obesity in mice. *Journal of immunology* 191: 5349-53
143. Nussbaum JC, Van Dyken SJ, von Moltke J, Cheng LE, Mohapatra A, Molofsky AB, Thornton EE, Krummel MF, Chawla A, Liang HE, Locksley RM. 2013. Type 2 innate lymphoid cells control eosinophil homeostasis. *Nature* 502: 245-8
144. Turcot V, Bouchard L, Faucher G, Garneau V, Tchernof A, Deshaies Y, Perusse L, Marceau S, Biron S, Lescelleur O, Biertho L, Vohl MC. 2012. Thymic stromal

lymphopoietin: an immune cytokine gene associated with the metabolic syndrome and blood pressure in severe obesity. *Clinical science* 123: 99-109
145. Lee MW, Odegaard JI, Mukundan L, Qiu Y, Molofsky AB, Nussbaum JC, Yun K, Locksley RM, Chawla A. 2015. Activated type 2 innate lymphoid cells regulate beige fat biogenesis. *Cell* 160: 74-87
146. Brestoff JR, Kim BS, Saenz SA, Stine RR, Monticelli LA, Sonnenberg GF, Thome JJ, Farber DL, Lutfy K, Seale P, Artis D. 2015. Group 2 innate lymphoid cells promote beiging of white adipose tissue and limit obesity. *Nature* 519: 242-6
147. Upadhyay V, Poroyko V, Kim TJ, Devkota S, Fu S, Liu D, Tumanov AV, Koroleva EP, Deng L, Nagler C, Chang EB, Tang H, Fu YX. 2012. Lymphotoxin regulates commensal responses to enable diet-induced obesity. *Nature immunology* 13: 947-53
148. Wang X, Ota N, Manzanillo P, Kates L, Zavala-Solorio J, Eidenschenk C, Zhang J, Lesch J, Lee WP, Ross J, Diehl L, van Bruggen N, Kolumam G, Ouyang W. 2014. Interleukin-22 alleviates metabolic disorders and restores mucosal immunity in diabetes. *Nature* 514: 237-41
149. Sonnenberg GF, Monticelli LA, Alenghat T, Fung TC, Hutnick NA, Kunisawa J, Shibata N, Grunberg S, Sinha R, Zahm AM, Tardif MR, Sathaliyawala T, Kubota M, Farber DL, Collman RG, Shaked A, Fouser LA, Weiner DB, Tessier PA, Friedman JR, Kiyono H, Bushman FD, Chang KM, Artis D. 2012. Innate lymphoid cells promote anatomical containment of lymphoid-resident commensal bacteria. *Science* 336: 1321-5
150. Hazenberg MD, Spits H. 2014. Human innate lymphoid cells. *Blood* 124: 700-9
151. Chen S, Yin P, Zhao X, Xing W, Hu C, Zhou L, Xu G. 2013. Serum lipid profiling of patients with chronic hepatitis B, cirrhosis, and hepatocellular carcinoma by ultra fast LC/IT-TOF MS. *Electrophoresis* 34: 2848-56
152. Fon Tacer K, Rozman D. 2011. Nonalcoholic Fatty liver disease: focus on lipoprotein and lipid deregulation. *Journal of lipids* 2011: 783976
153. Reddy JK, Rao MS. 2006. Lipid metabolism and liver inflammation. II. Fatty liver disease and fatty acid oxidation. *American journal of physiology. Gastrointestinal and liver physiology* 290: G852-8
154. Visser BJ, Wieten RW, Nagel IM, Grobusch MP. 2013. Serum lipids and lipoproteins in malaria--a systematic review and meta-analysis. *Malaria journal* 12: 442
155. Wu L, Parhofer KG. 2014. Diabetic dyslipidemia. *Metabolism: clinical and experimental* 63: 1469-79
156. Perz JF, Armstrong GL, Farrington LA, Hutin YJ, Bell BP. 2006. The contributions of hepatitis B virus and hepatitis C virus infections to cirrhosis and primary liver cancer worldwide. *Journal of hepatology* 45: 529-38
157. Mengshol JA, Golden-Mason L, Rosen HR. 2007. Mechanisms of Disease: HCV-induced liver injury. *Nature clinical practice. Gastroenterology & hepatology* 4: 622-34
158. Lawitz E, Mangia A, Wyles D, Rodriguez-Torres M, Hassanein T, Gordon SC, Schultz M, Davis MN, Kayali Z, Reddy KR, Jacobson IM, Kowdley KV, Nyberg L, Subramanian GM, Hyland RH, Arterburn S, Jiang D, McNally J, Brainard D,

Symonds WT, McHutchison JG, Sheikh AM, Younossi Z, Gane EJ. 2013. Sofosbuvir for previously untreated chronic hepatitis C infection. *The New England journal of medicine* 368: 1878-87

159. Mohd Hanafiah K, Groeger J, Flaxman AD, Wiersma ST. 2013. Global epidemiology of hepatitis C virus infection: new estimates of age-specific antibody to HCV seroprevalence. *Hepatology* 57: 1333-42
160. Poordad F, Hezode C, Trinh R, Kowdley KV, Zeuzem S, Agarwal K, Shiffman ML, Wedemeyer H, Berg T, Yoshida EM, Forns X, Lovell SS, Da Silva-Tillmann B, Collins CA, Campbell AL, Podsadecki T, Bernstein B. 2014. ABT-450/r-ombitasvir and dasabuvir with ribavirin for hepatitis C with cirrhosis. *The New England journal of medicine* 370: 1973-82
161. Sulkowski MS, Gardiner DF, Rodriguez-Torres M, Reddy KR, Hassanein T, Jacobson I, Lawitz E, Lok AS, Hinestrosa F, Thuluvath PJ, Schwartz H, Nelson DR, Everson GT, Eley T, Wind-Rotolo M, Huang SP, Gao M, Hernandez D, McPhee F, Sherman D, Hindes R, Symonds W, Pasquinelli C, Grasela DM. 2014. Daclatasvir plus sofosbuvir for previously treated or untreated chronic HCV infection. *The New England journal of medicine* 370: 211-21
162. Muir AJ, Naggie S. 2015. Hepatitis C Virus Treatment: Is It Possible To Cure All Hepatitis C Virus Patients? *Clinical gastroenterology and hepatology : the official clinical practice journal of the American Gastroenterological Association* 13: 2166-72
163. Castera L, Chouteau P, Hezode C, Zafrani ES, Dhumeaux D, Pawlotsky JM. 2005. Hepatitis C virus-induced hepatocellular steatosis. *The American journal of gastroenterology* 100: 711-5
164. Elkrief L, Chouinard P, Bendersky N, Hajage D, Larroque B, Babany G, Kutala B, Francoz C, Boyer N, Moreau R, Durand F, Marcellin P, Rautou PE, Valla D. 2014. Diabetes mellitus is an independent prognostic factor for major liver-related outcomes in patients with cirrhosis and chronic hepatitis C. *Hepatology* 60: 823-31
165. Herker E, Ott M. 2011. Unique ties between hepatitis C virus replication and intracellular lipids. *Trends in endocrinology and metabolism: TEM* 22: 241-8
166. Lambert JE, Bain VG, Ryan EA, Thomson AB, Clandinin MT. 2013. Elevated lipogenesis and diminished cholesterol synthesis in patients with hepatitis C viral infection compared to healthy humans. *Hepatology* 57: 1697-704
167. Lerat H, Kammoun HL, Hainault I, Merour E, Higgs MR, Callens C, Lemon SM, Foufelle F, Pawlotsky JM. 2009. Hepatitis C virus proteins induce lipogenesis and defective triglyceride secretion in transgenic mice. *The Journal of biological chemistry* 284: 33466-74
168. Perlemuter G, Sabile A, Letteron P, Vona G, Topilco A, Chretien Y, Koike K, Pessayre D, Chapman J, Barba G, Brechot C. 2002. Hepatitis C virus core protein inhibits microsomal triglyceride transfer protein activity and very low density lipoprotein secretion: a model of viral-related steatosis. *FASEB journal : official publication of the Federation of American Societies for Experimental Biology* 16: 185-94
169. Fukasawa M, Tanaka Y, Sato S, Ono Y, Nitahara-Kasahara Y, Suzuki T, Miyamura T, Hanada K, Nishijima M. 2006. Enhancement of de novo fatty

acid biosynthesis in hepatic cell line Huh7 expressing hepatitis C virus core protein. *Biological & pharmaceutical bulletin* 29: 1958-61

170. Kim KH, Hong SP, Kim K, Park MJ, Kim KJ, Cheong J. 2007. HCV core protein induces hepatic lipid accumulation by activating SREBP1 and PPARgamma. *Biochemical and biophysical research communications* 355: 883-8
171. Hellerstein MK, Christiansen M, Kaempfer S, Kletke C, Wu K, Reid JS, Mulligan K, Hellerstein NS, Shackleton CH. 1991. Measurement of de novo hepatic lipogenesis in humans using stable isotopes. *The Journal of clinical investigation* 87: 1841-52
172. Marques-Lopes I, Ansorena D, Astiasaran I, Forga L, Martinez JA. 2001. Postprandial de novo lipogenesis and metabolic changes induced by a high-carbohydrate, low-fat meal in lean and overweight men. *The American journal of clinical nutrition* 73: 253-61
173. Schwarz JM, Linfoot P, Dare D, Aghajanian K. 2003. Hepatic de novo lipogenesis in normoinsulinemic and hyperinsulinemic subjects consuming high-fat, low-carbohydrate and low-fat, high-carbohydrate isoenergetic diets. *The American journal of clinical nutrition* 77: 43-50
174. Diraison F, Beylot M. 1998. Role of human liver lipogenesis and reesterification in triglycerides secretion and in FFA reesterification. *The American journal of physiology* 274: E321-7
175. Lindenbach BD, Meuleman P, Ploss A, Vanwolleghem T, Syder AJ, McKeating JA, Lanford RE, Feinstone SM, Major ME, Leroux-Roels G, Rice CM. 2006. Cell culture-grown hepatitis C virus is infectious in vivo and can be recultured in vitro. *Proceedings of the National Academy of Sciences of the United States of America* 103: 3805-9
176. Shimizu Y, Hishiki T, Sugiyama K, Ogawa K, Funami K, Kato A, Ohsaki Y, Fujimoto T, Takaku H, Shimotohno K. 2010. Lipoprotein lipase and hepatic triglyceride lipase reduce the infectivity of hepatitis C virus (HCV) through their catalytic activities on HCV-associated lipoproteins. *Virology* 407: 152-9
177. Lam KK, Davey M, Sun B, Roth AF, Davis NG, Conibear E. 2006. Palmitoylation by the DHHC protein Pfa4 regulates the ER exit of Chs3. *The Journal of cell biology* 174: 19-25
178. Fiorentino M, Zadra G, Palescandolo E, Fedele G, Bailey D, Fiore C, Nguyen PL, Migita T, Zamponi R, Di Vizio D, Priolo C, Sharma C, Xie W, Hemler ME, Mucci L, Giovannucci E, Finn S, Loda M. 2008. Overexpression of fatty acid synthase is associated with palmitoylation of Wnt1 and cytoplasmic stabilization of beta-catenin in prostate cancer. *Laboratory investigation; a journal of technical methods and pathology* 88: 1340-8
179. Wei X, Schneider JG, Shenouda SM, Lee A, Towler DA, Chakravarthy MV, Vita JA, Semenkovich CF. 2011. De novo lipogenesis maintains vascular homeostasis through endothelial nitric-oxide synthase (eNOS) palmitoylation. *The Journal of biological chemistry* 286: 2933-45
180. Anania VG, Coscoy L. 2011. Palmitoylation of MIR2 is required for its function. *Journal of virology* 85: 2288-95
181. Chen BJ, Takeda M, Lamb RA. 2005. Influenza virus hemagglutinin (H3 subtype) requires palmitoylation of its cytoplasmic tail for assembly: M1

proteins of two subtypes differ in their ability to support assembly. *Journal of virology* 79: 13673-84

182. Rousso I, Mixon MB, Chen BK, Kim PS. 2000. Palmitoylation of the HIV-1 envelope glycoprotein is critical for viral infectivity. *Proceedings of the National Academy of Sciences of the United States of America* 97: 13523-5
183. Zhu YZ, Luo Y, Cao MM, Liu Y, Liu XQ, Wang W, Wu DG, Guan M, Xu QQ, Ren H, Zhao P, Qi ZT. 2012. Significance of palmitoylation of CD81 on its association with tetraspanin-enriched microdomains and mediating hepatitis C virus cell entry. *Virology* 429: 112-23
184. Narayana SK, Helbig KJ, McCartney EM, Eyre NS, Bull RA, Eltahla A, Lloyd AR, Beard MR. 2015. The Interferon-induced Transmembrane Proteins, IFITM1, IFITM2, and IFITM3 Inhibit Hepatitis C Virus Entry. *The Journal of biological chemistry* 290: 25946-59
185. Wakita T, Pietschmann T, Kato T, Date T, Miyamoto M, Zhao Z, Murthy K, Habermann A, Krausslich HG, Mizokami M, Bartenschlager R, Liang TJ. 2005. Production of infectious hepatitis C virus in tissue culture from a cloned viral genome. *Nature medicine* 11: 791-6
186. Blight KJ, McKeating JA, Rice CM. 2002. Highly permissive cell lines for subgenomic and genomic hepatitis C virus RNA replication. *Journal of virology* 76: 13001-14
187. Anderson R, Breazeale S, Elich T, Lee S. 2012. *USA*
188. van Elden LJ, Nijhuis M, Schipper P, Schuurman R, van Loon AM. 2001. Simultaneous detection of influenza viruses A and B using real-time quantitative PCR. *Journal of clinical microbiology* 39: 196-200
189. Petersen CP, Bordeleau ME, Pelletier J, Sharp PA. 2006. Short RNAs repress translation after initiation in mammalian cells. *Molecular cell* 21: 533-42
190. Taddeo EP, Laker RC, Breen DS, Akhtar YN, Kenwood BM, Liao JA, Zhang M, Fazakerley DJ, Tomsig JL, Harris TE, Keller SR, Chow JD, Lynch KR, Chokki M, Molkentin JD, Turner N, James DE, Yan Z, Hoehn KL. 2014. Opening of the mitochondrial permeability transition pore links mitochondrial dysfunction to insulin resistance in skeletal muscle. *Molecular metabolism* 3: 124-34
191. Watt MJ, Hoy AJ, Muoio DM, Coleman RA. 2012. Distinct roles of specific fatty acids in cellular processes: implications for interpreting and reporting experiments. *American journal of physiology. Endocrinology and metabolism* 302: E1-3
192. Park CY, Jun HJ, Wakita T, Cheong JH, Hwang SB. 2009. Hepatitis C virus nonstructural 4B protein modulates sterol regulatory element-binding protein signaling via the AKT pathway. *The Journal of biological chemistry* 284: 9237-46
193. Waris G, Felmlee DJ, Negro F, Siddiqui A. 2007. Hepatitis C virus induces proteolytic cleavage of sterol regulatory element binding proteins and stimulates their phosphorylation via oxidative stress. *Journal of virology* 81: 8122-30
194. Vahlensieck HF, Pridzun L, Reichenbach H, Hinnen A. 1994. Identification of the yeast ACC1 gene product (acetyl-CoA carboxylase) as the target of the polyketide fungicide soraphen A. *Current genetics* 25: 95-100

195. Boulant S, Targett-Adams P, McLauchlan J. 2007. Disrupting the association of hepatitis C virus core protein with lipid droplets correlates with a loss in production of infectious virus. *The Journal of general virology* 88: 2204-13
196. Shavinskaya A, Boulant S, Penin F, McLauchlan J, Bartenschlager R. 2007. The lipid droplet binding domain of hepatitis C virus core protein is a major determinant for efficient virus assembly. *The Journal of biological chemistry* 282: 37158-69
197. Ron D, Walter P. 2007. Signal integration in the endoplasmic reticulum unfolded protein response. *Nature reviews. Molecular cell biology* 8: 519-29
198. Tardif KD, Mori K, Siddiqui A. 2002. Hepatitis C virus subgenomic replicons induce endoplasmic reticulum stress activating an intracellular signaling pathway. *Journal of virology* 76: 7453-9
199. Zheng Y, Gao B, Ye L, Kong L, Jing W, Yang X, Wu Z. 2005. Hepatitis C virus non-structural protein NS4B can modulate an unfolded protein response. *Journal of microbiology* 43: 529-36
200. von dem Bussche A, Machida R, Li K, Loevinsohn G, Khander A, Wang J, Wakita T, Wands JR, Li J. 2010. Hepatitis C virus NS2 protein triggers endoplasmic reticulum stress and suppresses its own viral replication. *Journal of hepatology* 53: 797-804
201. Pavio N, Romano PR, Graczyk TM, Feinstone SM, Taylor DR. 2003. Protein synthesis and endoplasmic reticulum stress can be modulated by the hepatitis C virus envelope protein E2 through the eukaryotic initiation factor 2alpha kinase PERK. *Journal of virology* 77: 3578-85
202. Ke PY, Chen SS. 2011. Activation of the unfolded protein response and autophagy after hepatitis C virus infection suppresses innate antiviral immunity in vitro. *The Journal of clinical investigation* 121: 37-56
203. Sir D, Chen WL, Choi J, Wakita T, Yen TS, Ou JH. 2008. Induction of incomplete autophagic response by hepatitis C virus via the unfolded protein response. *Hepatology* 48: 1054-61
204. Koutsoudakis G, Romero-Brey I, Berger C, Perez-Vilaro G, Monteiro Perin P, Vondran FW, Kalesse M, Harmrolfs K, Muller R, Martinez JP, Pietschmann T, Bartenschlager R, Bronstrup M, Meyerhans A, Diez J. 2015. Soraphen A: A broad-spectrum antiviral natural product with potent anti-hepatitis C virus activity. *Journal of hepatology* 63: 813-21
205. Salaun C, Greaves J, Chamberlain LH. 2010. The intracellular dynamic of protein palmitoylation. *The Journal of cell biology* 191: 1229-38
206. Linder ME, Deschenes RJ. 2007. Palmitoylation: policing protein stability and traffic. *Nature reviews. Molecular cell biology* 8: 74-84
207. Hueging K, Doepke M, Vieyres G, Bankwitz D, Frentzen A, Doerrbecker J, Gumz F, Haid S, Wolk B, Kaderali L, Pietschmann T. 2014. Apolipoprotein E codetermines tissue tropism of hepatitis C virus and is crucial for viral cell-to-cell transmission by contributing to a postenvelopment step of assembly. *Journal of virology* 88: 1433-46
208. Tong L, Harwood HJ, Jr. 2006. Acetyl-coenzyme A carboxylases: versatile targets for drug discovery. *Journal of cellular biochemistry* 99: 1476-88

209. Harada N, Oda Z, Hara Y, Fujinami K, Okawa M, Ohbuchi K, Yonemoto M, Ikeda Y, Ohwaki K, Aragane K, Tamai Y, Kusunoki J. 2007. Hepatic de novo lipogenesis is present in liver-specific ACC1-deficient mice. *Molecular and cellular biology* 27: 1881-8
210. Kapadia SB, Chisari FV. 2005. Hepatitis C virus RNA replication is regulated by host geranylgeranylation and fatty acids. *Proceedings of the National Academy of Sciences of the United States of America* 102: 2561-6
211. Singaravelu R, Desrochers G, Srinivasan P, O'Hara S, Lyn R, Muller R, Jones D, Russell R, Pezacki J. 2015. Soraphen A: a probe for investigating the role of de novo lipogenesis during viral infection. *ACS Infectious Diseases* 1: 130-4
212. van Meer G, Voelker DR, Feigenson GW. 2008. Membrane lipids: where they are and how they behave. *Nature reviews. Molecular cell biology* 9: 112-24
213. Boson B, Granio O, Bartenschlager R, Cosset FL. 2011. A concerted action of hepatitis C virus p7 and nonstructural protein 2 regulates core localization at the endoplasmic reticulum and virus assembly. *PLoS pathogens* 7: e1002144
214. Etienne L, Blanchard E, Boyer A, Desvignes V, Gaillard J, Meunier JC, Roingeard P, Hourioux C. 2015. The Replacement of 10 Non-Conserved Residues in the Core Protein of JFH-1 Hepatitis C Virus Improves Its Assembly and Secretion. *PloS one* 10: e0137182
215. Syed GH, Siddiqui A. 2011. Effects of hypolipidemic agent nordihydroguaiaretic acid on lipid droplets and hepatitis C virus. *Hepatology* 54: 1936-46
216. Yang W, Hood BL, Chadwick SL, Liu S, Watkins SC, Luo G, Conrads TP, Wang T. 2008. Fatty acid synthase is up-regulated during hepatitis C virus infection and regulates hepatitis C virus entry and production. *Hepatology* 48: 1396-403
217. Liefhebber JM, Hague CV, Zhang Q, Wakelam MJ, McLauchlan J. 2014. Modulation of triglyceride and cholesterol ester synthesis impairs assembly of infectious hepatitis C virus. *The Journal of biological chemistry* 289: 21276-88
218. Moench SJ, Terry CE, Dewey TG. 1994. Fluorescence labeling of the palmitoylation sites of rhodopsin. *Biochemistry* 33: 5783-90
219. Yanai A, Huang K, Kang R, Singaraja RR, Arstikaitis P, Gan L, Orban PC, Mullard A, Cowan CM, Raymond LA, Drisdel RC, Green WN, Ravikumar B, Rubinsztein DC, El-Husseini A, Hayden MR. 2006. Palmitoylation of huntingtin by HIP14 is essential for its trafficking and function. *Nature neuroscience* 9: 824-31
220. Mashek DG, Li LO, Coleman RA. 2007. Long-chain acyl-CoA synthetases and fatty acid channeling. *Future lipidology* 2: 465-76
221. Castera L, Hezode C, Roudot-Thoraval F, Lonjon I, Zafrani ES, Pawlotsky JM, Dhumeaux D. 2004. Effect of antiviral treatment on evolution of liver steatosis in patients with chronic hepatitis C: indirect evidence of a role of hepatitis C virus genotype 3 in steatosis. *Gut* 53: 420-4
222. Ng CG, Coppens I, Govindarajan D, Pisciotta J, Shulaev V, Griffin DE. 2008. Effect of host cell lipid metabolism on alphavirus replication, virion

morphogenesis, and infectivity. *Proceedings of the National Academy of Sciences of the United States of America* 105: 16326-31
223. Martin-Acebes MA, Blazquez AB, Jimenez de Oya N, Escribano-Romero E, Saiz JC. 2011. West Nile virus replication requires fatty acid synthesis but is independent on phosphatidylinositol-4-phosphate lipids. *PloS one* 6: e24970
224. Perera R, Riley C, Isaac G, Hopf-Jannasch AS, Moore RJ, Weitz KW, Pasa-Tolic L, Metz TO, Adamec J, Kuhn RJ. 2012. Dengue virus infection perturbs lipid homeostasis in infected mosquito cells. *PLoS pathogens* 8: e1002584
225. Wang X, Diaz A, Hao L, Gancarz B, den Boon JA, Ahlquist P. 2011. Intersection of the multivesicular body pathway and lipid homeostasis in RNA replication by a positive-strand RNA virus. *Journal of virology* 85: 5494-503
226. Meng F, Wang K, Aoyama T, Grivennikov SI, Paik Y, Scholten D, Cong M, Iwaisako K, Liu X, Zhang M, Osterreicher CH, Stickel F, Ley K, Brenner DA, Kisseleva T. 2012. Interleukin-17 signaling in inflammatory, Kupffer cells, and hepatic stellate cells exacerbates liver fibrosis in mice. *Gastroenterology* 143: 765-76 e1-3
227. Kong X, Feng D, Wang H, Hong F, Bertola A, Wang FS, Gao B. 2012. Interleukin-22 induces hepatic stellate cell senescence and restricts liver fibrosis in mice. *Hepatology* 56: 1150-9
228. Radaeva S, Sun R, Pan HN, Hong F, Gao B. 2004. Interleukin 22 (IL-22) plays a protective role in T cell-mediated murine hepatitis: IL-22 is a survival factor for hepatocytes via STAT3 activation. *Hepatology* 39: 1332-42
229. Zenewicz LA, Yancopoulos GD, Valenzuela DM, Murphy AJ, Karow M, Flavell RA. 2007. Interleukin-22 but not interleukin-17 provides protection to hepatocytes during acute liver inflammation. *Immunity* 27: 647-59
230. Farhadi A, Gundlapalli S, Shaikh M, Frantzides C, Harrell L, Kwasny MM, Keshavarzian A. 2008. Susceptibility to gut leakiness: a possible mechanism for endotoxaemia in non-alcoholic steatohepatitis. *Liver international : official journal of the International Association for the Study of the Liver* 28: 1026-33
231. Dumoutier L, Louahed J, Renauld JC. 2000. Cloning and characterization of IL-10-related T cell-derived inducible factor (IL-TIF), a novel cytokine structurally related to IL-10 and inducible by IL-9. *Journal of immunology* 164: 1814-9
232. Kotenko SV, Izotova LS, Mirochnitchenko OV, Esterova E, Dickensheets H, Donnelly RP, Pestka S. 2001. Identification of the functional interleukin-22 (IL-22) receptor complex: the IL-10R2 chain (IL-10Rbeta) is a common chain of both the IL-10 and IL-22 (IL-10-related T cell-derived inducible factor, IL-TIF) receptor complexes. *The Journal of biological chemistry* 276: 2725-32
233. Wolk K, Kunz S, Witte E, Friedrich M, Asadullah K, Sabat R. 2004. IL-22 increases the innate immunity of tissues. *Immunity* 21: 241-54
234. Liang SC, Tan XY, Luxenberg DP, Karim R, Dunussi-Joannopoulos K, Collins M, Fouser LA. 2006. Interleukin (IL)-22 and IL-17 are coexpressed by Th17 cells and cooperatively enhance expression of antimicrobial peptides. *The Journal of experimental medicine* 203: 2271-9

235. Trifari S, Kaplan CD, Tran EH, Crellin NK, Spits H. 2009. Identification of a human helper T cell population that has abundant production of interleukin 22 and is distinct from T(H)-17, T(H)1 and T(H)2 cells. *Nature immunology* 10: 864-71
236. Duhen T, Geiger R, Jarrossay D, Lanzavecchia A, Sallusto F. 2009. Production of interleukin 22 but not interleukin 17 by a subset of human skin-homing memory T cells. *Nature immunology* 10: 857-63
237. Sutton CE, Lalor SJ, Sweeney CM, Brereton CF, Lavelle EC, Mills KH. 2009. Interleukin-1 and IL-23 induce innate IL-17 production from gammadelta T cells, amplifying Th17 responses and autoimmunity. *Immunity* 31: 331-41
238. Martin B, Hirota K, Cua DJ, Stockinger B, Veldhoen M. 2009. Interleukin-17-producing gammadelta T cells selectively expand in response to pathogen products and environmental signals. *Immunity* 31: 321-30
239. Intlekofer AM, Banerjee A, Takemoto N, Gordon SM, Dejong CS, Shin H, Hunter CA, Wherry EJ, Lindsten T, Reiner SL. 2008. Anomalous type 17 response to viral infection by CD8+ T cells lacking T-bet and eomesodermin. *Science* 321: 408-11
240. Gomez-Lechon MJ, Donato MT, Martinez-Romero A, Jimenez N, Castell JV, O'Connor JE. 2007. A human hepatocellular in vitro model to investigate steatosis. *Chemico-biological interactions* 165: 106-16
241. Wobser H, Dorn C, Weiss TS, Amann T, Bollheimer C, Buttner R, Scholmerich J, Hellerbrand C. 2009. Lipid accumulation in hepatocytes induces fibrogenic activation of hepatic stellate cells. *Cell research* 19: 996-1005
242. Malhi H, Bronk SF, Werneburg NW, Gores GJ. 2006. Free fatty acids induce JNK-dependent hepatocyte lipoapoptosis. *The Journal of biological chemistry* 281: 12093-101
243. Xiao YQ, Freire-de-Lima CG, Schiemann WP, Bratton DL, Vandivier RW, Henson PM. 2008. Transcriptional and translational regulation of TGF-beta production in response to apoptotic cells. *Journal of immunology* 181: 3575-85
244. Wang G, Yu Y, Sun C, Liu T, Liang T, Zhan L, Lin X, Feng XH. 2015. STAT3 selectively interacts with Smad3 to antagonize TGF-beta. *Oncogene*
245. Hoorweg K, Peters CP, Cornelissen F, Aparicio-Domingo P, Papazian N, Kazemier G, Mjosberg JM, Spits H, Cupedo T. 2012. Functional Differences between Human NKp44(-) and NKp44(+) RORC(+) Innate Lymphoid Cells. *Frontiers in immunology* 3: 72
246. Glatzer T, Killig M, Meisig J, Ommert I, Luetke-Eversloh M, Babic M, Paclik D, Bluthgen N, Seidl R, Seifarth C, Grone J, Lenarz M, Stolzel K, Fugmann D, Porgador A, Hauser A, Karlas A, Romagnani C. 2013. RORgammat(+) innate lymphoid cells acquire a proinflammatory program upon engagement of the activating receptor NKp44. *Immunity* 38: 1223-35
247. Viant C, Rankin LC, Girard-Madoux MJ, Seillet C, Shi W, Smyth MJ, Bartholin L, Walzer T, Huntington ND, Vivier E, Belz GT. 2016. Transforming growth factor-beta and Notch ligands act as opposing environmental cues in regulating the plasticity of type 3 innate lymphoid cells. *Science signaling* 9: ra46

248. Killig M, Glatzer T, Romagnani C. 2014. Recognition strategies of group 3 innate lymphoid cells. *Frontiers in immunology* 5: 142
249. Liu J, Abate W, Xu J, Corry D, Kaul B, Jackson SK. 2011. Three-dimensional spheroid cultures of A549 and HepG2 cells exhibit different lipopolysaccharide (LPS) receptor expression and LPS-induced cytokine response compared with monolayer cultures. *Innate immunity* 17: 245-55
250. Fabre T, Kared H, Friedman SL, Shoukry NH. 2014. IL-17A enhances the expression of profibrotic genes through upregulation of the TGF-beta receptor on hepatic stellate cells in a JNK-dependent manner. *Journal of immunology* 193: 3925-33
251. Simmonds P. 2013. The origin of hepatitis C virus. *Current topics in microbiology and immunology* 369: 1-15
252. Kapoor A, Simmonds P, Gerold G, Qaisar N, Jain K, Henriquez JA, Firth C, Hirschberg DL, Rice CM, Shields S, Lipkin WI. 2011. Characterization of a canine homolog of hepatitis C virus. *Proceedings of the National Academy of Sciences of the United States of America* 108: 11608-13
253. Burbelo PD, Dubovi EJ, Simmonds P, Medina JL, Henriquez JA, Mishra N, Wagner J, Tokarz R, Cullen JM, Iadarola MJ, Rice CM, Lipkin WI, Kapoor A. 2012. Serology-enabled discovery of genetically diverse hepaciviruses in a new host. *Journal of virology* 86: 6171-8
254. Gerth K, Bedorf N, Irschik H, Hofle G, Reichenbach H. 1994. The soraphens: a family of novel antifungal compounds from Sorangium cellulosum (Myxobacteria). I. Soraphen A1 alpha: fermentation, isolation, biological properties. *The Journal of antibiotics* 47: 23-31
255. Galdieri L, Vancura A. 2012. Acetyl-CoA carboxylase regulates global histone acetylation. *The Journal of biological chemistry* 287: 23865-76
256. Miller S, Krijnse-Locker J. 2008. Modification of intracellular membrane structures for virus replication. *Nature reviews. Microbiology* 6: 363-74
257. Welsch S, Miller S, Romero-Brey I, Merz A, Bleck CK, Walther P, Fuller SD, Antony C, Krijnse-Locker J, Bartenschlager R. 2009. Composition and three-dimensional architecture of the dengue virus replication and assembly sites. *Cell host & microbe* 5: 365-75
258. Samsa MM, Mondotte JA, Iglesias NG, Assuncao-Miranda I, Barbosa-Lima G, Da Poian AT, Bozza PT, Gamarnik AV. 2009. Dengue virus capsid protein usurps lipid droplets for viral particle formation. *PLoS pathogens* 5: e1000632
259. Berod L, Friedrich C, Nandan A, Freitag J, Hagemann S, Harmrolfs K, Sandouk A, Hesse C, Castro CN, Bahre H, Tschirner SK, Gorinski N, Gohmert M, Mayer CT, Huehn J, Ponimaskin E, Abraham WR, Muller R, Lochner M, Sparwasser T. 2014. De novo fatty acid synthesis controls the fate between regulatory T and T helper 17 cells. *Nature medicine* 20: 1327-33
260. Hall CH, Kassel R, Tacke RS, Hahn YS. 2010. HCV+ hepatocytes induce human regulatory CD4+ T cells through the production of TGF-beta. *PloS one* 5: e12154
261. Lee HC, Sung SS, Krueger PD, Jo YA, Rosen HR, Ziegler SF, Hahn YS. 2013. Hepatitis C virus promotes T-helper (Th)17 responses through thymic

stromal lymphopoietin production by infected hepatocytes. *Hepatology* 57: 1314-24
262. Waggoner SN, Hall CH, Hahn YS. 2007. HCV core protein interaction with gC1q receptor inhibits Th1 differentiation of CD4+ T cells via suppression of dendritic cell IL-12 production. *Journal of leukocyte biology* 82: 1407-19
263. Abe H, Kimura A, Tsuruta S, Fukaya T, Sakaguchi R, Morita R, Sekiya T, Shichita T, Chayama K, Fujii-Kuriyama Y, Yoshimura A. 2014. Aryl hydrocarbon receptor plays protective roles in ConA-induced hepatic injury by both suppressing IFN-gamma expression and inducing IL-22. *International immunology* 26: 129-37
264. Jie Z, Liang Y, Hou L, Dong C, Iwakura Y, Soong L, Cong Y, Sun J. 2014. Intrahepatic innate lymphoid cells secrete IL-17A and IL-17F that are crucial for T cell priming in viral infection. *Journal of immunology* 192: 3289-300
265. Kudira R, Malinka T, Kohler A, Dosch M, Gomez de Aguero M, Melin N, Haegele S, Starlinger P, Maharjan N, Saxena S, Keogh A, Stroka D, Candinas D, Beldi G. 2016. P2X1 regulated IL-22 secretion by innate lymphoid cells is required for efficient liver regeneration. *Hepatology*
266. Li J, Razumilava N, Gores GJ, Walters S, Mizuochi T, Mourya R, Bessho K, Wang YH, Glaser SS, Shivakumar P, Bezerra JA. 2014. Biliary repair and carcinogenesis are mediated by IL-33-dependent cholangiocyte proliferation. *The Journal of clinical investigation* 124: 3241-51
267. Yang Z, Tang T, Wei X, Yang S, Tian Z. 2015. Type 1 innate lymphoid cells contribute to the pathogenesis of chronic hepatitis B. *Innate immunity* 21: 665-73
268. McHedlidze T, Waldner M, Zopf S, Walker J, Rankin AL, Schuchmann M, Voehringer D, McKenzie AN, Neurath MF, Pflanz S, Wirtz S. 2013. Interleukin-33-dependent innate lymphoid cells mediate hepatic fibrosis. *Immunity* 39: 357-71
269. Matsumoto A, Kanai T, Mikami Y, Chu PS, Nakamoto N, Ebinuma H, Saito H, Sato T, Yagita H, Hibi T. 2013. IL-22-producing RORgammat-dependent innate lymphoid cells play a novel protective role in murine acute hepatitis. *PloS one* 8: e62853
270. Ohne Y, Silver JS, Thompson-Snipes L, Collet MA, Blanck JP, Cantarel BL, Copenhaver AM, Humbles AA, Liu YJ. 2016. IL-1 is a critical regulator of group 2 innate lymphoid cell function and plasticity. *Nature immunology*
271. Silver JS, Kearley J, Copenhaver AM, Sanden C, Mori M, Yu L, Pritchard GH, Berlin AA, Hunter CA, Bowler R, Erjefalt JS, Kolbeck R, Humbles AA. 2016. Inflammatory triggers associated with exacerbations of COPD orchestrate plasticity of group 2 innate lymphoid cells in the lungs. *Nature immunology*
272. Cella M, Otero K, Colonna M. 2010. Expansion of human NK-22 cells with IL-7, IL-2, and IL-1beta reveals intrinsic functional plasticity. *Proceedings of the National Academy of Sciences of the United States of America* 107: 10961-6
273. Vonarbourg C, Mortha A, Bui VL, Hernandez PP, Kiss EA, Hoyler T, Flach M, Bengsch B, Thimme R, Holscher C, Honig M, Pannicke U, Schwarz K, Ware CF, Finke D, Diefenbach A. 2010. Regulated expression of nuclear receptor

RORgammat confers distinct functional fates to NK cell receptor-expressing RORgammat(+) innate lymphocytes. *Immunity* 33: 736-51

274. Bernink JH, Krabbendam L, Germar K, de Jong E, Gronke K, Kofoed-Nielsen M, Munneke JM, Hazenberg MD, Villaudy J, Buskens CJ, Bemelman WA, Diefenbach A, Blom B, Spits H. 2015. Interleukin-12 and -23 Control Plasticity of CD127(+) Group 1 and Group 3 Innate Lymphoid Cells in the Intestinal Lamina Propria. *Immunity* 43: 146-60
275. Ishibashi H, Nakamura M, Komori A, Migita K, Shimoda S. 2009. Liver architecture, cell function, and disease. *Seminars in immunopathology* 31: 399-409
276. Ogawa Y, Imajo K, Yoneda M, Kessoku T, Tomeno W, Shinohara Y, Kato S, Mawatari H, Nozaki Y, Fujita K, Kirikoshi H, Maeda S, Saito S, Wada K, Nakajima A. 2013. Soluble CD14 levels reflect liver inflammation in patients with nonalcoholic steatohepatitis. *PloS one* 8: e65211
277. Kazankov K, Moller HJ, Lange A, Birkebaek NH, Holland-Fischer P, Solvig J, Horlyck A, Kristensen K, Rittig S, Handberg A, Vilstrup H, Gronbaek H. 2015. The macrophage activation marker sCD163 is associated with changes in NAFLD and metabolic profile during lifestyle intervention in obese children. *Pediatric obesity* 10: 226-33
278. Cinti S, Mitchell G, Barbatelli G, Murano I, Ceresi E, Faloia E, Wang S, Fortier M, Greenberg AS, Obin MS. 2005. Adipocyte death defines macrophage localization and function in adipose tissue of obese mice and humans. *Journal of lipid research* 46: 2347-55
279. Haukeland JW, Damas JK, Konopski Z, Loberg EM, Haaland T, Goverud I, Torjesen PA, Birkeland K, Bjoro K, Aukrust P. 2006. Systemic inflammation in nonalcoholic fatty liver disease is characterized by elevated levels of CCL2. *Journal of hepatology* 44: 1167-74
280. Egan CE, Daugherity EK, Rogers AB, Abi Abdallah DS, Denkers EY, Maurer KJ. 2013. CCR2 and CD44 promote inflammatory cell recruitment during fatty liver formation in a lithogenic diet fed mouse model. *PloS one* 8: e65247
281. Baeck C, Wehr A, Karlmark KR, Heymann F, Vucur M, Gassler N, Huss S, Klussmann S, Eulberg D, Luedde T, Trautwein C, Tacke F. 2012. Pharmacological inhibition of the chemokine CCL2 (MCP-1) diminishes liver macrophage infiltration and steatohepatitis in chronic hepatic injury. *Gut* 61: 416-26
282. Xiao F, Waldrop SL, Bronk SF, Gores GJ, Davis LS, Kilic G. 2015. Lipoapoptosis induced by saturated free fatty acids stimulates monocyte migration: a novel role for Pannexin1 in liver cells. *Purinergic signalling* 11: 347-59
283. Idrissova L, Malhi H, Werneburg NW, LeBrasseur NK, Bronk SF, Fingas C, Tchkonia T, Pirtskhalava T, White TA, Stout MB, Hirsova P, Krishnan A, Liedtke C, Trautwein C, Finnberg N, El-Deiry WS, Kirkland JL, Gores GJ. 2015. TRAIL receptor deletion in mice suppresses the inflammation of nutrient excess. *Journal of hepatology* 62: 1156-63
284. Kakazu E, Mauer AS, Yin M, Malhi H. 2016. Hepatocytes release ceramide-enriched pro-inflammatory extracellular vesicles in an IRE1alpha-dependent manner. *Journal of lipid research* 57: 233-45

285. Ibrahim SH, Hirsova P, Tomita K, Bronk SF, Werneburg NW, Harrison SA, Goodfellow VS, Malhi H, Gores GJ. 2016. Mixed lineage kinase 3 mediates release of C-X-C motif ligand 10-bearing chemotactic extracellular vesicles from lipotoxic hepatocytes. *Hepatology* 63: 731-44
286. Nakagawa H, Umemura A, Taniguchi K, Font-Burgada J, Dhar D, Ogata H, Zhong Z, Valasek MA, Seki E, Hidalgo J, Koike K, Kaufman RJ, Karin M. 2014. ER stress cooperates with hypernutrition to trigger TNF-dependent spontaneous HCC development. *Cancer cell* 26: 331-43
287. Dixon LJ, Flask CA, Papouchado BG, Feldstein AE, Nagy LE. 2013. Caspase-1 as a central regulator of high fat diet-induced non-alcoholic steatohepatitis. *PloS one* 8: e56100
288. Csak T, Ganz M, Pespisa J, Kodys K, Dolganiuc A, Szabo G. 2011. Fatty acid and endotoxin activate inflammasomes in mouse hepatocytes that release danger signals to stimulate immune cells. *Hepatology* 54: 133-44
289. Hendrikx T, Bieghs V, Walenbergh SM, van Gorp PJ, Verheyen F, Jeurissen ML, Steinbusch MM, Vaes N, Binder CJ, Koek GH, Stienstra R, Netea MG, Hofker MH, Shiri-Sverdlov R. 2013. Macrophage specific caspase-1/11 deficiency protects against cholesterol crystallization and hepatic inflammation in hyperlipidemic mice. *PloS one* 8: e78792
290. Ye D, Li FY, Lam KS, Li H, Jia W, Wang Y, Man K, Lo CM, Li X, Xu A. 2012. Toll-like receptor-4 mediates obesity-induced non-alcoholic steatohepatitis through activation of X-box binding protein-1 in mice. *Gut* 61: 1058-67
291. Wigg AJ, Roberts-Thomson IC, Dymock RB, McCarthy PJ, Grose RH, Cummins AG. 2001. The role of small intestinal bacterial overgrowth, intestinal permeability, endotoxaemia, and tumour necrosis factor alpha in the pathogenesis of non-alcoholic steatohepatitis. *Gut* 48: 206-11
292. Miele L, Valenza V, La Torre G, Montalto M, Cammarota G, Ricci R, Masciana R, Forgione A, Gabrieli ML, Perotti G, Vecchio FM, Rapaccini G, Gasbarrini G, Day CP, Grieco A. 2009. Increased intestinal permeability and tight junction alterations in nonalcoholic fatty liver disease. *Hepatology* 49: 1877-87
293. Imajo K, Fujita K, Yoneda M, Nozaki Y, Ogawa Y, Shinohara Y, Kato S, Mawatari H, Shibata W, Kitani H, Ikejima K, Kirikoshi H, Nakajima N, Saito S, Maeyama S, Watanabe S, Wada K, Nakajima A. 2012. Hyperresponsivity to low-dose endotoxin during progression to nonalcoholic steatohepatitis is regulated by leptin-mediated signaling. *Cell metabolism* 16: 44-54
294. Zwolak A, Szuster-Ciesielska A, Daniluk J, Slabczynska O, Kandefer-Szerszen M. 2015. Hyperreactivity of Blood Leukocytes in Patients with NAFLD to Ex Vivo Lipopolysaccharide Treatment Is Modulated by Metformin and Phosphatidylcholine but Not by Alpha Ketoglutarate. *PloS one* 10: e0143851
295. Duffield JS, Forbes SJ, Constandinou CM, Clay S, Partolina M, Vuthoori S, Wu S, Lang R, Iredale JP. 2005. Selective depletion of macrophages reveals distinct, opposing roles during liver injury and repair. *The Journal of clinical investigation* 115: 56-65
296. Fallowfield JA, Mizuno M, Kendall TJ, Constandinou CM, Benyon RC, Duffield JS, Iredale JP. 2007. Scar-associated macrophages are a major source of

hepatic matrix metalloproteinase-13 and facilitate the resolution of murine hepatic fibrosis. *Journal of immunology* 178: 5288-95

297. Ramachandran P, Pellicoro A, Vernon MA, Boulter L, Aucott RL, Ali A, Hartland SN, Snowdon VK, Cappon A, Gordon-Walker TT, Williams MJ, Dunbar DR, Manning JR, van Rooijen N, Fallowfield JA, Forbes SJ, Iredale JP. 2012. Differential Ly-6C expression identifies the recruited macrophage phenotype, which orchestrates the regression of murine liver fibrosis. *Proceedings of the National Academy of Sciences of the United States of America* 109: E3186-95
298. Song E, Ouyang N, Horbelt M, Antus B, Wang M, Exton MS. 2000. Influence of alternatively and classically activated macrophages on fibrogenic activities of human fibroblasts. *Cellular immunology* 204: 19-28
299. Schnoor M, Cullen P, Lorkowski J, Stolle K, Robenek H, Troyer D, Rauterberg J, Lorkowski S. 2008. Production of type VI collagen by human macrophages: a new dimension in macrophage functional heterogeneity. *Journal of immunology* 180: 5707-19
300. Wan J, Benkdane M, Teixeira-Clerc F, Bonnafous S, Louvet A, Lafdil F, Pecker F, Tran A, Gual P, Mallat A, Lotersztajn S, Pavoine C. 2014. M2 Kupffer cells promote M1 Kupffer cell apoptosis: a protective mechanism against alcoholic and nonalcoholic fatty liver disease. *Hepatology* 59: 130-42
301. Asanuma T, Ono M, Kubota K, Hirose A, Hayashi Y, Saibara T, Inanami O, Ogawa Y, Enzan H, Onishi S, Kuwabara M, Oben JA. 2010. Super paramagnetic iron oxide MRI shows defective Kupffer cell uptake function in non-alcoholic fatty liver disease. *Gut* 59: 258-66
302. Henning JR, Graffeo CS, Rehman A, Fallon NC, Zambirinis CP, Ochi A, Barilla R, Jamal M, Deutsch M, Greco S, Ego-Osuala M, Bin-Saeed U, Rao RS, Badar S, Quesada JP, Acehan D, Miller G. 2013. Dendritic cells limit fibroinflammatory injury in nonalcoholic steatohepatitis in mice. *Hepatology* 58: 589-602
303. Jiao J, Sastre D, Fiel MI, Lee UE, Ghiassi-Nejad Z, Ginhoux F, Vivier E, Friedman SL, Merad M, Aloman C. 2012. Dendritic cell regulation of carbon tetrachloride-induced murine liver fibrosis regression. *Hepatology* 55: 244-55
304. Connolly MK, Bedrosian AS, Mallen-St Clair J, Mitchell AP, Ibrahim J, Stroud A, Pachter HL, Bar-Sagi D, Frey AB, Miller G. 2009. In liver fibrosis, dendritic cells govern hepatic inflammation in mice via TNF-alpha. *The Journal of clinical investigation* 119: 3213-25
305. Miyake T, Akbar SM, Yoshida O, Chen S, Hiasa Y, Matsuura B, Abe M, Onji M. 2010. Impaired dendritic cell functions disrupt antigen-specific adaptive immune responses in mice with nonalcoholic fatty liver disease. *Journal of gastroenterology* 45: 859-67
306. Rehman A, Hemmert KC, Ochi A, Jamal M, Henning JR, Barilla R, Quesada JP, Zambirinis CP, Tang K, Ego-Osuala M, Rao RS, Greco S, Deutsch M, Narayan S, Pachter HL, Graffeo CS, Acehan D, Miller G. 2013. Role of fatty-acid synthesis in dendritic cell generation and function. *Journal of immunology* 190: 4640-9
307. Ibrahim J, Nguyen AH, Rehman A, Ochi A, Jamal M, Graffeo CS, Henning JR, Zambirinis CP, Fallon NC, Barilla R, Badar S, Mitchell A, Rao RS, Acehan D,

Frey AB, Miller G. 2012. Dendritic cell populations with different concentrations of lipid regulate tolerance and immunity in mouse and human liver. *Gastroenterology* 143: 1061-72

308. Everts B, Tussiwand R, Dreesen L, Fairfax KC, Huang SC, Smith AM, O'Neill CM, Lam WY, Edelson BT, Urban JF, Jr., Murphy KM, Pearce EJ. 2016. Migratory CD103+ dendritic cells suppress helminth-driven type 2 immunity through constitutive expression of IL-12. *The Journal of experimental medicine* 213: 35-51
309. Gadd VL, Skoien R, Powell EE, Fagan KJ, Winterford C, Horsfall L, Irvine K, Clouston AD. 2014. The portal inflammatory infiltrate and ductular reaction in human nonalcoholic fatty liver disease. *Hepatology* 59: 1393-405
310. Liang W, Lindeman JH, Menke AL, Koonen DP, Morrison M, Havekes LM, van den Hoek AM, Kleemann R. 2014. Metabolically induced liver inflammation leads to NASH and differs from LPS- or IL-1beta-induced chronic inflammation. *Laboratory investigation; a journal of technical methods and pathology* 94: 491-502
311. Rensen SS, Slaats Y, Nijhuis J, Jans A, Bieghs V, Driessen A, Malle E, Greve JW, Buurman WA. 2009. Increased hepatic myeloperoxidase activity in obese subjects with nonalcoholic steatohepatitis. *The American journal of pathology* 175: 1473-82
312. Ikura Y, Ohsawa M, Suekane T, Fukushima H, Itabe H, Jomura H, Nishiguchi S, Inoue T, Naruko T, Ehara S, Kawada N, Arakawa T, Ueda M. 2006. Localization of oxidized phosphatidylcholine in nonalcoholic fatty liver disease: impact on disease progression. *Hepatology* 43: 506-14
313. Rensen SS, Bieghs V, Xanthoulea S, Arfianti E, Bakker JA, Shiri-Sverdlov R, Hofker MH, Greve JW, Buurman WA. 2012. Neutrophil-derived myeloperoxidase aggravates non-alcoholic steatohepatitis in low-density lipoprotein receptor-deficient mice. *PloS one* 7: e52411
314. Strauss RS. 1999. Comparison of serum concentrations of alpha-tocopherol and beta-carotene in a cross-sectional sample of obese and nonobese children (NHANES III). National Health and Nutrition Examination Survey. *The Journal of pediatrics* 134: 160-5
315. Inzaugarat ME, Ferreyra Solari NE, Billordo LA, Abecasis R, Gadano AC, Chernavsky AC. 2011. Altered phenotype and functionality of circulating immune cells characterize adult patients with nonalcoholic steatohepatitis. *Journal of clinical immunology* 31: 1120-30
316. Novo E, Busletta C, Bonzo LV, Povero D, Paternostro C, Mareschi K, Ferrero I, David E, Bertolani C, Caligiuri A, Cannito S, Tamagno E, Compagnone A, Colombatto S, Marra F, Fagioli F, Pinzani M, Parola M. 2011. Intracellular reactive oxygen species are required for directional migration of resident and bone marrow-derived hepatic pro-fibrogenic cells. *Journal of hepatology* 54: 964-74
317. Talukdar S, Oh da Y, Bandyopadhyay G, Li D, Xu J, McNelis J, Lu M, Li P, Yan Q, Zhu Y, Ofrecio J, Lin M, Brenner MB, Olefsky JM. 2012. Neutrophils mediate insulin resistance in mice fed a high-fat diet through secreted elastase. *Nature medicine* 18: 1407-12

318. Sanyal AJ, Chalasani N, Kowdley KV, McCullough A, Diehl AM, Bass NM, Neuschwander-Tetri BA, Lavine JE, Tonascia J, Unalp A, Van Natta M, Clark J, Brunt EM, Kleiner DE, Hoofnagle JH, Robuck PR. 2010. Pioglitazone, vitamin E, or placebo for nonalcoholic steatohepatitis. *The New England journal of medicine* 362: 1675-85
319. Alkhouri N, Morris-Stiff G, Campbell C, Lopez R, Tamimi TA, Yerian L, Zein NN, Feldstein AE. 2012. Neutrophil to lymphocyte ratio: a new marker for predicting steatohepatitis and fibrosis in patients with nonalcoholic fatty liver disease. *Liver international : official journal of the International Association for the Study of the Liver* 32: 297-302
320. Kara M, Dogru T, Genc H, Sertoglu E, Celebi G, Gurel H, Kayadibi H, Cicek AF, Ercin CN, Sonmez A. 2015. Neutrophil-to-lymphocyte ratio is not a predictor of liver histology in patients with nonalcoholic fatty liver disease. *European journal of gastroenterology & hepatology* 27: 1144-8
321. Krizhanovsky V, Yon M, Dickins RA, Hearn S, Simon J, Miething C, Yee H, Zender L, Lowe SW. 2008. Senescence of activated stellate cells limits liver fibrosis. *Cell* 134: 657-67
322. Radaeva S, Wang L, Radaev S, Jeong WI, Park O, Gao B. 2007. Retinoic acid signaling sensitizes hepatic stellate cells to NK cell killing via upregulation of NK cell activating ligand RAE1. *American journal of physiology. Gastrointestinal and liver physiology* 293: G809-16
323. Muhanna N, Abu Tair L, Doron S, Amer J, Azzeh M, Mahamid M, Friedman S, Safadi R. 2011. Amelioration of hepatic fibrosis by NK cell activation. *Gut* 60: 90-8
324. Schnabl B, Purbeck CA, Choi YH, Hagedorn CH, Brenner D. 2003. Replicative senescence of activated human hepatic stellate cells is accompanied by a pronounced inflammatory but less fibrogenic phenotype. *Hepatology* 37: 653-64
325. Yoshimoto S, Loo TM, Atarashi K, Kanda H, Sato S, Oyadomari S, Iwakura Y, Oshima K, Morita H, Hattori M, Honda K, Ishikawa Y, Hara E, Ohtani N. 2013. Obesity-induced gut microbial metabolite promotes liver cancer through senescence secretome. *Nature* 499: 97-101
326. Tosello-Trampont AC, Krueger P, Narayanan S, Landes SG, Leitinger N, Hahn YS. 2016. NKp46(+) natural killer cells attenuate metabolism-induced hepatic fibrosis by regulating macrophage activation in mice. *Hepatology* 63: 799-812
327. Kramer B, Korner C, Kebschull M, Glassner A, Eisenhardt M, Nischalke HD, Alexander M, Sauerbruch T, Spengler U, Nattermann J. 2012. Natural killer p46High expression defines a natural killer cell subset that is potentially involved in control of hepatitis C virus replication and modulation of liver fibrosis. *Hepatology* 56: 1201-13
328. Kahraman A, Schlattjan M, Kocabayoglu P, Yildiz-Meziletoglu S, Schlensak M, Fingas CD, Wedemeyer I, Marquitan G, Gieseler RK, Baba HA, Gerken G, Canbay A. 2010. Major histocompatibility complex class I-related chains A and B (MIC A/B): a novel role in nonalcoholic steatohepatitis. *Hepatology* 51: 92-102

329. Jeong WI, Park O, Suh YG, Byun JS, Park SY, Choi E, Kim JK, Ko H, Wang H, Miller AM, Gao B. 2011. Suppression of innate immunity (natural killer cell/interferon-gamma) in the advanced stages of liver fibrosis in mice. *Hepatology* 53: 1342-51
330. Bendelac A, Lantz O, Quimby ME, Yewdell JW, Bennink JR, Brutkiewicz RR. 1995. CD1 recognition by mouse NK1+ T lymphocytes. *Science* 268: 863-5
331. Eberl G, Lees R, Smiley ST, Taniguchi M, Grusby MJ, MacDonald HR. 1999. Tissue-specific segregation of CD1d-dependent and CD1d-independent NK T cells. *Journal of immunology* 162: 6410-9
332. Kita H, Naidenko OV, Kronenberg M, Ansari AA, Rogers P, He XS, Koning F, Mikayama T, Van De Water J, Coppel RL, Kaplan M, Gershwin ME. 2002. Quantitation and phenotypic analysis of natural killer T cells in primary biliary cirrhosis using a human CD1d tetramer. *Gastroenterology* 123: 1031-43
333. Tang XZ, Jo J, Tan AT, Sandalova E, Chia A, Tan KC, Lee KH, Gehring AJ, De Libero G, Bertoletti A. 2013. IL-7 licenses activation of human liver intrasinusoidal mucosal-associated invariant T cells. *Journal of immunology* 190: 3142-52
334. Syn WK, Oo YH, Pereira TA, Karaca GF, Jung Y, Omenetti A, Witek RP, Choi SS, Guy CD, Fearing CM, Teaberry V, Pereira FE, Adams DH, Diehl AM. 2010. Accumulation of natural killer T cells in progressive nonalcoholic fatty liver disease. *Hepatology* 51: 1998-2007
335. Tajiri K, Shimizu Y, Tsuneyama K, Sugiyama T. 2009. Role of liver-infiltrating CD3+CD56+ natural killer T cells in the pathogenesis of nonalcoholic fatty liver disease. *European journal of gastroenterology & hepatology* 21: 673-80
336. Xu CF, Yu CH, Li YM, Xu L, Du J, Shen Z. 2007. Association of the frequency of peripheral natural killer T cells with nonalcoholic fatty liver disease. *World journal of gastroenterology* 13: 4504-8
337. Kremer M, Thomas E, Milton RJ, Perry AW, van Rooijen N, Wheeler MD, Zacks S, Fried M, Rippe RA, Hines IN. 2010. Kupffer cell and interleukin-12-dependent loss of natural killer T cells in hepatosteatosis. *Hepatology* 51: 130-41
338. Li Z, Soloski MJ, Diehl AM. 2005. Dietary factors alter hepatic innate immune system in mice with nonalcoholic fatty liver disease. *Hepatology* 42: 880-5
339. Wehr A, Baeck C, Heymann F, Niemietz PM, Hammerich L, Martin C, Zimmermann HW, Pack O, Gassler N, Hittatiya K, Ludwig A, Luedde T, Trautwein C, Tacke F. 2013. Chemokine receptor CXCR6-dependent hepatic NK T Cell accumulation promotes inflammation and liver fibrosis. *Journal of immunology* 190: 5226-36
340. Syn WK, Agboola KM, Swiderska M, Michelotti GA, Liaskou E, Pang H, Xie G, Philips G, Chan IS, Karaca GF, Pereira Tde A, Chen Y, Mi Z, Kuo PC, Choi SS, Guy CD, Abdelmalek MF, Diehl AM. 2012. NKT-associated hedgehog and osteopontin drive fibrogenesis in non-alcoholic fatty liver disease. *Gut* 61: 1323-9
341. Solari NEF, Inzaugarat ME, Baz P, De Matteo E, Lezama C, Galoppo M, Galoppo C, Chernavsky AC. 2012. The Role of Innate Cells Is Coupled to a Th1-

Polarized Immune Response in Pediatric Nonalcoholic Steatohepatitis. *Journal of clinical immunology* 32: 611-21

342. Boujedidi H, Robert O, Bignon A, Cassard-Doulcier AM, Renoud ML, Gary-Gouy H, Hemon P, Tharinger H, Prevot S, Bachelerie F, Naveau S, Emilie D, Balabanian K, Perlemuter G. 2015. CXCR4 dysfunction in non-alcoholic steatohepatitis in mice and patients. *Clinical science* 128: 257-67
343. Sutti S, Jindal A, Locatelli I, Vacchiano M, Gigliotti L, Bozzola C, Albano E. 2014. Adaptive immune responses triggered by oxidative stress contribute to hepatic inflammation in NASH. *Hepatology* 59: 886-97
344. Tang Y, Bian Z, Zhao L, Liu Y, Liang S, Wang Q, Han X, Peng Y, Chen X, Shen L, Qiu D, Li Z, Ma X. 2011. Interleukin-17 exacerbates hepatic steatosis and inflammation in non-alcoholic fatty liver disease. *Clinical and experimental immunology* 166: 281-90
345. Tan Z, Qian X, Jiang R, Liu Q, Wang Y, Chen C, Wang X, Ryffel B, Sun B. 2013. IL-17A plays a critical role in the pathogenesis of liver fibrosis through hepatic stellate cell activation. *Journal of immunology* 191: 1835-44
346. Wagner NM, Brandhorst G, Czepluch F, Lankeit M, Eberle C, Herzberg S, Faustin V, Riggert J, Oellerich M, Hasenfuss G, Konstantinides S, Schafer K. 2013. Circulating regulatory T cells are reduced in obesity and may identify subjects at increased metabolic and cardiovascular risk. *Obesity* 21: 461-8
347. Ma X, Hua J, Mohamood AR, Hamad AR, Ravi R, Li Z. 2007. A high-fat diet and regulatory T cells influence susceptibility to endotoxin-induced liver injury. *Hepatology* 46: 1519-29
348. Feuerer M, Herrero L, Cipolletta D, Naaz A, Wong J, Nayer A, Lee J, Goldfine AB, Benoist C, Shoelson S, Mathis D. 2009. Lean, but not obese, fat is enriched for a unique population of regulatory T cells that affect metabolic parameters. *Nature medicine* 15: 930-9
349. Chatzigeorgiou A, Chung KJ, Garcia-Martin R, Alexaki VI, Klotzsche-von Ameln A, Phieler J, Sprott D, Kanczkowski W, Tzanavari T, Bdeir M, Bergmann S, Cartellieri M, Bachmann M, Nikolakopoulou P, Androutsellis-Theotokis A, Siegert G, Bornstein SR, Muders MH, Boon L, Karalis KP, Lutgens E, Chavakis T. 2014. Dual role of B7 costimulation in obesity-related nonalcoholic steatohepatitis and metabolic dysregulation. *Hepatology* 60: 1196-210
350. Montes VN, Turner MS, Subramanian S, Ding Y, Hayden-Ledbetter M, Slater S, Goodspeed L, Wang S, Omer M, Den Hartigh LJ, Averill MM, O'Brien KD, Ledbetter J, Chait A. 2013. T cell activation inhibitors reduce CD8+ T cell and pro-inflammatory macrophage accumulation in adipose tissue of obese mice. *PloS one* 8: e67709
351. Poggi M, Engel D, Christ A, Beckers L, Wijnands E, Boon L, Driessen A, Cleutjens J, Weber C, Gerdes N, Lutgens E. 2011. CD40L deficiency ameliorates adipose tissue inflammation and metabolic manifestations of obesity in mice. *Arteriosclerosis, thrombosis, and vascular biology* 31: 2251-60
352. Guo CA, Kogan S, Amano SU, Wang M, Dagdeviren S, Friedline RH, Aouadi M, Kim JK, Czech MP. 2013. CD40 deficiency in mice exacerbates obesity-induced adipose tissue inflammation, hepatic steatosis, and insulin

resistance. *American journal of physiology. Endocrinology and metabolism* 304: E951-63

353. Leveille C, Bouillon M, Guo W, Bolduc J, Sharif-Askari E, El-Fakhry Y, Reyes-Moreno C, Lapointe R, Merhi Y, Wilkins JA, Mourad W. 2007. CD40 ligand binds to alpha5beta1 integrin and triggers cell signaling. *The Journal of biological chemistry* 282: 5143-51
354. Zirlik A, Maier C, Gerdes N, MacFarlane L, Soosairajah J, Bavendiek U, Ahrens I, Ernst S, Bassler N, Missiou A, Patko Z, Aikawa M, Schonbeck U, Bode C, Libby P, Peter K. 2007. CD40 ligand mediates inflammation independently of CD40 by interaction with Mac-1. *Circulation* 115: 1571-80

APPENDIX

Included in part in "Narayanan S, Surette FA, and Hahn YS. The immune landscape in nonalcoholic steatohepatitis. *Immune Network*." (manuscript in press).

Contribution of immune cells to the pathogenesis of NASH

The immune response accelerates and magnifies the extent of injury, yet paradoxically facilitates the resolution of inflammation and fibrosis in NASH (Figure A1). Although several studies have helped define precise roles for immune cells in the development of NAFLD, continued investigation of the interplay between various immune compartments is necessary to arrive at a complete understanding of the immunopathogenesis of NASH.

Monocytes and macrophages

As the first line of defense against potentially pathogenic content draining from the gut, the liver must maintain a large population of phagocytic cells that can engulf and clear a diverse array of foreign compounds and bacterial products. It is perhaps for this reason that over 80% of the body's macrophages reside in the liver, including liver-resident Kupffer cells and their monocyte-derived counterparts, both of which play significant roles in the pathogenesis of NASH (275). Indeed, macrophage markers have been proposed as potential biomarkers of disease severity as levels of soluble CD163 and CD14 in the blood of NASH patients correlate with NAFLD activity score, degree of steatosis, fibrosis, and inflammation (276, 277).

Macrophages first appear in damaged adipose tissue, where they engulf dying adipocytes to form histological hallmarks called crown-like structures (278). Subsequent recruitment of monocytes to the liver is driven by chemotactic factors, such as monocyte chemotactic protein-1 (MCP-1). Production of MCP-1 is initiated by hepatocytes during simple steatosis and is sustained by infiltrating macrophages in a feedforward loop (128, 279). As a result, blockade or absence of MCP-1 or CCR2, the receptor for MCP-1, reduces the influx of monocytes and macrophages into NASH livers, effectively halting the development of chronic inflammation (280, 281). Although MCP-1 is arguably the most well studied macrophage chemotactic factor in NASH, recent studies have identified additional molecules that regulate the influx of monocytes and macrophages into the liver, including the release of ATP or TRAIL from lipid-laden hepatocytes (282, 283). In addition, extracellular vesicles containing ceramide or CXCL10 released from injured hepatocytes are highly chemotactic to a number of immune cells, including macrophages (284, 285). Although these studies use bone marrow derived macrophages and cell lines to assess migration, their findings suggest that the trafficking of monocytes and macrophages to injured hepatocytes in NASH is a multifactorial process that can be targeted for therapeutic intervention. In fact, inhibition of CCR2 in NASH patients with fibrosis is an ongoing phase 2 clinical trial (NCT02217475). While such advances are promising, it will be interesting to determine whether the influx of monocytes occurs in parallel to *in situ* proliferation of liver-resident Kupffer cells and to further identify the relative contributions of each population toward the pathogenesis of NASH.

Upon infiltrating the liver during NASH, macrophages produce copious amounts of inflammatory cytokines such as TNF-α and IL-1β, which enhance steatosis and

facilitate the development of fibrosis and hepatocellular carcinoma (128, 286, 287). Pro-inflammatory cytokine production is triggered by imbalances in macrophage fatty acid and cholesterol metabolism or in response to damage associated molecular patterns released by injured hepatocytes (288, 289). These stimuli act in concert with toll-like receptors (TLRs), which are stimulated by elevated levels of endotoxin and other TLR ligands, as small intestinal bacterial overgrowth and loss of intestinal barrier integrity is characteristic of patients and animal models of disease (290-292). Moreover, in a mouse model of NASH, Kupffer cells were hyperresponsive to low-levels of endotoxin, which was paralleled in blood monocytes of NAFLD patients (293, 294). These observations underscore a critical role for the gut-liver axis in NAFLD, wherein damage initiated in lipotoxic hepatocytes is converted to inflammation by recruited macrophages and further propagated by immunogenic products leaking from the intestine.

The pro-inflammatory nature of classically activated M1 macrophages that initiate NASH is in contrast to the anti-inflammatory phenotype of alternatively activated M2 macrophages that aid in the repair of damaged liver tissue. For instance, ablation of macrophages during liver fibrosis improves scarring; however, loss of macrophages during recovery from fibrosis increases scar formation, as macrophages are a critical source of collagenases that remodel fibrotic tissue (295, 296). In a carbon tetrachloride (CCl_4) model of liver injury, restorative macrophages expressing some markers of both M1 and M2 macrophages infiltrate the liver at a late stage of disease, phagocytose dying cells, and resolve scar formation (297). Conversely, M2 macrophages induce proliferation and collagen production in fibroblasts and are strongly correlated with the expression of fibrogenic genes (298). Additionally, macrophages can directly contribute

to fibrogenesis through collagen secretion (299). Crosstalk between M1 and M2 macrophages can also regulate inflammation as M2 macrophages induce apoptosis of M1 macrophages in a mouse model of alcoholic fatty liver disease (300). Nonetheless, in unresolved NASH, the restorative capacity of macrophages is perturbed given the decrease in their phagocytic ability, which correlates to the degree of steatosis (301). Promoting M2 macrophages or reducing M1 macrophages early in disease thus appear to ameliorate the progression of NASH, while sustained M2 skewing later in disease impairs effective wound healing responses and contributes to fibrogenesis.

Dendritic cells (DCs)

DCs are highly efficient antigen presenting cells that regulate immune responses through cytokine production and activation of T cells. Similar to macrophages, DCs play a dichotomous role in the pathogenesis of NASH and liver fibrosis. For instance, in a mouse model of NASH, DCs steadily accumulate in the liver in early stages of disease and produce significant amounts of the pro-inflammatory cytokines TNF-α, IL-6, and MCP-1 and the anti-inflammatory cytokine IL-10 (302). Surprisingly, depletion of DCs did not ameliorate disease and instead lead to increased hepatic infiltration of immune cells, elevated levels of pro-inflammatory cytokine production, notable loss in IL-10 production, and upregulation of fibrogenic markers (302). The beneficial effects of DCs in liver fibrosis are in part due to their ability to clear apoptotic debris and produce matrix metalloproteinases that enable clearance of fibrotic deposits (302, 303). Fibrosis is mediated by the activation and proliferation of hepatic stellate cells (HSCs), which are the pericytes of the liver that differentiate into myofibroblasts during fibrosis. In contrast

to the net beneficial effect of DCs in fibrosis, culturing DCs from fibrotic livers with HSCs results in HSC proliferation and inflammatory cytokine production, suggesting that the effect of DCs in liver disease may vary by cell type (304).

Interestingly, DCs from fibrotic livers are able to induce robust cytolytic and proliferative antigen-specific T cell responses (304). On the contrary, DCs obtained from extrahepatic sites in high fat diet-fed mice are unable to initiate robust T cell responses (305). Although these studies differ in the models used, including a purely fibrosis model or diet-induced models of liver injury, they suggest that DC responses may be distinct between hepatic and extrahepatic sites in NASH and/or liver fibrosis. One explanation for these discrepancies may be intrinsic differences in lipid metabolism of liver-resident DCs compared to DCs in extrahepatic sites. Indeed, inhibiting global fatty acid synthesis resulted in ~20% loss of DCs from the spleen and bone marrow, while hepatic DCs were reduced by 80% (306). The increased sensitivity of hepatic DCs to changes in lipid metabolism may provide a potential therapeutic avenue, especially since DCs enriched in lipids are more immunogenic when compared to DCs with lower lipid content (307). Lastly, the distinct subsets of DCs in the liver could also be differentially modulated to alter local immune responses. A recent report of liver fibrosis following infection with *Schistosoma mansoni* found that a subset of DCs suppresses Th2 responses that lead to liver fibrosis (308). Moreover, DC depletion in a mouse model of NASH altered the ratio of CD8:CD4 T cells and reduced the intrahepatic frequency of regulatory T cells that dampen inflammation (302). Modulating DC responses may thus be an approach to limit T cell mediated liver injury (discussed below) in NASH.

Neutrophils

Neutrophils are myeloid cells of the granulocytic lineage that are among the first cells to arrive at the site of inflammation. Unlike macrophages and T cells, neutrophils are not as prolific in the hepatic inflammatory infiltrate in NASH (309). Their muted presence may be reflective of the inflammatory mileu, as high-fat diet fed mice treated with LPS and IL-1β had an increased influx of mononuclear cells, while hepatic injury via carbohydrates and cholesterol stimulated the influx of both mononuclear and polymorphonuclear cells (310). Given the increased levels of endotoxins and metabolic insults in the liver during NASH, the resulting heterogeneity of the inflammatory infiltrate may thus mask the contribution of neutrophils to the progression of NASH. Nonetheless, a number of mouse models and neutrophil markers in NASH patients have helped identify effector mechanisms by which neutrophils contribute to the immunopathology of NASH. Specifically, expression of myeloperoxidase (MPO), an enzyme stored in the azurophilic granules of neutrophils that generates cytotoxic hypochlorous acid, is increased in the plasma and livers of NASH patients compared to patients with simple steatosis (311). MPO can oxidize phosphatidylcholine that further activates neutrophils and acts as a ligand for scavenger receptors, which in turn exacerbates fibrogenesis (312). Consequently, it is not surprising that deficiency of MPO results in a marked reduction in the production of pro-inflammatory cytokines and development of hepatic fibrosis (311, 313).

Release of MPO is part of the respiratory burst of activated neutrophils, which results in the production of reactive oxygen species (ROS). The importance of ROS in NASH pathogenesis is underscored by decreased circulating levels of antioxidants in

obese children (314). Furthermore, neutrophils in the peripheral blood of NASH patients produce elevated levels of ROS upon stimulation when compared to controls (315). Local production of ROS can lead to lipid peroxidation and HSC migration, thus facilitating cellular injury and fibrosis (316). In addition to oxidative mechanisms of injury, neutrophils also secrete neutrophil elastase, which promotes hepatic insulin resistance by degrading insulin receptor substrate-1 (317). It is therefore conceivable that inhibitors of MPO, ROS, and neutrophil elastase may provide therapeutic benefit in NASH. Indeed, treatment of NASH patients with the antioxidant vitamin E reduced steatosis and serum levels of liver enzymes (318). Given the potential benefit in reducing neutrophil involvement during NASH, the increased ratio of neutrophils to lymphocytes in blood has been proposed as a potential noninvasive marker of disease severity (319). Although there is some debate as to the usefulness of this ratio in patients with comorbidites such as type 2 diabetes mellitus, further investigation of the role of neutrophils in the development of NASH may improve strategies for their use in diagnosis and treatment of disease (320).

NK cells

NK cells develop from common lymphoid progenitors, yet like many innate immune cells, respond to immunogenic insults early and in an antigen-independent manner. Mice lacking NK cells are resistant to developing steatosis following a high fructose diet, indicating that NK cells may have a role in facilitating the transition from NAFLD to NASH (127). Moreover, NK cells play a prominent role in chronic liver diseases, as they are critical players in inhibiting the development of fibrosis through

direct killing of newly activated and senescent HSCs (321, 322). The increased cytolytic activity of NK cells is triggered by upregulation of activating stress ligands or downregulation of inhibitory ligands on HSCs (322, 323). However, HSCs that are "fully activated" or fail to become senescent are resistant to killing by NK cells (321, 322). In contrast, senescent HSCs downregulate fibrogenic programs and upregulate inflammatory genes (324). Considering that HSCs are chronically activated in the proinflammatory environment of the liver during NASH, these findings may be indicative of dysregulated senescence of HSCs in NASH. Yoshimoto, et al. demonstrate that induction of the senescence phenotype in HSCs is associated with increased rates of hepatocellular carcinoma in mice exposed to a carcinogen that were fed a high-fat diet compared to normal diet fed mice (325). Given that these experiments were conducted in mice with intact immune responses, these data may be indicative of defective NK cell function in NAFLD, as NK cells kill senescent HSCs.

We recently reported that depletion of hepatic NK cells expressing the activating marker NKp46 promotes fibrogenesis by skewing macrophages toward M2 phenotypes late in disease (326). The importance of NKp46 expression in regulating HSC activity was previously demonstrated in fibrosis resulting from viral hepatitis, as loss of robust NKp46 expression was inversely related to fibrosis grade (327). Moreover, blockade of NKp46 results in decreased NK cell degranulation, IFN-γ production, and HSC killing upon *in vitro* co-culture with HSCs (327). In contrast, total NK cells and expression of the NK cell activating receptor NKG2D and its ligand MIC A/B are elevated in NASH patients and are associated with increased fibrosis grade (328). While the authors of this study interpret the data as indicative of a potential pathogenic role for NKG2D-MIC A/B

interaction in NASH, their findings could also reflect a compensatory, yet ineffective, increase in NK cell activity. This alternative interpretation further implies that NK cell responses may be compromised in NASH, thus permitting uncontrolled HSC proliferation and activation. Indeed, in a CCl_4 model of liver fibrosis, production of IFN-γ by NK cells was diminished in advanced stages of disease (329). Interestingly, the reduction in NK cell IFN-γ production was partly alleviated by blocking TGF-β released from HSCs (329). Continued investigation is thus required to thoroughly understand the complex interactions among NK cells, HSCs, macrophages, and likely other immune and nonimmune cells in NASH.

Natural killer T (NKT) cells

NKT cells are defined by the co-expression of an invariant T cell receptor and NK cell markers and recognize lipid antigens presented by the non-classical antigen presenting molecule CD1 (330). Classical CD1d reactive hepatic NKT cells are differentially distributed in mice and humans, where Vα14Jα18 NKT cells constitute ~22% of hepatic mononuclear cells in mice, while the human homologue Vα24Vβ11 NKT cells comprise only ~0.6% of $CD3^+$ cells that bind CD1d tetramers (331, 332). However, the counterpart to mouse invariant NKTs may instead be human mucosal associated invariant T (MAIT) cells, which make up ~15% of intrasinusoidal lymphocytes in humans (333). Given the differences between NKT cells in mice and humans, translating data obtained from mouse models of NASH to human disease may require caution.

NKT cell accumulation during NAFLD and NASH has been reported by several studies in both the liver and blood of patients (334, 335). Yet, other studies report that hepatic NKT cells are decreased in NASH patients and associate decreased frequencies of NKT cells in the peripheral blood with an increased risk of NAFLD (336, 337). These differences may in part reflect when and how NKT cells were detected. For instance, in a mouse model of NASH, NKT cells were selectively increased in the liver, but were unchanged in the spleen (338). However, the same study reported that NKT cells that infiltrate steatotic livers undergo apoptosis (338). Identifying the kinetics of NKT cell infiltration into the liver during the progression of disease in NASH patients may provide further insight into the frequency of NKT cells in NAFLD.

Influx of NKT cells into the liver during NASH is mediated by enhanced expression of the chemokine CXCL16 on endothelial cells and macrophages, which binds CXCR6 on the surface of NKT cells (339). Upregulation of CXCL16 coincides with the production of IL-4 and IFN-γ by NKT cells, which aggravates inflammation via macrophage activation (339). Activation of the Hedgehog pathway has also been implicated in NKT cell recruitment in NASH livers. Specifically, overactivation of Hedgehog signaling recruits increased numbers of NKT cells to the livers of methionine choline-deficient diet-fed mice, which developed higher grade fibrosis compared to wild type mice (334). $CD1d^{-/-}$ mice lacking NKT cells did not develop fibrosis, suggesting that Hedgehog mediated NKT cell responses are pathogenic in NASH (334). Indeed, activation of the Hedgehog pathway in NKT cells upregulates expression of osteopontin production, which drives HSC activation and fibrogenesis (340). Thus, the net contribution of NKT cells appears to be pathogenic in NASH. Nonetheless, modulating

the ability of NKT cells to produce cytokines may permit tuning of macrophage responses to favor the resolution of inflammation and clearance of fibrotic tissue.

T cells

T cells are a diverse class of lymphocytes that include CD4 and CD8 T cells, which respond to antigens displayed on MHCII and MHCI, respectively, to exert effector functions such as cytokine production and cytolysis. T cells play a critical role in the development and progression of NAFLD as high fructose-diet fed mice lacking T cells fail to develop steatosis and hepatic inflammation (127). These findings are validated in NASH patients as they have increased frequencies of IFN-γ^+ memory CD4 and CD8 T cells (315). Elevated peripheral blood T cells in NASH patients are reflective of cells infiltrating the inflamed liver (341). One of the molecular mechanisms driving T cell infiltration into the liver is dysfunctional chemotaxis, as peripheral CD4 T cells from obese mice and NASH patients migrate more readily toward the chemokine CXCL12 when compared to T cells from healthy mice or donors (342). These results suggest that imbalances in systemic lipid metabolism may result in intrinsic alterations in immune cells. In addition, increased oxidative stress in the hepatic microenvironment of NASH livers generates neoantigens that can induce the recruitment of T cells (343). Collectively, these studies identify T cells as a prominent immune population in NASH that plays a critical role in influencing the course of disease.

Functionally, CD4 T cell responses in NASH are skewed toward Th1 and Th17 phenotypes. Th1 responses in NASH are characterized by secretion of IFN-γ and TNF-α, which in turn help polarize macrophages toward M1 responses (315, 341, 343). Although

the lack of steatosis and inflammation in the absence of T cells would suggest that T cell derived IFN-γ is pathogenic in NASH, there are no studies to date that detail the progression of disease upon neutralization of IFN-γ (127). In contrast, IL-17 is well known to propagate NASH via multiple mechanisms, including neutrophil activation. Moreover, exposure of HepG2 cells to fatty acids in the presence of recombinant IL-17 promotes accumulation of intracellular triglycerides (344). Additionally, IL-17 signaling in HSCs upregulates expression of profibrotic genes while lack of IL-17 in a chemically-induced murine model of liver fibrosis reduces the levels of proinflamamtory cytokines and extent of cell death (226, 345). Interestingly, fibrosis was exacerbated in mice lacking expression of IL-22, a cytokine produced by Th17 cells that promotes epithelial regeneration (226). Although the above studies provide ample evidence for a pathogenic role of Th17 cells in NASH, perhaps tuning Th17 responses to increase IL-22 production may uncover a beneficial role for the increased presence of this population in NASH livers.

The marked increase in Th1 and Th17 responses in NASH is complemented by a loss in regulatory T cells (Treg) in the adipose tissues, peripheral blood, or livers of NASH patients or mice that replicate facets of the disease (346-348). In the liver, the reduced presence of Tregs is not only relative to the influx of other T cell subsets, but may also be due to increased susceptibility to death by oxidative damage (347). Importantly, adoptive transfer of Tregs into high-fat diet mice decreases hepatic inflammation and serum levels of liver enzymes, indicating that Tregs may regulate the transition from NAFLD to NASH (347). These findings were corroborated by the association of elevated hepatic lipogenesis and inflammation and reduced Treg frequency

in mice lacking expression of the costimulatory molecules CD80 and CD86 (349). Interestingly, blockade of CD80 and CD86 in mice with an intact Treg compartment had the opposite effect as the grade of steatosis and fibrosis was decreased with a concurrent improvement in glucose tolerance (349). These contrasting results indicate that modulating costimulatory molecules in the presence of Tregs may be an attractive means to regulate T cell responses in NASH. Indeed, blockade or genetic deficiency of another costimulatory molecule, CD40L, impeded inflammation in both adipose tissues and livers of mice fed obesogenic diets (350, 351). Surprisingly, deficiency of CD40, which binds CD40L, produces the opposite results, as steatosis and insulin resistance were exacerbated in $CD40^{-/-}$ mice compared to wild type controls despite reduced hepatic levels of inflammatory cytokines (352). CD40L can also bind the integrins $\alpha5\beta1$ and Mac-1 (353, 354). The contrasting progression of disease in CD40 and CD40L deficient mice may thus reflect interactions that are independent of CD40 and T cells as $\alpha5\beta1$ and Mac-1 are expressed on several cells of nonlymphocytic origin.

Figure A1. Immunopathogenesis of nonalcoholic steatohepatitis (NASH).

Interactions between immune cells and steatotic hepatocytes or HSCs in NASH can exacerbate or ameliorate disease.

DCs, dendritic cells; IL, interleukin; TNF, tumor necrosis factor; DAMPs, damage associated molecular patterns; IFN, interferon; NK cell, natural killer cell; NKT, natural killer T cell HSC, hepatic stellate cell; MPO, myeloperoxidase; ROS, reactive oxygen species.

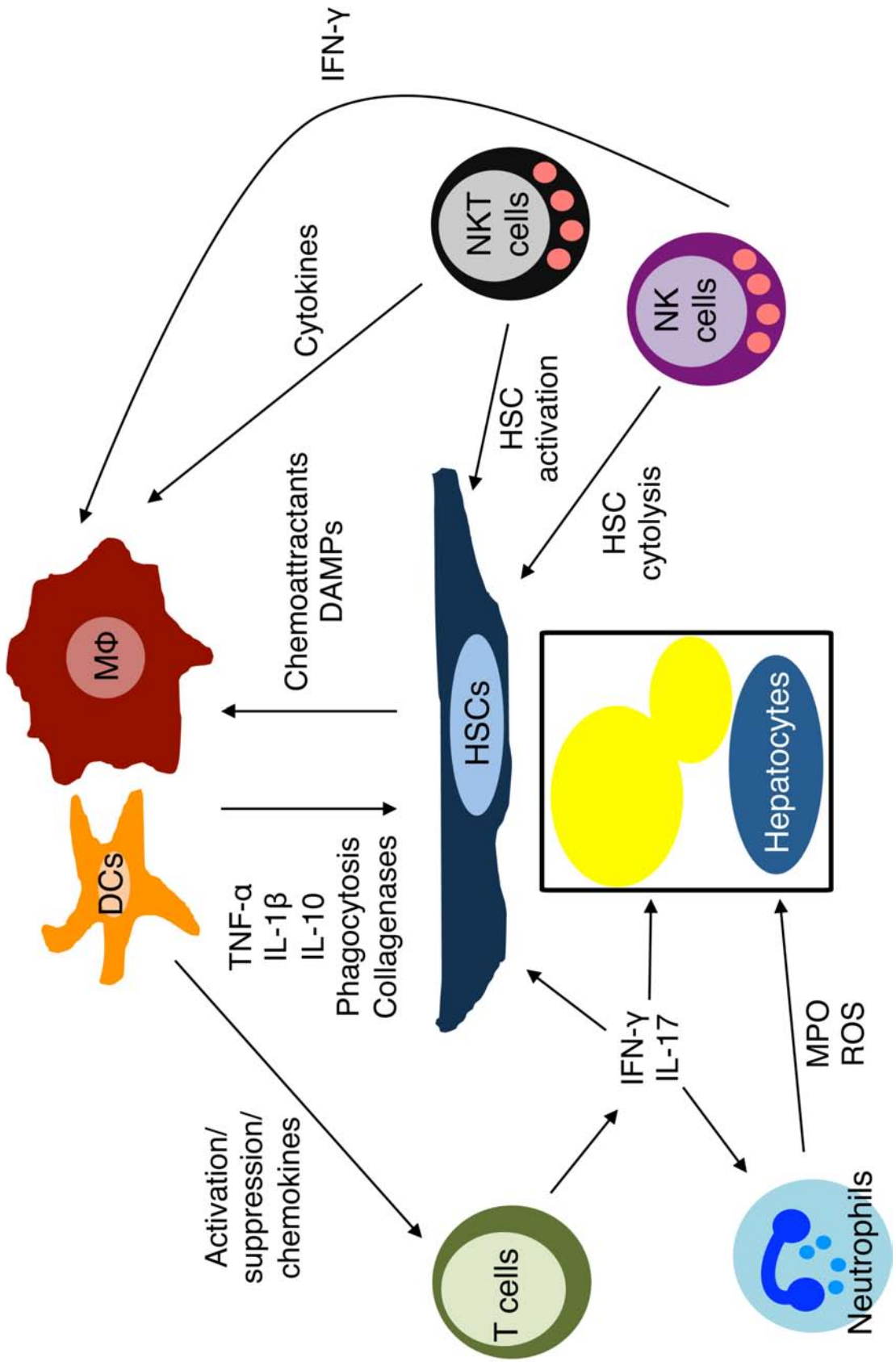
IFN-γ
Cytokines
NKT cells
NK cells
HSC activation
HSC cytolysis
Chemoattractants DAMPs
MΦ
DCs
HSCs
Hepatocytes
TNF-α
IL-1β
IL-10
Phagocytosis
Collagenases
Activation/ suppression/ chemokines
T cells
IFN-γ
IL-17
MPO
ROS
Neutrophils

Appendix Table 1. Lipidomics of uninfected hepatocytes treated with ACC inhibitors. Uninfected Huh7.5.1 cells were treated with DMSO, 1 μM K1, or 100 nM soraphen A for 3 days. Indicated lipids were quantified by mass spectrometry and mean values were used to determine significant changes in K1 and soraphen A-treated cells compared to DMSO control. The column "*p* value" was determined by student's *t* test and $p<0.05$ (bolded) was considered significant. The column "corrected *p* value" was adjusted for false discovery rate (FDR). Because FDR is more stringent than a *t* test, $p<0.1$ (bolded) was considered significant. Positive and negative values in the column "Log (fold change)" indicate an increase or decrease in the lipid, respectively. NA indicates insufficient replicates to calculate value. Results are the mean ± SEM of 3-4 independent experiments.

Metabolite	**Average±SD (relative abundance)**			***p* value (*t* test)**		**Corrected *p* value (FDR adjusted)**		**Log (fold change)**	
	DMSO	K1	Soraphen A	K1	Soraphen A	K1	Soraphen A	K1	Soraphen A
Phosphatidylserine (PS)									
16:0 16:0 PS	61.46±7.18	129.05±79.15	92.60±11.63	0.276836	**0.006090**	1.000000	0.651642	1.070	0.591
16:0 18:2 PS	459.85±58.42	356.67±234.59	461.03±53.95	0.528232	0.977408	1.000000	1.000000	-0.367	0.004
16:0 20:3, 18:1 18:2 PS	723.28±168.96	457.20±315.13	740.16±131.93	0.280463	0.880338	1.000000	1.000000	-0.662	0.033
16:0 20:4 PS	262.61±32.39	293.02±187.08	446.18±102.35	0.805824	**0.031650**	1.000000	1.000000	0.158	0.765
16:0 22:6 PS	151.61±19.68	230.88±152.85	310.27±48.06	0.464249	**0.003698**	1.000000	0.414150	0.607	1.033
18:0 18:1 PS	644.37±154.27	500.58±259.89	574.21±263.01	0.455663	0.665306	1.000000	1.000000	-0.364	-0.166
18:0 20:2 PS	313.72±93.94	182.90±113.02	172.31±48.26	0.180673	**0.049161**	1.000000	1.000000	-0.778	-0.864
18:0 22:5 PS	623.20±149.49	566.34±327.92	588.52±232.24	0.800484	0.811501	1.000000	1.000000	-0.138	-0.083
18:0 22:6, 20:2 20:4 PS	1701.98±232.89	1451.93±885.51	1322.42±301.20	0.676506	0.096246	1.000000	1.000000	-0.229	-0.364
18:1 18:1, 18:0 18:2 PS	1151.68±171.17	643.62±399.46	743.39±179.52	0.146459	**0.016626**	1.000000	1.000000	-0.839	-0.632
18:1 20:4, 18:0 20:5 PS	466.73±30.82	887.30±575.90	1109.63±276.59	0.333277	**0.018082**	1.000000	1.000000	0.927	1.249
18:1 22:6 PS	251.53±20.83	583.50±370.68	558.61±97.57	0.260851	**0.006659**	1.000000	0.705836	1.214	1.151
Phosphatidic acid (PA)									
16:0 16:0 PA	17.02±12.65	24.66±18.09	16.48±5.34	0.570766	0.941035	1.000000	1.000000	0.535	-0.047
16:0 18:1 PA	32.57±11.62	25.76±13.21	24.24±9.60	0.516462	0.313084	1.000000	1.000000	-0.338	-0.426
16:0 18:2 PA	17.12±5.61	10.29±2.27	10.78±4.16	0.089335	0.123558	1.000000	1.000000	-0.735	-0.667
16:0 20:3 PA	15.61±2.38	9.20±6.52	7.99±1.65	0.225066	**0.002692**	1.000000	0.304156	-0.763	-0.967
16:0 20:4 PA	15.51±2.06	16.37±5.64	16.50±7.47	0.822935	0.814432	1.000000	1.000000	0.077	0.088
16:0 22:4 PA	3.71±.95	3.88±0.95	3.86±NA	0.857248	NA	1.000000	NA	0.066	0.059
16:0 22:6 PA	75.66±34.68	22.98±11.75	16.66±6.08	**0.049468**	**0.040269**	1.000000	1.000000	-1.719	-2.183
18:0 18:1 PA	15.65±5.52	19.30±9.89	14.39±4.39	0.606177	0.749308	1.000000	1.000000	0.302	-0.122
18:0 18:2 PA	38.96±12.13	16.30±11.23	17.73±3.86	0.054654	**0.033936**	1.000000	1.000000	-1.257	-1.136
18:0 20:2 PA	11.62±10.74	1.55±0.94	29.77±23.42	0.157368	0.460855	1.000000	1.000000	-2.905	1.358
18:0 20:4 PA	95.21±17.63	67.35±42.34	66.88±23.71	0.375263	0.107561	1.000000	1.000000	-0.500	-0.510
18:0 20:5 PA	1.62±NA	2.18±1.74	NA±NA	NA	NA	NA	NA	0.431	NA
18:0 22:5 PA	57.97±10.30	19.88±8.98	16.59±3.29	**0.003892**	**0.002356**	0.439843	0.270900	-1.544	-1.805
18:0 22:6 PA	130.17±47.91	63.86±38.70	54.36±19.81	0.099844	**0.043108**	1.000000	1.000000	-1.028	-1.260
18:1 18:2 PA	9.88±2.58	24.05±16.89	17.22±4.80	0.282387	**0.046752**	1.000000	1.000000	1.283	0.802
18:1 20:3 PA	9.51±6.47	20.42±14.34	14.89±4.75	0.318208	0.232358	1.000000	1.000000	1.103	0.648
18:1 20:4 PA	14.36±2.97	36.64±23.54	37.43±10.49	0.241794	**0.017901**	1.000000	1.000000	1.351	1.382
18:1 22:6 PA	314.07±77.96	164.14±93.72	148.39±15.39	0.089334	**0.021656**	1.000000	1.000000	-0.936	-1.082

Phosphatidylethanolamine (PE)									
16:0 16:0 PE	0.10±.02	0.05±0.04	0.05±0.03	0.171983	**0.024378**	1.000000	1.000000	-0.983	-1.008
16:0 18:0 PE	0.07±.03	0.06±0.04	0.05±0.02	0.839950	0.446573	1.000000	1.000000	-0.128	-0.362
16:0 18:1 PE	0.76±.11	0.59±0.32	0.70±0.12	0.450814	0.451206	1.000000	1.000000	-0.373	-0.131
16:0 18:2 PE	2.03±.24	1.63±0.96	2.31±0.53	0.546086	0.384106	1.000000	1.000000	-0.317	0.188
16:0 20:3, 18:1 18:2 PE	2.32±.40	1.77±1.13	2.53±0.64	0.495863	0.590728	1.000000	1.000000	-0.386	0.129
16:0 20:4 PE	2.16±.33	1.42±0.79	2.38±0.60	0.243171	0.551197	1.000000	1.000000	-0.603	0.140
16:0 22:6 PE	1.37±.19	1.35±0.83	2.27±0.47	0.969544	**0.023030**	1.000000	1.000000	-0.022	0.729
18:0 18:1 PE	0.22±.04	0.22±0.12	0.27±0.05	0.981689	0.175478	1.000000	1.000000	0.012	0.287
18:1 18:1, 18:0 18:2 PE	1.12±.15	1.31±0.74	1.56±0.36	0.703641	0.090774	1.000000	1.000000	0.225	0.475
18:1 20:3, 18:0 20:4 PE	3.62±.38	2.52±1.47	2.87±0.52	0.322963	0.063487	1.000000	1.000000	-0.522	-0.335
18:1 20:4, 18:0 20:5 PE	2.38±.19	2.54±1.40	3.75±0.76	0.862999	**0.033806**	1.000000	1.000000	0.093	0.653
Phosphatidylcholine (PC)									
16:0 16:0 PC	30.63±4.33	16.17±8.76	15.99±2.59	0.086347	**0.002272**	1.000000	0.263603	-0.921	-0.938
16:0 18:0 PC	9.03±1.17	3.93±2.30	4.23±0.59	**0.043706**	**0.001231**	1.000000	0.143983	-1.201	-1.095
16:0 18:1 PC	98.81±10.55	40.71±23.68	49.61±4.20	**0.037068**	**0.001057**	1.000000	0.124674	-1.279	-0.994
16:0 18:2 PC	85.09±5.16	62.63±39.99	77.54±12.01	0.433360	0.311017	1.000000	1.000000	-0.442	-0.134
16:0 20:3 PC	42.27±4.59	24.72±17.67	33.40±5.24	0.223669	**0.044452**	1.000000	1.000000	-0.774	-0.340
16:0 20:4 PC	22.11±3.14	19.58±13.44	32.03±5.90	0.777347	**0.034892**	1.000000	1.000000	-0.175	0.535
16:0 22:6 PC	8.25±.72	7.84±4.85	13.96±2.17	0.898011	**0.009456**	1.000000	0.992875	-0.073	0.759
18:0 18:1 PC	11.43±1.72	6.18±3.45	7.04±0.62	0.101935	**0.009968**	1.000000	1.000000	-0.888	-0.700
18:1 18:1 PC	34.90±4.05	24.89±15.67	31.33±3.06	0.384337	0.212577	1.000000	1.000000	-0.487	-0.156
18:1 20:3 PC	14.31±.86	11.19±7.55	14.77±2.67	0.549774	0.756886	1.000000	1.000000	-0.354	0.046
18:1 20:4 PC	8.56±.49	10.56±6.76	17.90±2.67	0.659558	**0.005059**	1.000000	0.556438	0.303	1.065
Diacylglycerol (DAG)									
16:0 18:1 DAG	0.91±.22	0.09±0.01	0.11±0.03	**0.005293**	**0.005168**	0.561096	0.563286	-3.318	-3.007
16:0 18:2 DAG	0.39±.06	0.04±0.01	0.04±0.02	**0.001140**	**0.000790**	0.133428	**0.093974**	-3.455	-3.335
18:1 18:2 DAG	0.34±.10	0.10±0.02	0.10±0.03	**0.012605**	**0.011401**	1.000000	1.000000	-1.774	-1.798
18:2 18:2 DAG	0.06±.03	0.04±0.01	0.04±0.03	0.179644	0.424218	1.000000	1.000000	-0.687	-0.613
Lysophosphatidic acid (LPA)									
16:0 LPA	0.73±.29	0.43±0.26	0.61±0.43	0.210079	0.649122	1.000000	1.000000	-0.768	-0.270
16:1 LPA	1.08±.27	0.45±0.18	0.60±0.26	**0.013640**	**0.042644**	1.000000	1.000000	-1.257	-0.854
18:0 LPA	6.74±1.78	2.90±0.72	3.87±1.92	**0.016188**	0.071703	1.000000	1.000000	-1.218	-0.799
18:1 LPA	0.74±.26	1.09±0.28	1.47±0.67	0.165844	0.113120	1.000000	1.000000	0.557	0.987
18:2 LPA	0.52±.15	0.34±0.08	0.50±0.18	0.101926	0.887885	1.000000	1.000000	-0.590	-0.048
20:4 LPA	1.07±.38	1.12±0.27	1.40±0.46	0.856662	0.310911	1.000000	1.000000	0.062	0.386

Sphingomyelin (SM)									
SM 13:0	2.47±.76	1.81±0.88	2.42±0.27	0.356782	0.894839	1.000000	1.000000	-0.447	-0.034
SM 13:1	0.25±.18	0.09±0.11	0.32±0.31	0.269832	0.709503	1.000000	1.000000	-1.432	0.354
SM 14:0	8.30±1.83	6.10±4.87	7.57±1.86	0.522602	0.597473	1.000000	1.000000	-0.444	-0.132
SM 14:1	0.50±.09	0.62±0.35	0.73±0.18	0.609971	0.074684	1.000000	1.000000	0.314	0.545
SM 15:0	10.51±2.45	6.92±5.26	8.36±1.97	0.361935	0.222044	1.000000	1.000000	-0.603	-0.331
SM 15:1	0.60±.37	0.49±0.23	0.71±0.15	0.680441	0.606231	1.000000	1.000000	-0.298	0.247
SM 16:0	164.43±63.95	92.27±58.75	108.54±25.46	0.186340	0.181026	1.000000	1.000000	-0.834	-0.599
SM 16:1	23.33±2.16	13.98±8.70	19.87±3.96	0.199549	0.190045	1.000000	1.000000	-0.738	-0.232
SM 17:0	8.03±1.20	3.07±1.62	4.41±1.00	**0.014338**	**0.003858**	1.000000	0.428237	-1.387	-0.866
SM 17:1	2.38±.19	1.03±0.54	2.14±0.35	**0.040440**	0.302932	1.000000	1.000000	-1.200	-0.148
SM 18:0	10.63±1.14	3.18±1.25	6.09±1.37	**0.001025**	**0.002456**	0.120920	0.280030	-1.740	-0.804
SM 18:1	5.82±.54	2.28±0.77	4.30±0.73	**0.004093**	**0.017502**	0.458437	1.000000	-1.355	-0.437
SM 19:0	1.34±.33	0.36±0.15	1.09±0.24	**0.005063**	0.276143	0.546848	1.000000	-1.891	-0.295
SM 19:1	0.75±.71	0.14±0.05	0.47±0.24	0.179079	0.494765	1.000000	1.000000	-2.442	-0.684
SM 20:0	6.35±1.49	2.05±0.76	6.03±0.84	**0.005189**	0.722155	0.555172	1.000000	-1.632	-0.075
SM 20:1	2.59±.87	0.75±0.34	2.34±0.60	**0.017466**	0.652120	1.000000	1.000000	-1.780	-0.147
SM 21:0	1.74±.59	0.57±0.18	1.95±0.52	**0.022833**	0.613483	1.000000	1.000000	-1.616	0.164
SM 21:1	0.60±.31	0.24±0.17	0.79±0.09	0.116738	0.299969	1.000000	1.000000	-1.305	0.416
SM 22:0	9.57±2.48	3.43±1.06	8.82±1.64	**0.009815**	0.633666	0.991318	1.000000	-1.479	-0.118
SM 22:1	9.66±4.07	3.13±0.77	8.49±1.21	**0.046073**	0.615500	1.000000	1.000000	-1.625	-0.186
SM 22:2	0.79±.32	0.24±0.07	0.79±0.13	**0.037756**	0.995647	1.000000	1.000000	-1.725	0.002
SM 23:0	2.72±.75	0.99±0.38	2.81±0.24	**0.012840**	0.832108	1.000000	1.000000	-1.451	0.047
SM 23:1	4.23±1.97	1.62±0.74	4.48±0.28	0.071267	0.818331	1.000000	1.000000	-1.386	0.082
SM 24:0	7.65±1.19	2.95±1.06	5.12±0.88	**0.003232**	**0.015934**	0.371704	1.000000	-1.373	-0.579
SM 24:1	21.37±5.40	7.41±2.85	15.86±2.76	**0.008079**	0.135468	0.837892	1.000000	-1.528	-0.430
SM 24:2	6.29±2.20	2.96±0.99	5.59±0.62	0.050264	0.579353	1.000000	1.000000	-1.085	-0.169
SM 24:3	0.53±.30	0.28±0.10	0.61±0.13	0.198341	0.639483	1.000000	1.000000	-0.913	0.208
SM 25:0	0.63±.20	0.20±0.12	0.38±0.12	**0.018864**	0.086227	1.000000	1.000000	-1.629	-0.746
SM 25:1	1.42±.30	0.46±0.32	0.89±0.21	**0.013596**	**0.030229**	1.000000	1.000000	-1.610	-0.677
SM 26:0	0.18±.05	0.06±0.06	0.13±0.07	**0.049209**	0.249483	1.000000	1.000000	-1.713	-0.506
SM 26:1	0.50±.18	0.16±0.09	0.36±0.13	**0.028438**	0.264169	1.000000	1.000000	-1.595	-0.479
SM 26:2	0.42±.14	0.20±0.08	0.33±0.10	0.051785	0.362251	1.000000	1.000000	-1.077	-0.336

Glucosylceramide (GlcCer)									
GlcCer 16:0	60.37±13.44	3.61±0.74	104.30±70.68	**0.003397**	0.303993	0.387309	1.000000	-4.065	0.789
GlcCer 18:0	6.15±2.21	0.31±0.04	10.75±8.63	**0.013232**	0.369416	1.000000	1.000000	-4.326	0.806
GlcCer 20:0	2.01±.79	0.08±0.01	2.11±1.79	**0.016589**	0.927866	1.000000	1.000000	-4.566	0.066
GlcCer 21:1	0.34±.08	0.03±0.01	0.32±0.13	**0.004678**	0.830330	0.509853	1.000000	-3.661	-0.076
GlcCer 21:2	2.14±1.14	0.06±0.00	1.14±0.38	**0.035659**	0.179633	1.000000	1.000000	-5.202	-0.906
GlcCer 22:0	1.33±.55	0.07±0.02	1.41±0.94	**0.019346**	0.886406	1.000000	1.000000	-4.213	0.086
GlcCer 22:1	0.29±.04	0.03±0.02	0.24±0.08	**0.000150**	0.312411	**0.017955**	1.000000	-3.176	-0.285
GlcCer 23:0	0.50±.16	0.02±0.01	0.34±0.16	**0.009489**	0.191781	0.967874	1.000000	-4.447	-0.580
GlcCer 23:1	0.48±.15	0.02±0.00	0.28±0.09	**0.008057**	0.061262	0.837892	1.000000	-4.494	-0.806
GlcCer 24:0	1.72±.43	0.07±0.02	0.78±0.23	**0.004439**	**0.013487**	0.488249	1.000000	-4.614	-1.145
GlcCer 24:1	1.09±.37	0.06±0.01	0.62±0.19	**0.011030**	0.075936	1.000000	1.000000	-4.248	-0.823
Dihydroceramide (DCer)									
DCer 16:0	6.25±3.68	10.23±1.04	11.62±9.37	0.116242	0.347703	1.000000	1.000000	0.711	0.894
DCer 18:0	0.71±.32	1.42±0.65	1.15±0.57	0.189456	0.238602	1.000000	1.000000	0.992	0.695
DCer 20:0	1.01±.66	1.52±0.13	2.45±1.74	0.225889	0.200646	1.000000	1.000000	0.586	1.276
DCer 22:0	0.68±.45	0.99±0.42	1.09±0.56	0.394907	0.307237	1.000000	1.000000	0.537	0.671
DCer 24:0	1.28±.73	2.21±0.59	1.86±0.74	0.122433	0.311916	1.000000	1.000000	0.786	0.535
DCer 24:1	1.43±.86	2.22±0.40	2.18±1.60	0.177695	0.449824	1.000000	1.000000	0.630	0.607
Ceramide (Cer)									
Cer 16:0	1.66±1.66	53.25±8.66	77.23±4.87	**0.006659**	**0.000378**	0.699152	**0.045390**	-1.037	-0.501
Cer 18:0	12.86±.82	7.15±2.25	8.45±1.57	**0.037621**	**0.005400**	1.000000	0.583193	-0.847	-0.607
Cer 18:1	2.45±.09	1.34±0.02	2.66±0.66	**0.000075**	0.568950	**0.009042**	1.000000	-0.868	0.120
Cer 20:0	10.05±4.60	2.37±0.48	9.44±4.92	**0.043427**	0.862275	1.000000	1.000000	-2.082	-0.090
Cer 20:1	1.10±.21	0.62±0.36	1.21±0.47	0.131770	0.679930	1.000000	1.000000	-0.830	0.142
Cer 20:2	1.85±.48	0.81±0.30	2.66±1.61	**0.017173**	0.399373	1.000000	1.000000	-1.191	0.519
Cer 22:0	11.06±1.37	6.55±1.03	12.67±1.68	**0.004290**	0.188985	0.476216	1.000000	-0.755	0.196
Cer 22:1	1.93±.60	1.10±0.25	1.96±0.42	0.064876	0.949445	1.000000	1.000000	-0.814	0.018
Cer 23:0	10.19±1.89	5.74±2.45	14.97±5.13	0.063934	0.159206	1.000000	1.000000	-0.829	0.555
Cer 24:0	20.62±2.62	9.21±1.70	13.88±2.60	**0.000954**	**0.010614**	0.113486	1.000000	-1.163	-0.571
Cer 24:1	29.63±3.45	17.40±2.39	24.36±2.65	**0.002650**	0.054442	0.307414	1.000000	-0.768	-0.282

Appendix Table 2. Lipidomics of HCV-infected hepatocytes treated with ACC inhibitors. Infected Huh7.5.1 cells were treated with DMSO, 1 μM K1, or 100 nM soraphen A for 3 days. Indicated lipids were quantified by mass spectrometry and mean values were used to determine significant changes in K1 and soraphen A-treated cells compared to DMSO control. The column "*p* value" was determined by student's *t* test and $p<0.05$ (bolded) was considered significant. The column "corrected *p* value" was adjusted for false discovery rate (FDR). Because FDR is more stringent than a *t* test, $p<0.1$ (bolded) was considered significant. Positive and negative values in the column "Log (fold change)" indicate an increase or decrease in the lipid, respectively. Results are the mean ± SEM of 3-4 independent experiments.

Metabolite	Average±SD (relative abundance)			*p* value (*t* test)		Corrected *p* value (FDR adjusted)		Log (fold change)	
	DMSO	K1	Soraphen A	K1	Soraphen A	K1	Soraphen A	K1	Soraphen A
Phosphatidylserine (PS)									
16:0 16:0 PS	49.71±19.46	91.77±40.11	86.48±27.83	0.202178	0.133616	1.000000	1.000000	0.885	0.799
16:0 18:2 PS	402.35±94.31	330.43±199.23	419.17±153.36	0.607921	0.877173	1.000000	1.000000	-0.284	0.059
16:0 20:3 PS, 18:1 18:2 PS	729.21±181.59	432.57±281.26	656.49±296.05	0.202504	0.731185	1.000000	1.000000	-0.753	-0.152
16:0 20:4 PS	271.54±54.51	276.47±224.96	365.93±159.65	0.973495	0.416058	1.000000	1.000000	0.026	0.430
16:0 22:6 PS	248.20±87.76	249.86±185.07	268.11±95.09	0.989547	0.790307	1.000000	1.000000	0.010	0.111
18:0 18:1 PS	1003.80±275.01	542.50±292.46	488.46±177.84	0.097034	**0.030274**	1.000000	1.000000	-0.888	-1.039
18:0 20:2 PS	395.79±67.84	228.58±107.80	183.13±20.74	0.094620	**0.005188**	1.000000	0.513156	-0.792	-1.112
18:0 22:5 PS	1049.85±109.94	764.96±502.66	566.11±110.52	0.430640	**0.003291**	1.000000	0.342243	-0.457	-0.891
18:0 22:6 PS, 20:2 20:4 PS	3040.31±407.08	2053.23±1264.91	1555.42±239.81	0.307414	**0.001991**	1.000000	0.223047	-0.566	-0.967
18:1 18:1 PS, 18:0 18:2 PS	1329.13±264.22	640.52±361.86	670.65±197.64	0.056837	**0.013070**	1.000000	1.000000	-1.053	-0.987
18:1 20:4 PS, 18:0 20:5 PS	755.60±64.14	1047.70±706.97	1038.00±322.00	0.548803	0.266329	1.000000	1.000000	0.472	0.458
18:1 22:6 PS	411.16±59.44	795.01±435.24	676.60±115.15	0.265282	**0.039797**	1.000000	1.000000	0.951	0.719
Phosphatidic acid (PA)									
16:0 16:0 PA	19.56±13.97	17.07±10.50	14.45±0.89	0.798690	0.517809	1.000000	1.000000	-0.196	-0.437
16:0 18:1 PA	32.88±20.65	32.41±18.84	17.43±7.21	0.976040	0.239222	1.000000	1.000000	-0.021	-0.916
16:0 18:2 PA	17.29±7.25	8.96±0.18	8.62±4.64	0.184750	0.168513	1.000000	1.000000	-0.949	-1.004
16:0 20:3 PA	9.68±4.77	10.03±8.90	5.99±1.56	0.958634	0.463828	1.000000	1.000000	0.051	-0.693
16:0 20:4 PA	17.43±2.57	14.20±9.75	13.84±3.65	0.632087	0.290376	1.000000	1.000000	-0.296	-0.333
16:0 22:4 PA	8.36±5.11	2.69±4.43	1.69±0.86	0.179393	0.076512	1.000000	1.000000	-1.638	-2.309
16:0 22:6 PA	334.94±100.01	48.31±38.41	21.96±10.88	**0.006083**	**0.007678**	0.626550	0.744748	-2.794	-3.931
18:0 18:1 PA	22.12±5.84	16.13±10.68	16.55±2.05	0.446274	0.163634	1.000000	1.000000	-0.456	-0.418
18:0 18:2 PA	40.69±15.69	19.11±13.44	14.62±1.64	0.110047	**0.043915**	1.000000	1.000000	-1.090	-1.477
18:0 20:2 PA	42.95±26.46	10.41±4.09	27.78±18.24	0.163047	0.464960	1.000000	1.000000	-2.045	-0.629
18:0 20:4 PA	165.51±24.19	102.26±60.82	72.05±20.79	0.205899	**0.003088**	1.000000	0.324194	-0.695	-1.200
18:0 20:5 PA	8.33±4.58	1.82±0.88	2.58±0.33	0.126623	0.160536	1.000000	1.000000	-2.192	-1.693
18:0 22:5 PA	159.65±46.21	31.16±20.22	17.69±3.15	**0.006336**	**0.008332**	0.639964	0.791513	-2.357	-3.174
18:0 22:6 PA	578.15±231.02	99.73±45.11	76.33±1.64	**0.022753**	**0.022511**	1.000000	1.000000	-2.535	-2.921
18:1 18:2 PA	7.99±7.26	18.70±15.51	10.73±6.09	0.377838	0.704392	1.000000	1.000000	1.227	0.425
18:1 20:3 PA	9.87±5.44	19.11±10.47	15.95±7.23	0.263489	0.296354	1.000000	1.000000	0.952	0.692
18:1 20:4 PA	13.49±7.42	39.61±27.98	29.98±9.22	0.243901	0.066850	1.000000	1.000000	1.554	1.152
18:1 22:6 PA	1084.59±337.31	295.80±75.73	232.78±40.75	**0.015397**	**0.014032**	1.000000	1.000000	-1.874	-2.220

Phosphatidylethanolamine (PE)									
16:0 16:0 PE	0.39±0.13	0.16±0.07	0.12±0.03	**0.036451**	**0.025404**	1.000000	1.000000	-1.278	-1.645
16:0 18:0 PE	0.23±0.07	0.12±0.07	0.10±0.03	0.095342	**0.019541**	1.000000	1.000000	-0.969	-1.224
16:0 18:1 PE	2.46±0.32	1.45±0.78	1.18±0.31	0.142141	**0.001146**	1.000000	0.129508	-0.765	-1.061
16:0 18:2 PE	4.37±1.33	3.59±2.12	3.81±1.13	0.612640	0.542886	1.000000	1.000000	-0.283	-0.199
16:0 20:3 PE, 18:1 18:2 PE	3.93±1.42	3.08±1.94	3.82±1.46	0.561254	0.919111	1.000000	1.000000	-0.352	-0.040
16:0 20:4 PE	3.44±0.65	2.32±1.61	3.17±1.24	0.353082	0.723740	1.000000	1.000000	-0.567	-0.115
16:0 22:6 PE	3.23±0.76	2.66±1.86	3.32±1.23	0.653674	0.910816	1.000000	1.000000	-0.284	0.037
18:0 18:1 PE	0.86±0.17	0.68±0.40	0.47±0.09	0.526964	**0.012904**	1.000000	1.000000	-0.336	-0.860
18:1 18:1 PE, 18:0 18:2 PE	3.06±0.82	3.24±1.91	2.74±0.71	0.887555	0.582379	1.000000	1.000000	0.084	-0.157
18:1 20:3 PE, 18:0 20:4 PE	5.88±1.06	4.39±2.43	4.02±1.09	0.404677	0.050434	1.000000	1.000000	-0.421	-0.548
18:1 20:4 PE, 18:0 20:5 PE	4.25±0.98	4.93±3.46	5.51±2.05	0.771312	0.324530	1.000000	1.000000	0.213	0.375
Phosphatidylcholine (PC)									
16:0 16:0 PC	102.20±5.97	36.45±23.05	26.89±6.02	**0.033288**	**0.000002**	1.000000	**0.000250**	-1.488	-1.926
16:0 18:0 PC	31.58±0.90	10.76±7.41	7.00±2.08	**0.038406**	**0.000023**	1.000000	**0.002759**	-1.553	-2.173
16:0 18:1 PC	320.84±1.81	106.08±77.31	78.24±22.22	**0.040537**	**0.000195**	1.000000	**0.022981**	-1.597	-2.036
16:0 18:2 PC	196.41±17.84	137.13±93.06	116.79±28.58	0.384970	**0.005132**	1.000000	0.513156	-0.518	-0.750
16:0 20:3 PC	91.81±14.73	49.41±34.05	47.30±12.67	0.151887	**0.003982**	1.000000	0.410105	-0.894	-0.957
16:0 20:4 PC	63.14±4.93	40.45±28.02	47.70±15.93	0.294961	0.146204	1.000000	1.000000	-0.642	-0.405
16:0 22:6 PC	29.05±2.15	20.50±16.73	18.77±6.09	0.469672	**0.036769**	1.000000	1.000000	-0.503	-0.631
18:0 18:1 PC	45.74±2.43	17.58±13.00	11.24±3.37	0.060773	**0.000007**	1.000000	**0.000841**	-1.379	-2.024
18:1 18:1 PC	96.16±3.64	66.50±50.36	45.89±11.99	0.415027	**0.002140**	1.000000	0.233270	-0.532	-1.067
18:1 20:3 PC	36.23±3.79	27.98±21.70	22.33±4.98	0.578989	**0.005149**	1.000000	0.513156	-0.373	-0.698
18:1 20:4 PC	26.02±0.54	28.91±22.54	25.97±8.11	0.844969	0.990615	1.000000	1.000000	0.152	-0.003
Diacylglycerol (DAG)									
16:0 18:1 DAG	2.32±0.19	0.26±0.03	0.20±0.06	**0.000143**	**0.000054**	**0.017416**	**0.006436**	-3.142	-3.549
16:0 18:2 DAG	0.75±0.09	0.12±0.02	0.08±0.04	**0.000501**	**0.000215**	**0.058570**	**0.025206**	-2.642	-3.165
18:1 18:2 DAG	0.66±0.09	0.26±0.08	0.22±0.08	**0.002285**	**0.000401**	0.255877	**0.045726**	-1.351	-1.557
18:2 18:2 DAG	0.17±0.02	0.08±0.04	0.10±0.04	**0.029427**	**0.034102**	1.000000	1.000000	-1.116	-0.735
Lysophosphatidic acid (LPA)									
16:0 LPA	0.49±0.25	0.71±0.10	0.77±0.01	0.282166	0.203665	1.000000	1.000000	0.518	0.636
16:1 LPA	0.88±0.15	0.81±0.11	1.07±0.38	0.498958	0.490176	1.000000	1.000000	-0.123	0.274
18:0 LPA	8.59±0.76	5.74±0.89	6.38±1.29	**0.011156**	0.076047	1.000000	1.000000	-0.582	-0.429
18:1 LPA	0.88±0.34	1.94±0.26	2.10±0.27	**0.014968**	**0.009320**	1.000000	0.876099	1.142	1.262
18:2 LPA	0.44±0.19	0.52±0.09	0.65±0.15	0.532144	0.162008	1.000000	1.000000	0.225	0.565
20:4 LPA	1.37±0.38	2.02±0.38	1.99±0.35	0.081698	0.078755	1.000000	1.000000	0.559	0.537

Sphingomyelin (SM)									
SM 13:0	6.70±0.81	2.20±0.51	3.86±1.13	**0.000301**	**0.008078**	**0.035866**	0.775466	-1.608	-0.794
SM 13:1	1.15±0.14	0.27±0.21	0.48±0.32	**0.006176**	**0.016830**	0.629968	1.000000	-2.114	-1.264
SM 14:0	12.08±1.47	14.20±0.75	11.20±2.33	0.059186	0.547937	1.000000	1.000000	0.233	-0.110
SM 14:1	0.68±0.26	1.19±0.17	0.85±0.37	**0.025966**	0.483112	1.000000	1.000000	0.806	0.324
SM 15:0	17.79±4.72	16.71±1.63	13.46±2.53	0.694089	0.171895	1.000000	1.000000	-0.090	-0.403
SM 15:1	0.52±0.32	0.72±0.21	1.06±0.67	0.364432	0.215315	1.000000	1.000000	0.472	1.027
SM 16:0	284.22±61.23	210.69±41.84	177.57±27.60	0.118086	**0.031748**	1.000000	1.000000	-0.432	-0.679
SM 16:1	32.30±7.14	27.34±1.44	31.55±6.38	0.260248	0.879598	1.000000	1.000000	-0.241	-0.034
SM 17:0	11.05±1.86	6.38±1.41	7.03±0.74	**0.012996**	**0.016602**	1.000000	1.000000	-0.793	-0.653
SM 17:1	2.74±0.76	2.74±0.06	2.96±0.40	0.996469	0.639693	1.000000	1.000000	-0.001	0.109
SM 18:0	17.18±2.23	6.42±1.68	9.74±0.81	**0.000777**	**0.004029**	**0.089300**	0.410988	-1.421	-0.819
SM 18:1	7.78±1.01	4.43±0.48	7.49±1.86	**0.003066**	0.792757	0.334196	1.000000	-0.812	-0.056
SM 19:0	1.58±0.20	0.78±0.36	1.78±0.37	**0.039957**	0.395339	1.000000	1.000000	-1.031	0.170
SM 19:1	0.47±0.20	0.24±0.03	0.63±0.15	0.105426	0.251236	1.000000	1.000000	-0.966	0.427
SM 20:0	7.52±1.23	3.17±1.24	8.81±0.42	**0.007897**	0.123190	0.789704	1.000000	-1.247	0.229
SM 20:1	2.76±0.25	1.17±0.09	3.48±0.47	**0.000310**	**0.046283**	**0.036544**	1.000000	-1.232	0.336
SM 21:0	1.87±0.37	0.99±0.43	2.77±0.38	**0.047068**	**0.014477**	1.000000	1.000000	-0.918	0.565
SM 21:1	0.73±0.14	0.47±0.15	1.00±0.21	0.073739	0.080126	1.000000	1.000000	-0.643	0.454
SM 22:0	10.66±1.14	5.03±2.11	13.44±1.83	**0.026818**	**0.049042**	1.000000	1.000000	-1.083	0.334
SM 22:1	9.09±0.98	4.99±1.17	12.89±1.11	**0.008351**	**0.002260**	0.826705	0.244048	-0.865	0.503
SM 22:2	0.71±0.35	0.47±0.13	1.41±0.40	0.268133	**0.039734**	1.000000	1.000000	-0.607	0.986
SM 23:0	3.30±0.30	1.75±0.78	3.79±0.98	0.063349	0.396060	1.000000	1.000000	-0.915	0.201
SM 23:1	4.22±0.99	2.30±0.74	6.72±0.88	**0.032752**	**0.009610**	1.000000	0.893712	-0.875	0.671
SM 24:0	9.26±1.55	5.46±1.77	7.54±0.83	**0.040821**	0.112845	1.000000	1.000000	-0.761	-0.296
SM 24:1	22.13±1.57	11.95±2.91	23.34±2.44	**0.013193**	0.443613	1.000000	1.000000	-0.889	0.076
SM 24:2	6.69±0.56	5.22±0.52	8.69±1.14	**0.017856**	**0.029834**	1.000000	1.000000	-0.358	0.379
SM 24:3	0.56±0.14	0.59±0.12	1.02±0.11	0.777744	**0.002429**	1.000000	0.259912	0.074	0.865
SM 25:0	0.65±0.09	0.46±0.14	0.67±0.15	0.120852	0.885684	1.000000	1.000000	-0.493	0.029
SM 25:1	1.28±0.11	0.96±0.16	1.43±0.48	**0.049447**	0.579077	1.000000	1.000000	-0.404	0.160
SM 26:0	0.21±0.11	0.14±0.05	0.15±0.06	0.381259	0.426109	1.000000	1.000000	-0.576	-0.502
SM 26:1	0.60±0.14	0.40±0.07	0.52±0.11	0.113538	0.449407	1.000000	1.000000	-0.601	-0.214
SM 26:2	0.35±0.18	0.42±0.04	0.49±0.24	0.509427	0.389852	1.000000	1.000000	0.262	0.489

Glucosylceramide (GlcCer)									
GlcCer 16:0	166.12±39.31	7.56±2.69	154.12±70.17	**0.003839**	0.778191	0.406884	1.000000	-4.458	-0.108
GlcCer 18:0	15.22±3.42	0.71±0.27	15.39±8.69	**0.003272**	0.971997	0.353400	1.000000	-4.426	0.016
GlcCer 20:0	3.71±0.77	0.16±0.03	3.36±2.51	**0.002681**	0.801857	0.297637	1.000000	-4.575	-0.145
GlcCer 21:1	0.69±0.09	0.04±0.01	0.49±0.18	**0.000675**	0.105091	**0.078310**	1.000000	-4.245	-0.500
GlcCer 21:2	3.41±1.28	0.13±0.02	1.69±0.85	**0.014272**	0.073064	1.000000	1.000000	-4.689	-1.011
GlcCer 22:0	3.02±1.15	0.12±0.02	2.07±1.27	**0.015058**	0.311919	1.000000	1.000000	-4.696	-0.545
GlcCer 22:1	0.55±0.18	0.04±0.00	0.40±0.25	**0.010844**	0.370702	1.000000	1.000000	-3.765	-0.457
GlcCer 23:0	1.03±0.25	0.05±0.02	0.70±0.46	**0.004494**	0.277920	0.471912	1.000000	-4.269	-0.549
GlcCer 23:1	0.78±0.21	0.04±0.01	0.48±0.28	**0.005393**	0.133275	0.560847	1.000000	-4.147	-0.719
GlcCer 24:0	3.12±1.01	0.14±0.02	1.38±0.49	**0.009664**	**0.032506**	0.937428	1.000000	-4.530	-1.177
GlcCer 24:1	2.32±0.89	0.12±0.01	1.23±0.45	**0.015819**	0.088016	1.000000	1.000000	-4.305	-0.913
Dihydroceramide (DCer)									
DCer 16:0	33.97±5.41	28.47±7.47	23.20±13.84	0.348048	0.222329	1.000000	1.000000	-0.255	-0.550
DCer 18:0	3.74±0.88	3.46±1.19	3.16±0.66	0.744985	0.331663	1.000000	1.000000	-0.115	-0.246
DCer 20:0	5.64±1.58	4.56±0.95	2.99±2.11	0.315644	0.095184	1.000000	1.000000	-0.306	-0.916
DCer 22:0	3.58±0.92	3.02±1.39	2.27±0.45	0.588981	0.058173	1.000000	1.000000	-0.242	-0.657
DCer 24:0	5.00±0.70	4.86±0.62	4.27±1.97	0.787436	0.524919	1.000000	1.000000	-0.042	-0.228
DCer 24:1	7.81±1.59	6.95±2.18	4.72±2.39	0.600409	0.082206	1.000000	1.000000	-0.167	-0.725
Ceramide (Cer)									
Cer 16:0	270.73±39.69	119.80±7.65	133.62±17.98	**0.003651**	**0.002803**	0.390629	0.297066	-1.176	-1.019
Cer 18:0	35.05±4.06	10.94±0.67	15.35±3.16	**0.000969**	**0.000344**	0.110420	**0.039885**	-1.680	-1.191
Cer 18:1	6.08±1.16	2.78±0.22	4.74±1.30	**0.009031**	0.176240	0.885021	1.000000	-1.128	-0.359
Cer 20:0	24.67±6.52	7.59±1.32	17.34±8.32	**0.011315**	0.217307	1.000000	1.000000	-1.700	-0.509
Cer 20:1	2.67±0.89	1.03±0.44	1.98±0.60	**0.027171**	0.247543	1.000000	1.000000	-1.379	-0.437
Cer 20:2	4.00±0.95	1.28±0.09	3.86±2.03	**0.009895**	0.910702	0.949943	1.000000	-1.647	-0.049
Cer 22:0	33.90±4.65	12.37±3.69	20.34±3.48	**0.001082**	**0.004177**	0.122302	0.421879	-1.455	-0.737
Cer 22:1	4.39±0.23	2.00±0.27	3.16±0.36	**0.000247**	**0.002038**	**0.029835**	0.226179	-1.136	-0.476
Cer 23:0	31.70±11.78	10.85±3.71	29.19±10.96	**0.032164**	0.766056	1.000000	1.000000	-1.547	-0.119
Cer 24:0	71.75±8.25	20.60±3.62	26.81±4.21	**0.000251**	**0.000362**	**0.030143**	**0.041607**	-1.800	-1.420
Cer 24:1	76.85±10.45	40.71±7.17	41.53±7.54	**0.002901**	**0.002095**	0.319120	0.230429	-0.916	-0.888